Report No. NADC-90048-60

INVESTIGATION OF CURRENT AND PROPOSED AIRCRAFT DEPARTURE SUSCEPTIBILITY CRITERIA WITH APPLICATION TO FUTURE FIGHTER AIRCRAFT

Robert M. Seltzer
Air Vehicle and Crew Systems Technology Department (Code 6053)
NAVAL AIR DEVELOPEMENT CENTER
Warminster, PA 18774-5000

31 MAY 1990

FINAL REPORT
Period Covering January 1989 to January 1990
Task No. 4.5
Project No. RR-22-A41
Work Unit No. ZX170
Program Element No. 62122N

Approved for Public Release: Distribution is Unlimited

Prepared for
OFFICE OF NAVAL TECHNOLOGY
800 N. Quincy St.
Arlington, Va 22217

NOTICES

REPORT NUMBERING SYSTEM — The numbering of technical project reports issued by the Naval Air Warfare Center, Aircraft Division, Warminster is arranged for specific identification purposes. Each number consists of the Center acronym, the calendar year in which the number was assigned, the sequence number of the report within the specific calendar year, and the official 2-digit correspondence code of the Functional Department responsible for the report. For example: Report No. NAWCADWAR-92001-60 indicates the first Center report for the year 1992 and prepared by the Air Vehicle and Crew Systems Technology Department. The numerical codes are as follows:

CODE	OFFICE OR DEPARTMENT
00	Commanding Officer, NAWCADWAR
01	Technical Director, NAWCADWAR
05	Computer Department
10	AntiSubmarine Warfare Systems Department
20	Tactical Air Systems Department
30	Warfare Systems Analysis Department
50	Mission Avionics Technology Department
60	Air Vehicle & Crew Systems Technology Department
70	Systems & Software Technology Department
80	Engineering Support Group
90	Test & Evaluation Group

PRODUCT ENDORSEMENT — The discussion or instructions concerning commercial products herein do not constitute an endorsement by the Government nor do they convey or imply the license or right to use such products.

Reviewed By: John W. Clark Jr. **Date:** 8-5-92
Branch Head

Reviewed By: K. A. Green **Date:** 8/10/92
Division Head

Reviewed By: J. H. Frost **Date:** 8/12/92
Director/Deputy Director

REPORT DOCUMENTATION PAGE

Form Approved
OMB No. 0704-0188

1a REPORT SECURITY CLASSIFICATION Unclassified	1b RESTRICTIVE MARKINGS
2a SECURITY CLASSIFICATION AUTHORITY	3. DISTRIBUTION/AVAILABILITY OF REPORT Approved for Public Release; Distribution is Unlimited
2b. DECLASSIFICATION/DOWNGRADING SCHEDULE	
4 PERFORMING ORGANIZATION REPORT NUMBER(S) NADC - 90048-60	5 MONITORING ORGANIZATION REPORT NUMBER(S)
6a NAME OF PERFORMING ORGANIZATION Air Vehicle and Crew Systems Technology Department 6b OFFICE SYMBOL (If applicable) 6053	7a. NAME OF MONITORING ORGANIZATION
6c. ADDRESS (City, State, and ZIP Code) Naval Air Development Center Warminster, PA 18974-5000	7b ADDRESS (City, State, and ZIP Code)
8a. NAME OF FUNDING/SPONSORING ORGANIZATION Office of Naval Technology 8b OFFICE SYMBOL (If applicable) ONT	9 PROCUREMENT INSTRUMENT IDENTIFICATION NUMBER
8c. ADDRESS (City, State, and ZIP Code) 800 North Quincy St. Arlington, VA 22217-5000	10 SOURCE OF FUNDING NUMBERS PROGRAM ELEMENT NO: 62122N PROJECT NO: RR-22-A41 TASK NO: 4.5 WORK UNIT ACCESSION NO: ZX170

11. TITLE (Include Security Classification)
Investigation of Current and Proposed Aircraft Departure Susceptibility Criteria with Application to Future Fighter Aircraft.

12 PERSONAL AUTHOR(S)
Robert M. Seltzer

13a. TYPE OF REPORT	13b TIME COVERED	14 DATE OF REPORT (Year, Month, Day)	15 PAGE COUNT
Final	FROM 1/89 TO 1/90	1990 MAY 31	172

16 SUPPLEMENTARY NOTATION

17 COSATI CODES			18 SUBJECT TERMS (Continue on reverse if necessary and identify by block number)
FIELD	GROUP	SUB-GROUP	Aircraft Departure Criteria, High Angle-of-Attack Equations-of Motion.
01	03	03	

19 ABSTRACT (Continue on reverse if necessary and identify by block number)

This report entails a brief review of the derivation, application and implied limitations of the aircraft departure susceptibility criteria presented in the MIL-STD-1797A Flying Qualities Specification. To begin the discussion, the six degree-of-freedom rigid body aircraft equations-of-motion and aircraft stability concepts are reviewed, focusing on their application to determine the susceptibility of an aircraft to depart from controlled flight. A methodology is then suggested that allows a designer to determine the departure susceptibility of an aircraft configuration through the course of its design (up to and including flight test) with increasing levels of accuracy as the design progresses.

20 DISTRIBUTION/AVAILABILITY OF ABSTRACT	21 ABSTRACT SECURITY CLASSIFICATION
☒ UNCLASSIFIED/UNLIMITED ☐ SAME AS RPT ☐ DTIC USERS	N/A
22a NAME OF RESPONSIBLE INDIVIDUAL Robert M. Seltzer	22b TELEPHONE (Include Area Code) 215-441-1356 22c OFFICE SYMBOL Code 6053

CONTENTS

Page

FIGURES v

TABLES ix

SYMBOLS x

INTRODUCTION 1

- Background 1
- Objective 2
- Scope 2
- Methodology 2

RESULTS AND DISCUSSION 4

- General 4
- Stability and the Rigid Aircraft Equations-of-Motion 24
- Chronological Review of the Developments of Aircraft Departure Susceptibility Criteria 43
  - (Unknown): C_{n_β}, C_{ℓ_β} 47
  - Moul & Paulson: $C_{n_{\beta DYN}}$ 50
  - Weissman: $C_{n_{\beta DYN}}$ vs LCDP 70
  - Johnston: $1/T_{\theta_3}$ 77
  - Kalviste: $C_{m_{\alpha COP}}$, $C_{n_{\beta COP}}$, K 88
  - Bihrle: C_{n_β} vs C_{ℓ_β} 93
  - Johnston: $1/T_{\phi_1}$ 97
  - Pelikan: $C_{n_{\beta APP}}$ 104
  - Kalviste: Dynamic Stability Parameters 108
  - Chody: Routh Criterion Parameters 115

CONCLUSIONS 123

CONTENTS

Page

RECOMMENDATIONS 125

REFERENCES 129

APPENDIX A: Glossary of Defined Terms A-1

FIGURES

Figure	Description	Page
1	Primary Causes Of Aircraft Departure From Controlled Flight	3
2	(a) Yaw Damping Derivative Versus Angle-of-Attack For the X-31A Aircraft	6
	(b) Roll Damping Derivative Versus Angle-of-Attack For the X-31A Aircraft	6
3	Effect Of Oscillation Amplitude On Damping In Roll	7
4	Range Of Data For The Yaw And Roll Damping Derivatives Of The X-31A Aircraft	8
5	Yawing Moment Coefficient Due To Roll Rate For The X-31A Aircraft (Nominal And Range Of Data)	10
6	Rolling Moment Coefficient Due To Yaw Rate For The X-31A Aircraft (Nominal Range Of Data).	11
7	Static Aerodynamic Cross-Coupling Data For The Preliminary Configuration Of The X-31A Aircraft	
	(a) Influence Of Sideslip On The Pitching Moment Coefficient	12
	(b) Influence Of Angle-Of-Attack On The Yawing, Moment, Coefficient	13
8	The Effect Of The Static Cross-Coupling Derivative M_β On The Pole-Zero Locations For The F-4 Aircraft ($\alpha_0 = 20^\circ$, $\beta_0 = 1^\circ$)	15
9	Comparison Of The Composite Pitch Damping Derivative ($C_{m_q} + C_{m_{\dot\alpha}}$) And The Sum Of The Pure Pitching (C_{m_q}) And Pure Plunging ($C_{m_{\dot\alpha}}$) Derivatives With Angle-of- Attack For A Preliminary Configuration Of The X-31A Aircraft.	18
10	Comparison Of The Composite Side Force Damping Derivative ($C_{Y_r} - C_{Y_{\dot\beta}}$)$_s$ And The Sum Of The Pure Yawing (C_{Y_r})$_s$ Derivatives With Angle-of-Attack For A Preliminary Configuration Of The X-31A Aircraft	19

FIGURES (CONT)

Figure	Description	Page
11	Comparison Of The Composite Derivative ($C_{l_r} - C_{l_{\dot{\beta}}}$) And The Sum Of The Pure Yawing $(C_{l_r})_s$ and Pure Sideslipping $(C_{l_{\dot{\beta}}})_s$ Derivatives With Angle-of-Attack For a Preliminary Configuration Of The X-31A Aircraft.	20
12	Comparison Of The Composite Yaw Damping Derivative $(C_{n_r} - C_{n_{\dot{\beta}}})_s$ And The Sum Of The Pure Yawing $(C_{n_r})_s$ and Pure Sideslipping $(C_{n_{\dot{\beta}}})_s$ Derivatives With Angle-of-Attack For A Preliminary Configuration Of The X-31A Aircraft.	21
13	Six Degree-of-Freedom, Nonlinear, Rigid Body Equations-of-Motion (Body-Axis; $I_{yz} = I_{xy} = 0$).	25
14	General Formulation Of The Linear State Equations For A Nonlinear System.	28
15	Nonlinear Rigid Aircraft Equations Of Motion In Perturbed State Space Form (Body-Axis).	31-32
16	Decoupled Longitudinal Body-Axis Stability Matrix.	34
17	Decoupled Lateral/Directional Body-Axis Stability Matrix.	35
18	Simplified Linear Stability Matrix Applicable To Asymmetric Maneuvering Flight.	36
19	Lateral/Directional Root Locus Plot Varying C_{l_p}.	48
20	Lateral/Directional Root Locus Plot Vary C_{n_p}.	48
21	Comparison Of The Lateral/Directional Characteristic Quartic C-Coefficient With $C_{n_{p_{DYN}}}$ For Two Configurations.	
	a. Configuration A	56
	b. Configuration B	57
22	Comparison Of $C_{n_{p_{DYN}}}$ And The C-Coefficient Of The Linear Lateral/Directional Characteristic Quartic For A Preliminary Configuration Of The X-31A Aircraft.	59

FIGURES (CONT)

Figure	Description	Page
23	$Cn_{\beta DYN}$ Stability Design Guide as Suggested by Reference (35).	60
24	Nondimensional Rolling and Yawing Moment Coefficient Versus Sideslip Angle for the F-18 Aircraft at 30 Degrees Angle-of-Attack.	61
25	Rudder Control Effectiveness for a Preliminary Configuration of the X-31A Aircraft.	62
26	The Effect of Differential Trailing-edge Flap Deflection on the Generation of Adverse Yaw at High Angles-of-Attack for a Preliminary Configuration of the X-31A Aircraft.	63
27	Typical Step Responses for Nonminimum Phase Systems.	68
28	Weissman $Cn_{\beta DYN}$ Versus *LCDP Departure Susceptibility Criterion Plane.*	70
29	Weissman LCDP Versus $Cn_{\beta DYN}$ Departure Susceptibility Criterion Plane as Modified by Show and Titiriga of Reference (37).	71
30	Weissman LCDP Versus $Cn_{\beta DYN}$ Departure Susceptibility Criterion Plane as Modified by STI of Reference (37).	72
31	Generalized Pole-Zero Relationships Associated with the Four Quadrants of the LCDP Versus $Cn_{\beta DYN}$ Criterion Plane.	74
32	Linear, Rigid, Six Degree-of-Freedom Coupled ($\beta \neq 0$) Equations-of-Motion for the Unaugmented A-7 Aircraft (Data for $\alpha_0 = 18.8^\circ$; $\beta_0 = 6^\circ$).	78
33	Comparison Between the Pole-Zero Locations of the $N^{\beta}_{\delta_e}/\Delta$ Transfer Function for the Uncoupled and Coupled 6 DOF Equation-of-Motion for the A-7 Aircraft ($\alpha_0 = 18.8^\circ$; $\beta_0 = 6^\circ$).	79
34	Comparison Between the Pole-Zero Locations of the $N^{\beta}_{\delta_e}/\Delta$ Transfer Function for the 6 DOF Equations-of-Motion and the 5 DOF Equations-of-Motion (No $\dot{U}$ - equation) for the A-7 Aircraft ($\alpha_0 = 18.8^\circ$; $\beta_0 = 6^\circ$).	81

FIGURES (CONT)

Figure	Description	Page
35	Root Locus Plot for the 6 DOF Coupled ($\beta \neq 0$) θ/δ_e Transfer Function (Data for the A-7 Aircraft; $\alpha_0 = 18.8^\circ$;$\beta_0 = 6^\circ$)	81
36	Digital Simulation of a Closed-Loop A-7 Departure to a Step Pitch Attitude Command ($\alpha_0 = 18.8^\circ$; $\beta_0 = 6^\circ$).	83
37	Effect of Not Including the $\mathcal{L}'_\alpha$ And N'_α (in the 6 DOF Equations-of-Motion) on the Pole-Zero Locations Cf The $N^\theta_{\delta_e}/\Delta$ Transfer Function of the A-7 Aircraft (Data for $\alpha_0 = 18.8^\circ$; $\beta_0 = 6^\circ$).	84
38	Effect of Not Including the Z_p and Z_r Terms (in the 6 DOF Equations-of-Motion) on the Pole-Zero Locations of the $N^\theta_{\delta_e}/\Delta$ Transfer Function Of The A-7 Aircraft (Data for $\alpha_0 = 18.8^\circ$; $\beta_0 = 6^\circ$).	85
39	Kalviste α Versus β Static Stability Plot.	91
40	Bihrle Applied Research Design Guidelines for Departure Susceptibility and Roll Reversal.	94
41	Typical Low Angle-of-Attack $\phi(s)/\delta_{STK}(s)$ Root Loci Plot.	97
42	Typical High Angle-of-Attack $\phi(s)/\delta_{STK}(s)$ Root Loci Plot.	98
43	$N^\phi_{\delta_{STK}}$ Root Migration with Angle-of-Attack for the F-4J Aircraft.	99
44	Departure Susceptibility Ratings Versus Lateral Closed-Loop Divergence Potential, $1/T_{\phi_1}$ or ζ_ϕ, ω_{n_ϕ}.	101
45	Illustration of the Tangent and Secant Slope Linearization Techniques.	106
46	Kalviste Stability Parameters Plotted Versus Angle-of-Attack and Sideslip Angle.	114

FIGURES (CONT)

Figure	Description	Page
47	Open-Loop Lateral/Directional Stability Boundaries Of Chody Based On The Routh Stability Criteria	116
48	Closed-Loop Lateral/Directional Stability Boundaries: Of Chody (Extension Of LCDP To Include The Aerodynamic Dynamic Derivatives).	118

TABLES

Table		Page
I	Dynamic Moment Derivatives	16
II	Relative Significance Of Dynamic Moment Derivatives For High Angle-of-Attack Flight.	23
III	Summary of The Effects of Altitude, Velocity, Aerodynamic Angles, and Steady Maneuvering on The Unaugmented Rigid Aircraft Stability	38
IV	Chronology of The Major Aircraft Departure Susceptibility Criteria Developements	44
V	Comparison of The Major Differences In Design Features and Characteristics Of Fighter/Attack Aircraft of the 1950's and 1960's Versus The Current Design period	120
VI	Recommended Methodology For Evaluation/Determination Of Aircraft Departure Susceptibility	124

SYMBOLS

SYMBOL	DEFINITION	UNITS
A, B, C, D, E	Coefficient of nth order polynomial from high to low, $As^n + Bs^{n-1} + ...Es^0$	-
b	Wing span	ft
c	Wing chord	ft
$\bar{c}$	Mean Aerodynamic chord (mac)	ft
C_D	Drag coefficient, $\frac{D}{\bar{q}S}$	-
C_L	Lift coefficient, $\frac{L}{\bar{q}S}$	-
C_ℓ	Aerodynamic non-dimensional, rolling moment coefficient, $\frac{\mathscr{L}}{\bar{q}Sb}$	-
C'_{ℓ_i}	Change in non-dimensional rolling moment coefficient with change in variable i (where i = V, p, r, δ_A, δ_R). Axis system is other than principal axis, $C'_{\ell_i} = [(C_{\ell_i} + I_{xz} C'_{n_i}/I_{xx})/(1 - I^2_{xz}/I_{xx} I_{zz})]$	-
C_m	Aerodynamic non-dimensional, pitching moment coefficient, $\frac{M}{\bar{q}S\bar{c}}$	-
C_n	Aerodynamic non-dimensional, yawing moment coefficient, $\frac{N}{\bar{q}Sb}$	-
C'_{n_i}	Change in non-dimensional yawing moment coefficient with change in variable i (where i = V, p, r, δ_A, δ_R). Axis system is other than principal axis, $C'_{n_i} = [(C_{n_i} + I_{xz} C_{\ell_i}/I_{zz})/(1 - I^2_{xz}/I_{xx} I_{zz})]$	-
$C_{n_{\beta DYN}}$	Dynamic Departure Susceptibility Parameter, $C_{n_\beta} \cos\alpha - (\frac{I_z}{I_x})_B C_{\ell_\beta} \sin\alpha$	1/deg
C_Y	Aerodynamic non-dimensional, side force coefficient, $\frac{F_Y}{\bar{q}S}$	-

SYMBOLS (CONT)

SYMBOL	DEFINITION	UNITS

NON-DIMENSIONAL AERODYNAMIC COEFFICIENTS AND DERIVATIVES

Z - force	X - force	Pitching moment
$C_Z = \frac{F_Z}{\bar{q}S}$	$C_X = \frac{F_X}{\bar{q}S}$	$C_m = \frac{M_Y}{\bar{q}S\bar{c}}$
$C_{Z_\alpha} = \frac{\partial C_Z}{\partial \alpha}$	$C_{X_\alpha} = \frac{\partial C_X}{\partial \alpha}$	$C_{m_\alpha} = \frac{\partial C_m}{\partial \alpha}$
$C_{Z_q} = \frac{\partial C_Z}{\partial \frac{q\bar{c}}{2V_T}}$	$C_{X_q} = \frac{\partial C_X}{\partial \frac{q\bar{c}}{2V_T}}$	$C_{m_q} = \frac{\partial C_m}{\partial \frac{q\bar{c}}{2V_T}}$
$C_{Z_{\dot\alpha}} = \frac{\partial C_Z}{\partial \frac{\dot\alpha\bar{c}}{2V_T}}$	$C_{X_{\dot\alpha}} = \frac{\partial C_X}{\partial \frac{\dot\alpha\bar{c}}{2V_T}}$	$C_{m_{\dot\alpha}} = \frac{\partial C_m}{\partial \frac{\dot\alpha\bar{c}}{2V_T}}$
$C_{Z_{\dot q}} = \frac{\partial C_Z}{\partial \frac{\dot q\bar{c}^2}{4V_T}}$	$C_{X_{\dot q}} = \frac{\partial C_X}{\partial \frac{\dot q\bar{c}^2}{4V_T}}$	$C_{m_{\dot q}} = \frac{\partial C_m}{\partial \frac{\dot q\bar{c}^2}{4V_T}}$

Rolling moment	Yawing moment	Side force
$C_\ell = \frac{\mathcal{L}}{q_\infty Sb}$	$C_n = \frac{N}{q_\infty Sb}$	$C_Y = \frac{F_Y}{q_\infty S}$
$C_{\ell_p} = \frac{\partial C_\ell}{\partial \frac{pb}{2V_T}}$	$C_{n_p} = \frac{\partial C_n}{\partial \frac{pb}{2V_T}}$	$C_{Y_p} = \frac{\partial C_Y}{\partial \frac{pb}{2V_T}}$
$C_{\ell_r} = \frac{\partial C_\ell}{\partial \frac{rb}{2V_T}}$	$C_{n_r} = \frac{\partial C_n}{\partial \frac{rb}{2V_T}}$	$C_{Y_r} = \frac{\partial C_Y}{\partial \frac{rb}{2V_T}}$
$C_{\ell_\beta} = \frac{\partial C_n}{\partial \beta}$	$C_{n_\beta} = \frac{\partial C_r}{\partial \beta}$	$C_{Y_\beta} = \frac{\partial C_Y}{\partial \beta}$
$C_{\ell_{\dot\beta}} = \frac{\partial C_\ell}{\partial \frac{\dot\beta b}{2V_T}}$	$C_{n_{\dot\beta}} = \frac{\partial C_n}{\partial \frac{\dot\beta b}{2V_T}}$	$C_{Y_{\dot\beta}} = \frac{\partial C_Y}{\partial \frac{\dot\beta b}{2V_T}}$
$C_{\ell_{\dot p}} = \frac{\partial C_\ell}{\partial \frac{\dot p b^2}{4V_T}}$	$C_{n_{\dot p}} = \frac{\partial C_n}{\partial \frac{\dot p b^2}{4V_T}}$	$C_{Y_{\dot p}} = \frac{\partial C_Y}{\partial \frac{\dot p b^2}{4V_T}}$

SYMBOLS (CONT)

SYMBOL	DEFINITION	UNITS
DIMENSIONAL AERODYNAMIC DERIVATIVES DEFINED BY CHODY (REFERENCE (36))		
Y^*_β	$= \frac{1}{V_T}\{(Y_\beta + D_0)\cos\beta_0 + (D_\beta - Y_0)\sin\beta_0 + \{g\,[\cos\beta_0(\cos\alpha_0 \sin\theta_0 - \sin\alpha_0 \cos\theta_0 \cos\phi_0) - \sin\beta_0 \cos\theta_0 \sin\phi_0]\}$	1/sec
Y^*_p	$= \sin\alpha_0 + \frac{1}{V_T}(Y_p\cos\beta_0 + D_p\sin\beta_0)$	rad
Y^*_r	$= -\cos\alpha_0 + \frac{1}{V_T}(Y_r\cos\beta + D_r\sin\beta_0)$	rad
Y^*_ϕ	$= \frac{g}{V_T}[\cos\beta_0(\sin\alpha_0 \cos\theta_0 \sin\phi_0) + \cos\beta_0 \cos\theta_0 \cos\phi_0]$	1/sec
L^*_β	$= L'_\beta$	$1/sec^2$
$L^*_{\dot\beta}$	$= L'_{\dot\beta}$	1/sec
L^*_p	$= L'_p + (-R_0 I_{xy} + Q_0 I_{xy})/I_x$	1/sec
L^*_r	$= L'_r + (-P_0 I_{xy} + Q_0 (I_y - I_z) - 2R_0 I_{xz})/I_x$	1/sec
L_Ω	$= L^*_p \cos\alpha_0 + L^*_r \sin\alpha_0$	1/sec
N^*_β	$= N'_\beta$	$1/sec^2$
$N^*_{\dot\beta}$	$= N'_{\dot\beta}$	1/sec
N^*_p	$= N'_r + (R_0 I_{yz} + Q_0 (I_x - I_y) + 2P_0 I_{xy})/I_z$	1/sec
N^*_r	$= N'_r + (-Q_0 I_{xz} + P_0 I_{yz})/I_z$	1/sec
N^*_Ω	$= N'_p \cos\alpha_0 + N'_r \sin\alpha_0$	1/sec
ϕ^*_p	$= 1$	-
ϕ^*_r	$= \tan\theta_0 \cos\phi_0$	rad
ϕ^*_ϕ	$= \dot\theta_0 \tan\theta_0$	rad

SYMBOLS (CONT)

SYMBOL	DEFINITION	UNITS
	DIMENSIONAL AERODYNAMIC DERIVATIVES DEFINED BY CHODY (REFERENCE (36))	
	Note, if $L'_{\dot{\beta}}$ and $N'_{\dot{\beta}}$ are not "small" then,	
	$L'_r = L'_r + L'_{\dot{\beta}} \cos\alpha_0$	$1/sec$
	$L'_p = L'_p + L'_{\dot{\beta}} \sin\alpha_0$	$1/sec$
	$N'_p = N'_p + N'_{\dot{\beta}} \sin\alpha_0$	$1/sec$
	$N'_r = N'_r + N'_{\dot{\beta}} \cos\alpha_0$	$1/sec$
C_{ℓ_i}, C_{m_i}	Dimensionless body-axis (other than principal) roll and yaw moment coefficient	-
D	Aerodynamic Drag	lb
F	Force	lb
g	Gravitational acceleration constant, 32.174	ft/sec^2
h	Altitude	ft
i	State Variable, i.e., α, β, θ, etc	-
I	Identity Matrix	-
I_X, I_Y, I_Z	Body-axis moments of inertia	$slug\text{-}ft^2$
I_{XZ}	Body-axis Product of inertia	$slug\text{-}ft^2$
$j\omega$	Imaginary part of Laplace transform variable $s = \sigma + j\omega$	-
ℓ_{VT}	Distance from the aircraft c.g. to the X-coordinate of the vertical tail aerodynamic center.	ft
L	Aerodynamic Lift	lb

SYMBOLS (CONT)

SYMBOL	DEFINITION	UNITS
L_i, M_i, N_i	$(\partial(\mathcal{L}_i)/\partial i) \cdot (1/I_x)$ $(\partial(M_i)/\partial i) \cdot (1/I_y)$ $(\partial(N_i)/\partial i) \cdot (1/I_z)$	
	where $i = v$	$\frac{1}{ft - sec}$
	$i = \beta, \alpha$	$\frac{1}{sec^2 - rad}$
	$i = p, q, r, \dot{\alpha}, \dot{\beta},$	$\frac{1}{sec - rad}$
	$i = \delta_i$	$\frac{1}{sec^2 - rad}$
$\mathcal{L}'_i$	Total incremental change in rolling acceleration due to incremental change in state variable quantity, $= (\mathcal{L}_i + \frac{I_{xz}}{I_x} N_i)/(1 - \frac{I_{xz}^2}{I_x I_z})$	(as applicable)
m	Aircraft mass	slugs
M	Mach number	-
M	Pitching moment about aircraft body axis	ft-lb
N	Yawing moment about aircraft body axis	ft-lb
N'_i	Total incremental change in yawing acceleration due to incremental change in state variable quantity, $= (N_i + \frac{I_{xz}}{I_z} L_i)/(1 - \frac{I_{xz}^2}{I_x I_z})$	(as applicable)
N_j^i	Aircraft transfer function numerator relating output, i, to control deflection, j, (i = p, q, r, etc; j = δ_a, δ_e, δ_r)	
p	Perturbed roll angular velocity about the X-body axis	rad/sec
P	Total roll rate about the X-body axis, $P = P_0 + p$	rad/sec
q	Perturbed pitch angular velocity about the y-body axis	rad/sec
Q	Total pitch rate about the y-body axis, $Q = Q_0 + q$	rad/sec
$\bar{q}$	Dynamic pressure, $\frac{1}{2}\rho V_T^2$	$\frac{lb}{ft^2}$

SYMBOLS (CONT)

SYMBOL	DEFINITION	UNITS
r	Perturbed, yaw angular velocity about the y-body axis	rad/sec
R	Total yaw rate about the z-body axis, $R = R_0 + r$	rad/sec
s	Laplace operator ($s = \sigma \pm j\omega$)	-
S	Aircraft wing area	ft^2
t	Time	sec
T	Thrust	lb
T_R	First order time constant of the roll subsidence mode	sec
T_s	First order time constant of the spiral mode	sec
T_{θ_1}, T_{θ_2}	First order time, constants of the conventional low and high frequency zeros of the pitch attitude numerator	sec
T_{θ_3}	First order time constant of the pitch altitude numerator which results from unsymmetrical flight	sec
T_{ϕ_1}, T_{ϕ_2}	First order time constants of the overdamped roll attitude numerator	sec
U	Control vector	-
u	Control perturbation vector	-
u	Perturbed linear velocity component along the x-axis	$\frac{ft}{sec}$
U	Total linear velocity along the (X body axis), $U = U_0 + u$	$\frac{ft}{sec}$
v	Perturbed linear velocity component along the (Y body axis)	
V	Total linear velocity along the (Y body axis), $V = V_0 + v$	$\frac{ft}{sec}$
V_T	Total linear velocity, $\sqrt{U^2 + V^2 + W^2}$	$\frac{ft}{sec}$
w	Perturbed linear velocity component along the (Z body axis)	$\frac{ft}{sec}$
W	Total linear velocity along the (Z body axis), $W = W_0 + w$	$\frac{ft}{sec}$
W	Weight	lb
X	State vector	-

SYMBOLS (CONT)

SYMBOL	DEFINITION	UNITS
x	State perturbation vector	-
X, Y, Z	Aerodynamic forces along the OXYZ body-axis system	lb
X_i, Y_i, Z_i	$[\partial(\ ) / \partial i]/m$ where i = u, v, w,	$\frac{1}{sec}$
	where i = p, q, r, $\dot{\alpha}$, β	$\frac{ft}{sec - rad}$
	where i = δ_j	$\frac{ft}{sec^2 - rad}$

GREEK	DEFINITION	UNITS
α	Angle of attack, $\tan^{-1} \frac{W}{V_T}$	deg
β	Sideslip angle, $\sin^{-1} \frac{V}{V_T}$	deg
γ	Flight path angle	deg
μ	Roll angle about the velocity vector	deg
ρ	Mass density	$\frac{slugs}{ft^3}$
Γ	Wing geometric dihedral angle	deg
δ_i	Surface deflection with subscript	deg
Δ	Transfer function denominator	-
ζ_i	Damping ratio with subscript	-
λ	Eigenvalue	-
ϕ, θ, ψ	Conventional perturbed Euler angles (roll, pitch, yaw)	deg
ϕ, θ, ψ	Conventional Euler angles between inertial axis and aircraft body axis (roll, pitch, yaw)	deg
σ	Real part of Laplace transform variable, $s = \sigma \pm j\omega$	rad/sec
$\omega_{(\ )}$	Natural frequency of the denominator or numerator root with subscript	rad/sec
ω_B^A	Rotational rate vector of reference frame A with respect to reference frame B coordinates	rad/sec
$\Lambda_{c/4}$	Sweepback angle at the quarter chord	deg

SYMBOLS (CONT)

MATHEMATICAL	DEFINITION
$\underline{\Lambda}$	Square diagonal Matrix whose diagonal elements are distinct eigenvalues
$\triangleq$	define
$(\dot{})$	derivative with respect to time, d/dt
∞	infinity (without bound)
∂	Partial derivative
$<$	less than
$>$	greater than
$\|\ \|$	norm
$(\vec{})$	Denotes Vector quantity
$(\bar{})$	Matrix Column Vector
[ ]	Square Matrix
T	Matrix Transpose
	Transfer functions are presented using the following shorthand notation,
	$(s + a) \triangleq (a)$, where $a = 1/\tau$
	$\left[s^2 + \zeta\omega_n s + \omega_n^2\right] \triangleq [\zeta, \omega_n]$

SYMBOLS (CONT)

Subscripts	Description
a	Aileron
APP	Apparent
B	Body axes
COP	Coupled stability axis system (of Kalviste.)
DR	Dutch-roll
DYN	Dynamic stability axis system of Kalviste
e	Elevator
I	Inertial axes
L	Left
ℓ	Aerodynamic moment about the x-axis
m	Aerodynamic moment about the y-axis
n	Aerodynamic moment about the z-axis
o	Reference or nominal value
p	Phugoid
r	Rudder
R	Right, Roll mode
s	Stability, Spiral mode
SP	Short period
SR	Coupled spiral-roll subsidence (lateral phugoid)
VT	Vertical Tail

SYMBOLS (CONT)

ACRONYMS	DEFINITION
ARI	Aileron-Rudder Interconnect
BVR	Beyond Visual Range
CIC	Close-In-Combat
DOF	Degree-of-Freedom
OOC	Out-of-Control
STI	Systems Technology Inc.
WVR	Within Visual Range

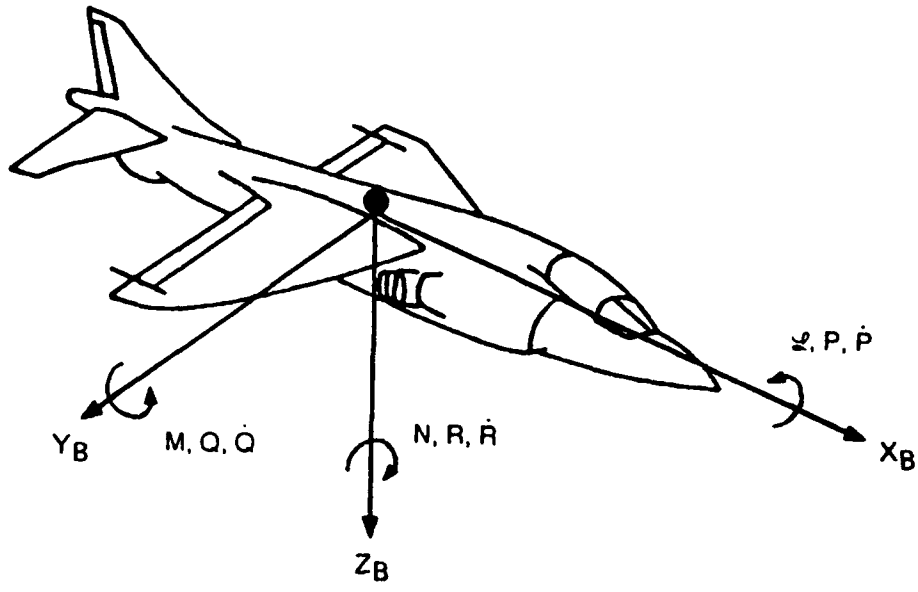

THE BODY AXIS SYSTEM IS DEFINED BY THE FOLLOWING:

X_B longitudinal body axis in the plane of symmetry of the aircraft, positive forward;

Y_B lateral body axis perpendicular to the plane of symmetry of the aircraft, usually taken in the plane of the wings, positive toward the right wing tip;

Z_B vertical body axis in the plane of symmetry of the aircraft, perpendicular to the longitudinal and lateral axes, positive down.

Figure I(a) Definition of Body Axis System (Reference (1))

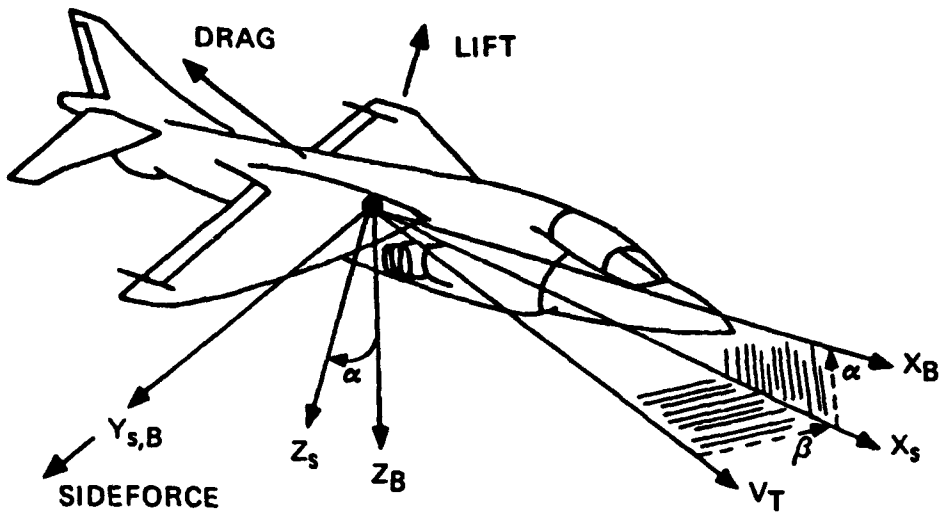

(B) Stability Axis

THE STABILITY AXIS SYSTEM IS DEFINED BY THE FOLLOWING:

X_s longitudinal stability axis, parallel to the projection of the total velocity (V_T) on the plane of symmetry of the aircraft, positive forward;

Y_s lateral stability axis, coincident with and positive in the same direction as the lateral body axis;

Z_s vertical stability axis in the plane of symmetry of the aircraft, perpendicular to the longitudinal and lateral axes, positive down.

Figure i(b) Definition of Stability Axis System (Reference (1))

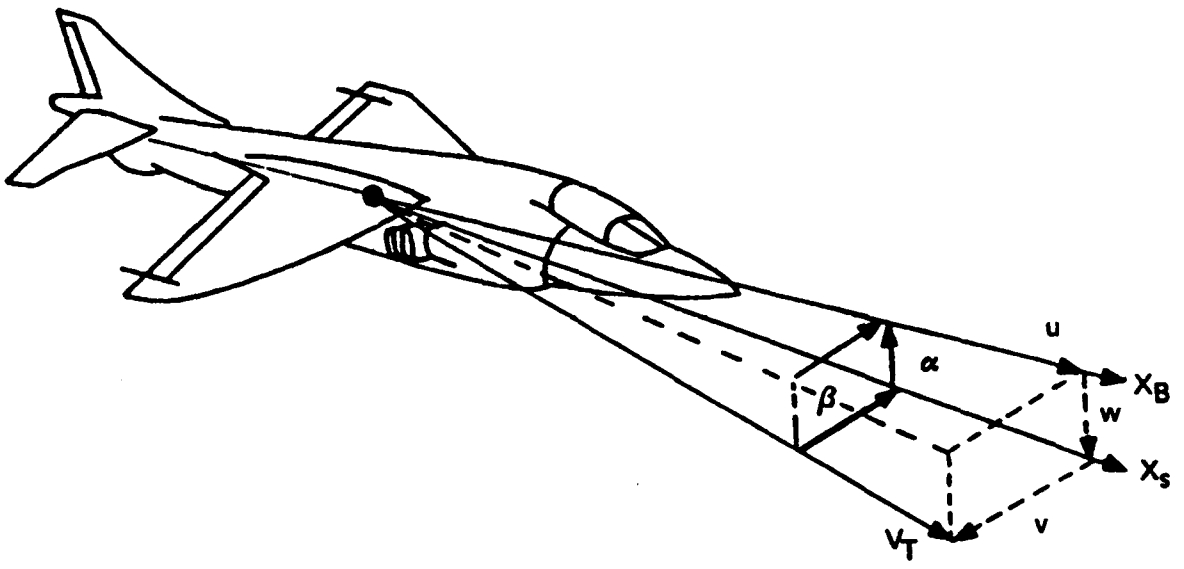

AERODYNAMIC ANGLES

α pitch angle of attack, angle between the X_S-axis and the X_B-axis, positive rotates the +Z-axis into the +X-axis:

$\alpha = \tan^{-1}(W/U)$, $-180^\circ \leq \alpha \leq 180^\circ$;

β angle of sideslip, angle between the total velocity (V_T) and its projection on the XZ-plane, positive rotates the $+Y_S$-axis into the $+X_S$-axis: $\beta = \sin^{-1}(V/V_T)$, $-90^\circ \leq \beta \leq 90^\circ$;

Figure ii Aerodynamic Angles (Reference(1))

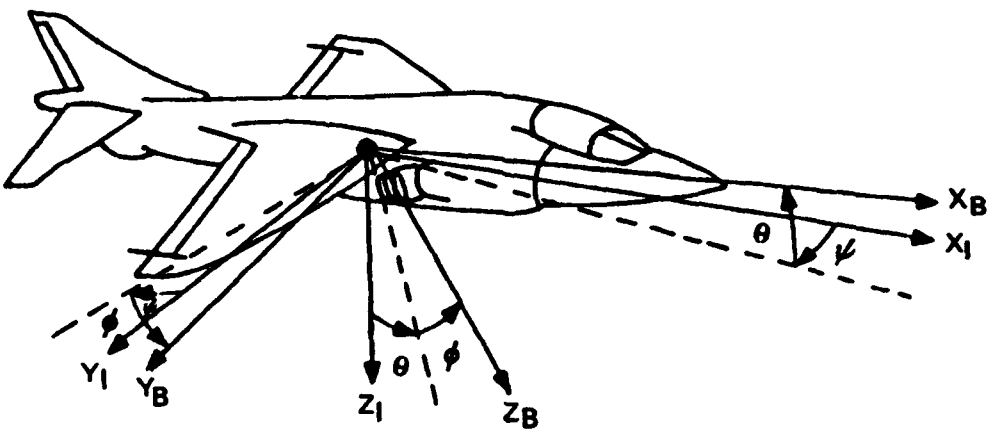

NOTE: Z_i IS COINCIDENT WITH THE LOCAL GRAVITY VECTOR.

ORIENTATION ANGLES:

yaw angle, positive clockwise about the +Z-axis direction;

pitch angle, positive clockwise about the +Y-axis direction;

roll angle, positive clockwise about the +X-axis direction;

ψ, θ, and ϕ form a system of three angles which uniquely defines the orientations of the Body Axes with respect to an inertial reference set of axes. Any orientation of the Body Axis System is obtained (uniquely) by rotationally displacing it from the reference system through each of the three angles in turn. The order of rotation is important and is defined to be yaw-pitch-roll.

Figure iii Earth-Body Orientation (Euler) Angles (Reference(1))

INTRODUCTION

BACKGROUND

Out-of-Control[1] (OOC) flight is not new to the Navy fleet. Aircraft departure[1] (from controlled flight) and OOC accidents have plagued aviation from it's infancy. The importance of being able to confidently predict when an aircraft has the potential to depart controlled flight is vividly illustrated using the F-14 as an example. From 1973 through 1987, thirty F-14 aircraft have been lost due to OOC accidents. This equates to one- third of all F-14 accidents. Not only is aircraft departure resistance an important safety issue, but it is also paramount in maintaining mission effectiveness in today's close-in-combat (CIC) environment. The CIC environment today, and in the near future, is projected to be characterized by: (1) short duration maneuvering, i.e., time compression, (2) an increase in importance placed on the transition between beyond-visual-range (BVR) and within-visual-range (WVR) maneuvering and (3) expansion of the combat arena into the low-speed post-stall flight envelope regime. These three characteristics require harder maneuvering and improved agility for today's and future aircraft. Improved agility over today's current fighters will result in aircraft capable of higher turn rates, increased acceleration and deceleration capability and probably, most importantly, skew maneuvering capability involving nose pointing at the expense of energy conservation. To make these improvements in maneuvering possible requires that the aircraft possess some degree of departure resistance. Understanding, predicting and designing for departure resistant aircraft (without sacrificing desired levels of maneuverability) has spurred the development of many aircraft departure susceptibility criteria and guidelines that originate with the development of the basic directional weathercock stability derivative, C_{n_β}. This report will expand on each of the major departure susceptibility criteria, and highlight each of their applications and limitations. A more detailed aircraft departure susceptible analysis approach is recommended to assess the effects of asymmetric flight and maneuvering dynamics.

---

1 See Appendix A, "Glossary Of Defined Terms"

OBJECTIVE

The primary objective of the study reported herein is to provide guidelines for the analytical determination of aircraft departure susceptibility applicable to the designs of future fighter aircraft.

SCOPE

This report entails a brief review of the derivation, application and implied limitations of the aircraft departure susceptibility criteria presented in the MIL-STD-1797A Flying Qualities specification (Reference (2)). To begin the discussion, the rigid body six degree-of-freedom equations-of-motion and aircraft stability concepts are reviewed, focusing on their application to determine the susceptibility of an aircraft to depart from controlled flight. Finally, a methodology is suggested that allows a designer to determine the departure susceptibility of an aircraft configuration through the course of its design (up to and including flight test) with increasing levels of accuracy as the design progresses.

METHODOLOGY

In providing guidelines for the analytical determination of aircraft departure susceptibility, the intent was not to endorse one criteria over another, or to rehash what MIL-STD-1797A recommends or even to propose a "new and improved" criteria. Rather an attempt is made to point out the departure susceptibility prediction techniques which are appropriate at various stages of the design phase as a function of the required accuracy. As pointed out in Reference (3), consistent simple prediction techniques are important early in the design phase to establish the configuration and make trade studies between performance and departure resistance. Later in the development cycle, increased accuracy is required to avoid costly configuration changes and reduce risk during flight test.

There are four primary contributors of aircraft departure from controlled flight. They are: (1) high angle-of-attack bare airframe aerodynamic flight characteristics, (2) use of aerodynamic flight controls (i.e., pilot in the loop), (3) inertial coupling and (4) kinematic coupling (see Figure 1). The influence of each of these factors

I **Aircraft Bare Airframe High-AOA Aerodynamic Flight Characteristics**

- Nonlinear with respect to angle-of-attack and sideslip
- Flow breakdown and Adverse Vortex Shedding Effects Common

Associated Causes of Departure

1. Aircraft unstable directionally with stable dihedral effect (or vice versa); Aircraft may depart but is not likely to be divergent

2. Aircraft is unstable directionally and has unstable dihedral effect divergent departure likely

II **Use of Aerodynamic Flight Controls**

- Aileron and rudder effectiveness greatly reduced

Associated Causes of Departure

1. Use of aileron may aggravate situation due to adverse yaw generated at high angle-of-attack becoming the dominant control effect.

2. Use of prolonged or misapplication (cross-controlling) of control inputs at high angle-of-attack could induce departure.

III **Inertial Coupling**

- Moments generated due to inertial coupling becoming more pronounced at large angles-of-attack.

Associated Cause of Departure

1. Increase in inertial coupling effect at large angle-of-attack likely to place the aircraft in a flight condition more susceptible to departure.

IV **Kinematic Coupling**

- Sideslip angle (angle-of-attack) generated due to kinematic coupling can become more pronounced with increasing angle-of-attack (sideslip).

Associated Cause of Departure

1. From a departure susceptibility viewpoint any generation of large amount of sideslip (or angle-of-attack) is undesirable because it has the potential to place the aircraft in a flight condition that is more susceptible to departure.

Figure 1 Primary Causes of Aircraft Departure from Controlled Flight (Reference (4))

as they contribute to the susceptibility of an aircraft to depart controlled flight has been investigated by many researchers to date. In addition, Kalviste has recently addressed each of the major departure causing elements with the exception of closed-loop pilot/flight control effects in a single methodology (See reference (5)).

RESULTS AND DISCUSSION

General

To achieve the accuracy at which to predict/analyze aircraft stability parameters and flying qualities at high angles-of-attack depends chiefly on the ability to formulate a "valid" aerodynamic mathematical model. This then assumes that the desired quantities (i.e., C_{l_β}, C_{l_q}, etc) can either be accurately measured in a wind tunnel or be calculated analytically with a good confidence level.

Of particular interest to the flight dynamicist's in terms of predicting an aircraft's tendency to depart from controlled flight are those flow phenomena that significantly vary with angle-of-attack and that can cause asymmetric effects even when the aircraft maintains a zero sideslip attitude. Two of the most important phenomena of this kind are (1) the formation and asymmetric shedding of forebody vortices and (2) the formation and asymmetric bursting of wing leading-edge vortices. These phenomena become even more complex if an oscillatory motion is superimposed on the primary steady flight trajectory (Reference (6)). These high angle-of-attack flow phenomena have large effects on all of the aerodynamic characteristics of the aircraft including, of course, the static and dynamic stability parameters. The most important of these effects on the dynamic stability parameters are (1) large nonlinear variations of stability parameters with angle-of-attack, angle-of-sideslip and rate of coning as well as with amplitude and frequency of oscillation, (2) significant aerodynamic cross-coupling between longitudinal and lateral degrees of freedom (i.e., C_{m_β}, C_{n_α}), (3) time-dependent and hysteresis effects and (4) strong

configuration dependence. Reference (6) discusses each of these four effects in great length, but for the purposes of this report, the focus will be on the impact each of these four elements have on the methodology required to accurately predict aircraft departure susceptibility.

To illustrate both the magnitude and the suddenness of the nonlinear variations in dynamic derivatives with angle-of-attack, the yaw and roll damping derivatives for the X-31A aircraft are presented in Figure 2. The yaw damping derivative (Figure 2a) exhibits a very sudden and very large (twice the low-α value and the sign reversed) unstable peak at an angle-of- attack of 40 degrees while the roll damping derivative (Figure 2b) exhibits an equally large and sudden variation (again about twice the low-α value and the sign reversed) with angle-of-attack such that it is undamped over the 28 to 50 degree AOA range. Work done at NASA Langley (References (8) and (9)) suggest that the primary mechanism for these effects is associated with the flow phenomena emanating from the aircraft's forebody. The studies showed the peak instabilities to be largely independent of the wing sweep angle and the presence of vertical tails.

In addition to dynamic derivatives exhibiting large nonlinear variations with angle-of-attack, they have also been shown to exhibit significant nonlinear variations with the frequency and amplitude of oscillation. This variation takes place, for the most part, where the derivatives change suddenly with angle-of-attack. An example of the variation of the roll damping derivative with oscillation amplitude is shown in Figure 3 for a fighter configuration at low subsonic speed (Reference (10)). The large unstable peak that occurs at an angle-of-attack of 35 degrees when the amplitude of oscillation is ± 5 degrees decreases at larger amplitudes and completely disappears at an amplitude of ± 20 degrees. With the knowledge of these frequency and amplitude effects, NASA Langley presented the forced oscillation test data of the X-31A aircraft with an envelope that encompassed the variability of the data due to the amplitude and frequency variations during the forced oscillation testing. Note that these are not "bands of uncertainty" but envelopes due to actual data taken.

Figure 4 illustrates the range of data for the yaw and roll damping derivatives for the X-31A aircraft.

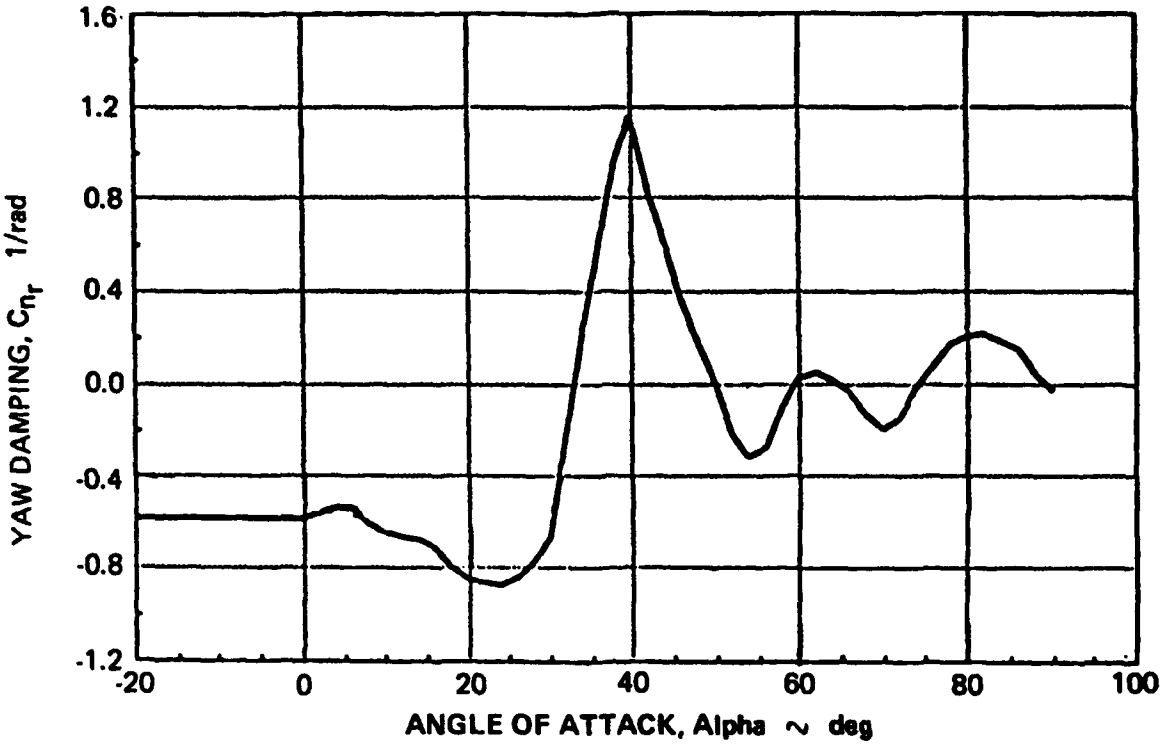

Figure 2a Yaw Damping Derivative Versus Angle-of-Attack for the X-31A Aircraft (Reference (7))

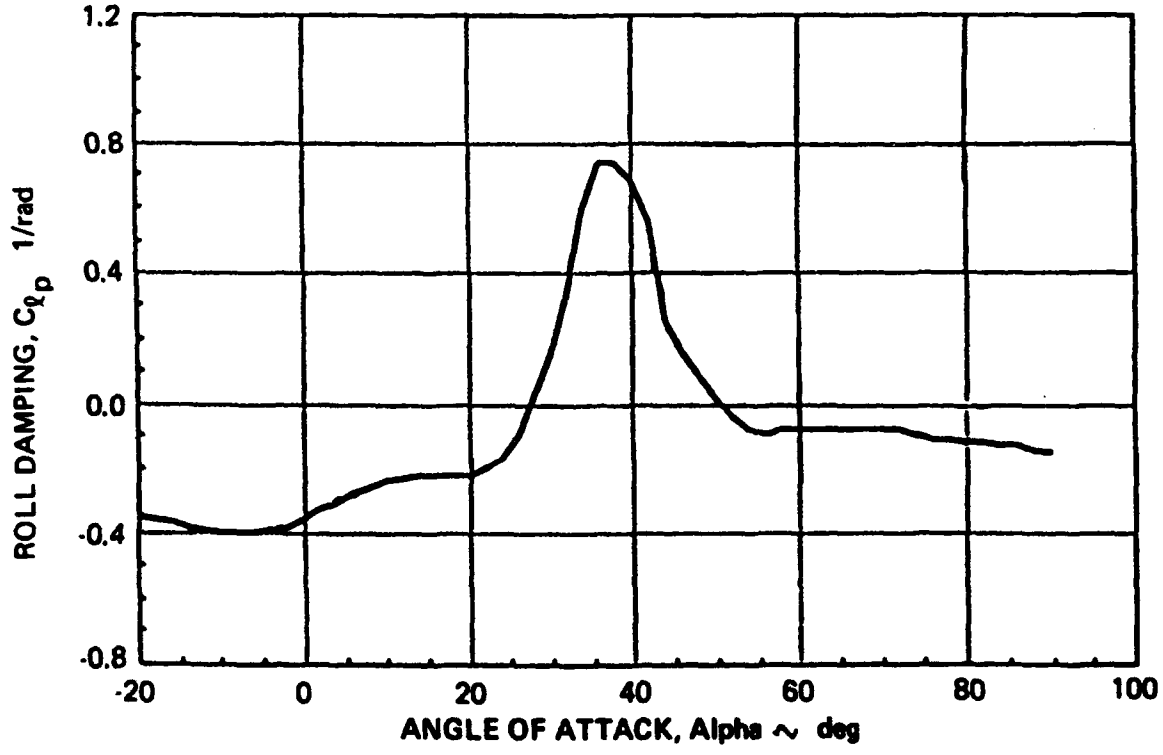

Figure 2b Roll Damping Derivative Versus Angle-of-Attack for the X-31A Aircraft (Reference (7))

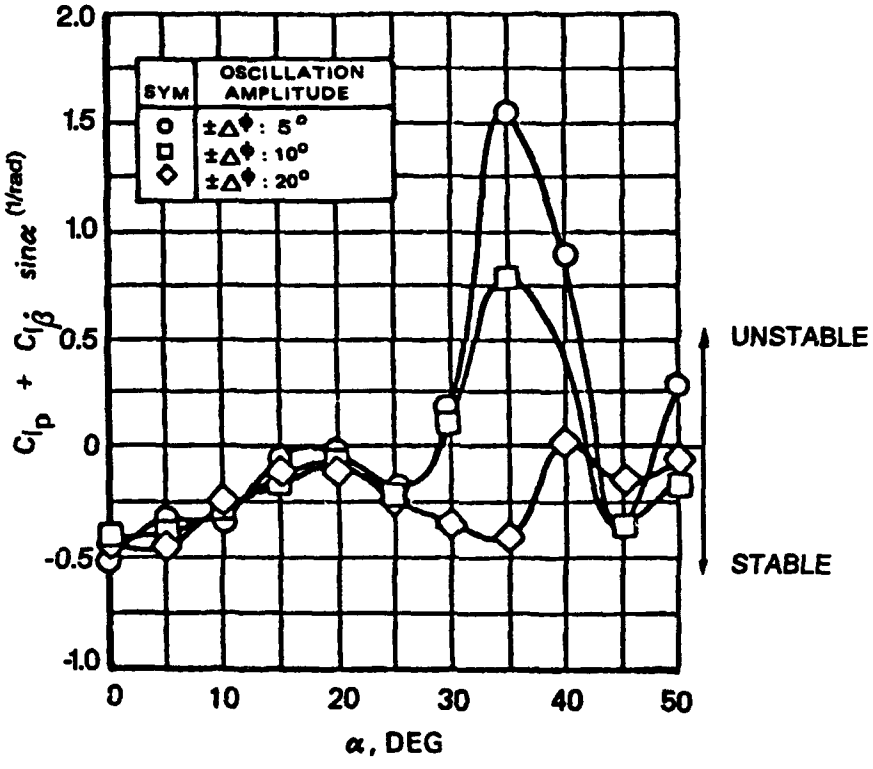

Figure 3 Effect of Oscillation Amplitude on Damping in Roll (Reference (10))

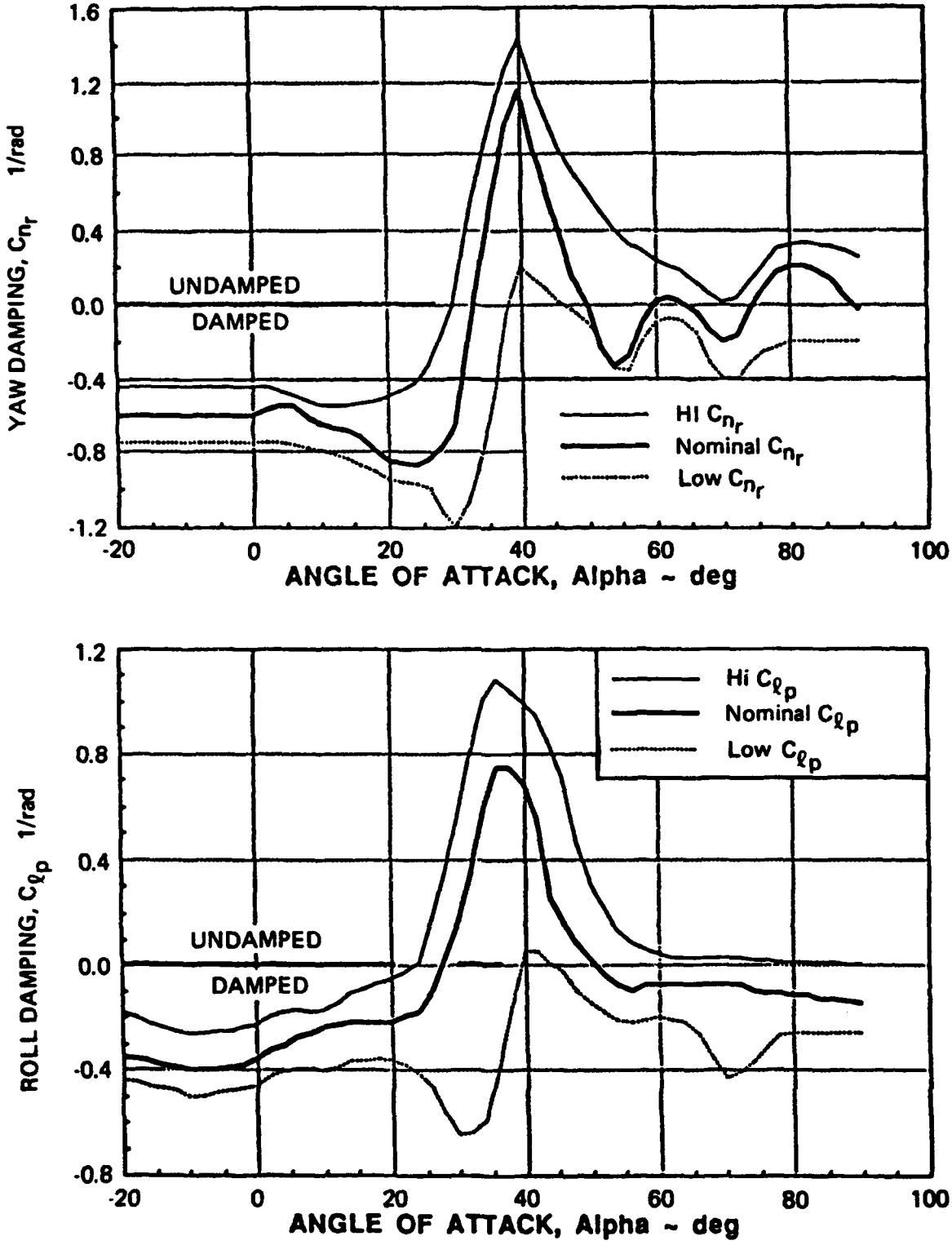

Figure 4 Range of Data for the Yaw and Roll Damping Derivatives of the X-31A Aircraft (Reference (7))

Additionally, the nominal and range of data of the cross-coupling dynamic derivatives, C_{n_p} and C_{l_r}, as a function of angle-of-attack, are shown in Figures 5 and 6 respectively.

In cases where the amplitude and frequency of oscillation effects are significant, the derivative concept becomes, at best, a "good" guess of the dependence of aerodynamic damping with angle-of-attack.

Aerodynamic Cross Coupling

The introduction of cross-coupling derivatives requires simultaneous consideration of the complete six degrees-of-freedom equations of motion of an aircraft, rather than the decoupled sets of equations for the longitudinal and lateral/directional degrees-of-freedom. The phenomena of aerodynamic cross-coupling can occur at high angles-of-attack when, 1) lateral aerodynamic reactions (such as caused by the lateral motions of the forebody vortices) may occur on an aircraft as a result of some longitudinal motion such as pitching or vertical translation or 2) longitudinal aerodynamic reactions (such as those caused by the longitudinal motion of the vortex burst locations) may occur on an aircraft as a result of some lateral motion such as rolling, yawing or lateral translation. Static cross-coupling data for an early version of the X-31A aircraft is presented in Figure 7. Figure 7a illustrates the pitching moment as a function of angle-of-attack and sideslip angle, while Figure 7b illustrates the yawing moment coefficient as a function of angle-of-attack and sideslip angle. For this version of the X-31A aircraft, it is apparent that aircraft aerodynamic pitching moment is a strong function of sideslip angle above -15 degrees (i.e., C_{m_β}). Likewise the aircraft aerodynamic yawing moment is a strong function of angle-of-attack (i.e., C_{n_α}). This aerodynamic cross-coupling phenomena is important and must be modelled to correctly analyze aircraft stability characteristics at high angles-of-attack. For further discussion on aerodynamic cross-coupling see reference (12). In reference (13) an analysis was conducted to determine the influence of the M_β term on the aircraft dynamics of the F-4 aircraft. This was done by calculating the θ/δ_e, ϕ/δ_a and r/δ_r transfer functions from the six degree-of-freedom coupled ($\beta \neq 0$) equations-of-motion. For this particular case (F-4 Aircraft; $\alpha_0 = 20^o$; $\beta_o = 1^0$), M_β principally affects the lateral and longitudinal short-period modes with a resultant increase in short period damping (ζ_{SP}) and

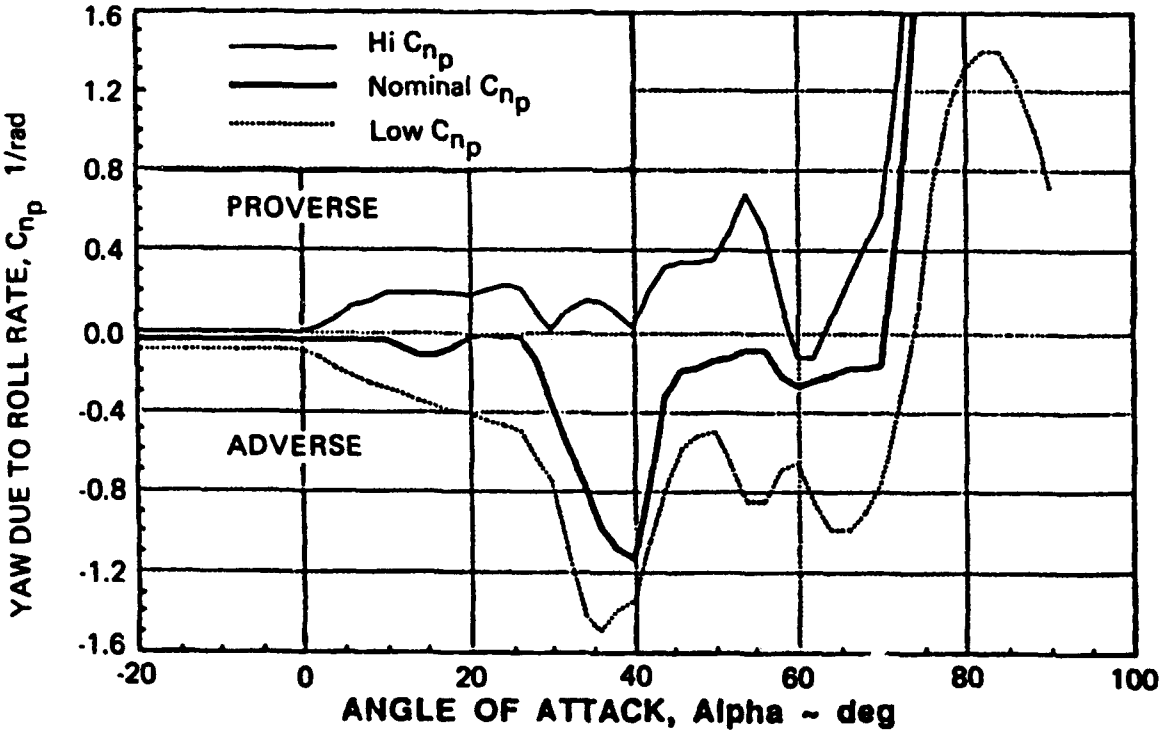

Figure 5 Yawing Moment Coefficient Due to Roll Rate for the X-31A Aircraft (Nominal and Range of Data) (Reference (7))

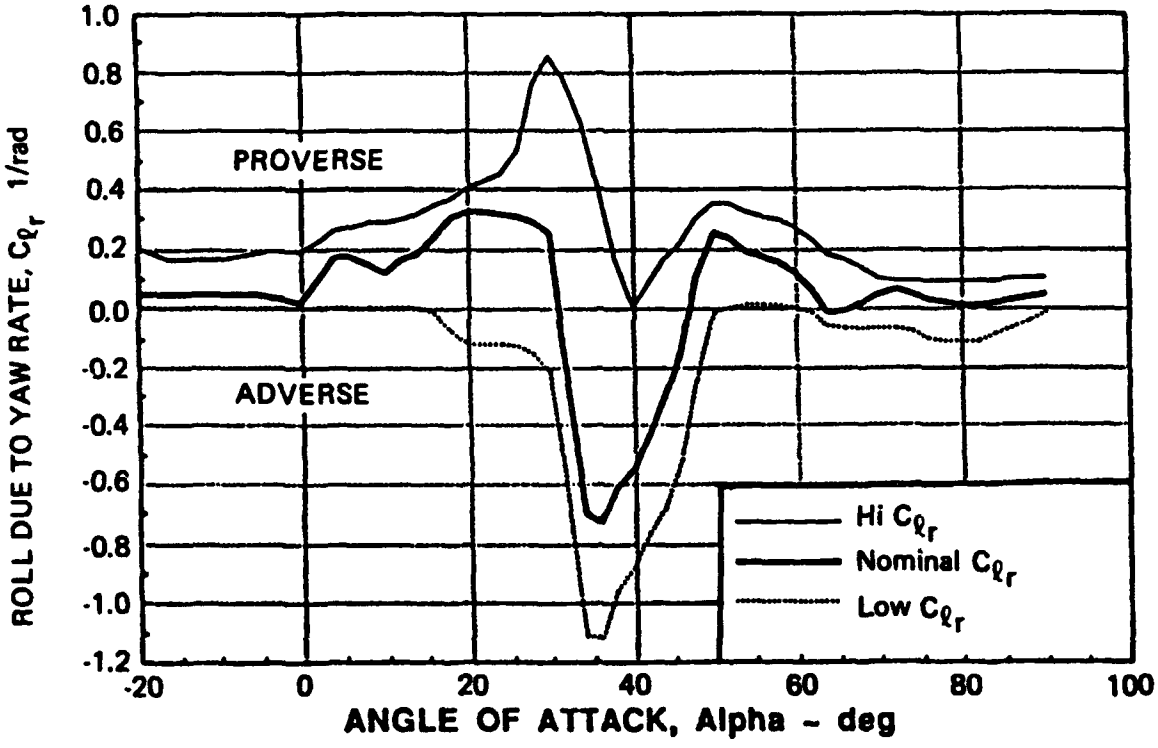

Figure 6 Rolling Moment Coefficient Due to Yaw Roll Rate for the X-31A Aircraft (Nominal and Range of Data) (Reference (7))

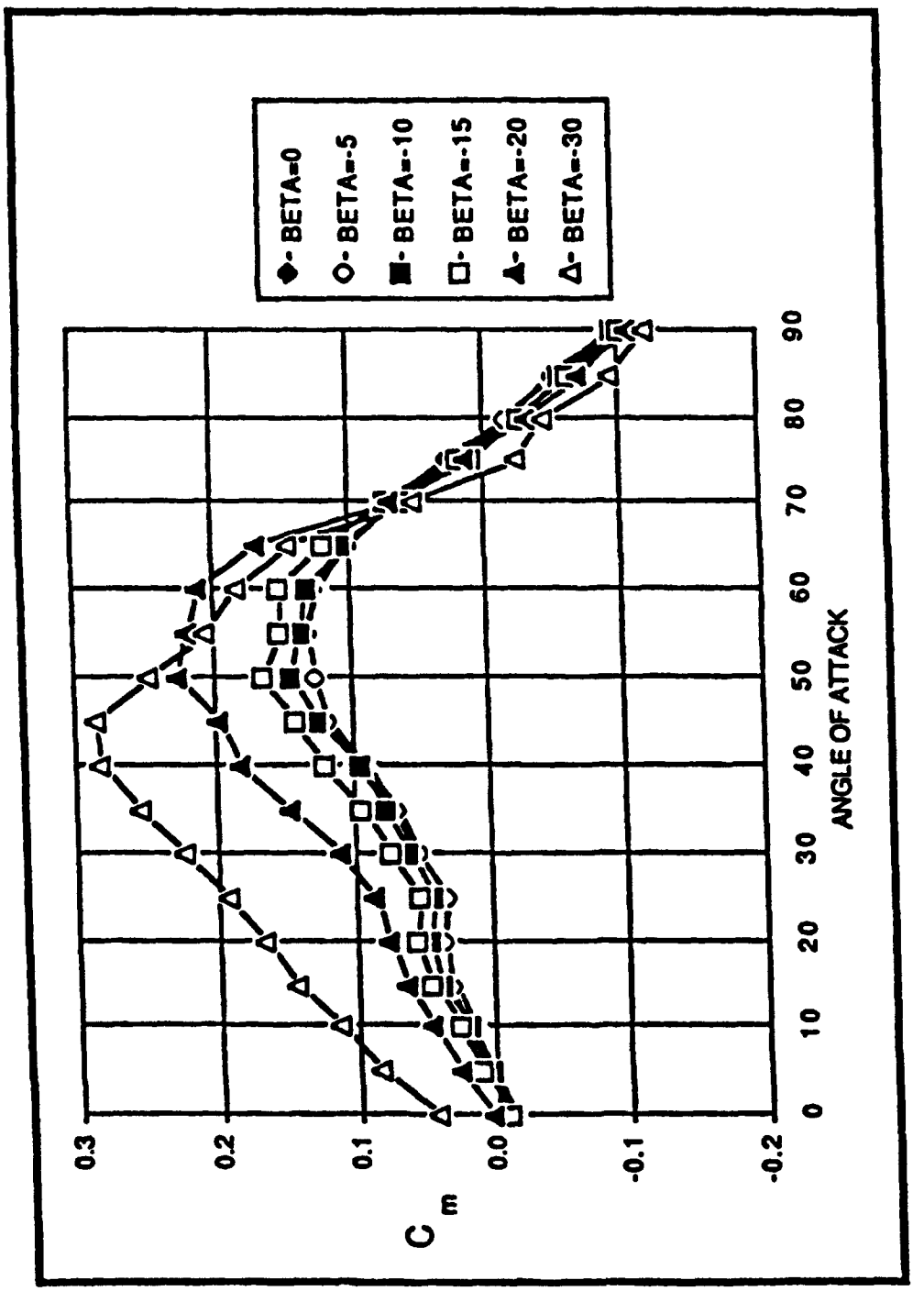

a. Influence of Sideslip on the Pitching Moment Coefficient

Figure 7 Static Aerodynamic Cross-Coupling Data for the Preliminary Configuration of the X-31 Aircraft (Reference (11))

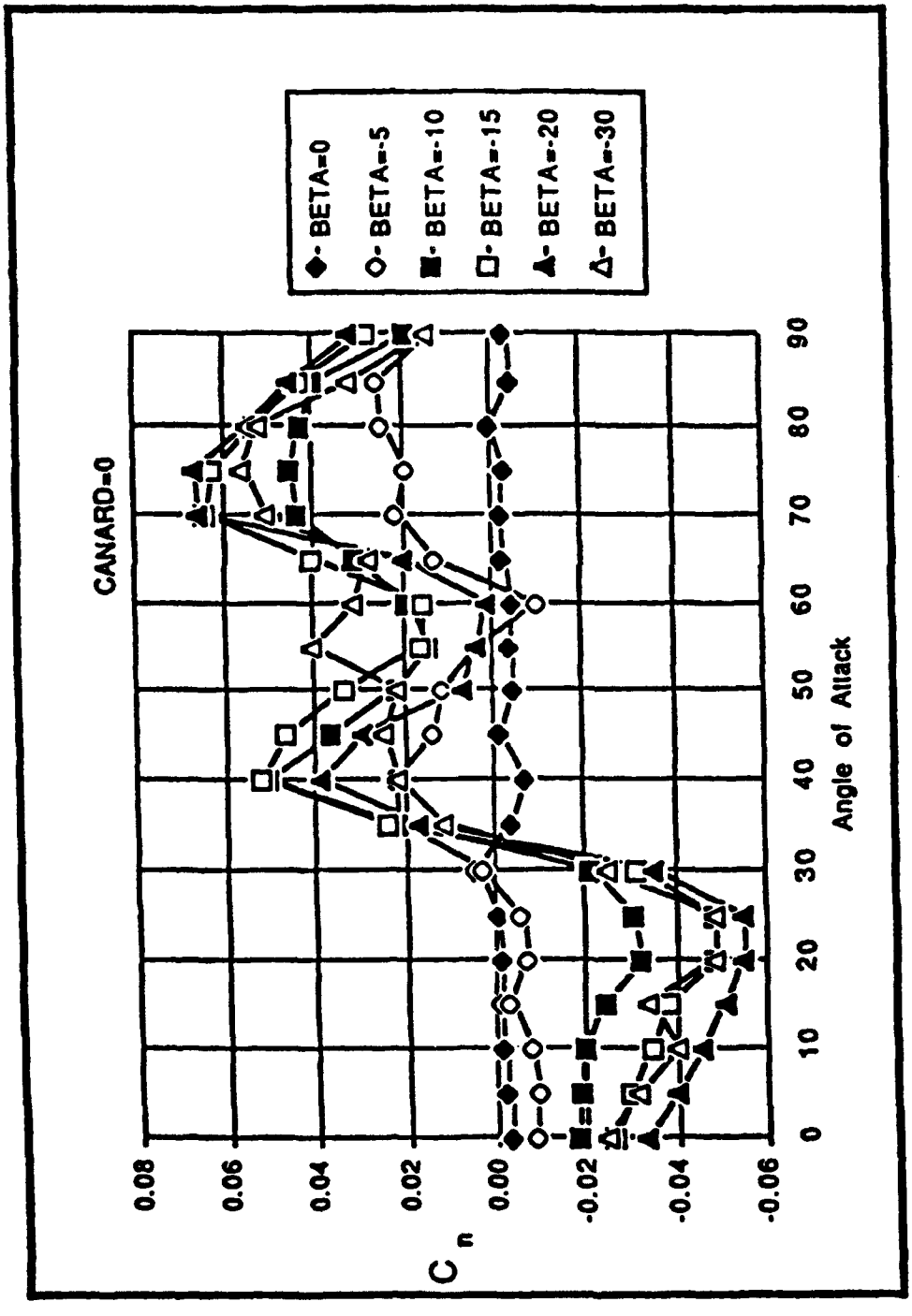

b. Influence of Angle-of Attack on the Yawing Moment Coefficient.

Figure 7 (Concluded) Static Aerodynamic Cross-Coupling Data for the Preliminary Configuration of the X-31 Aircraft (Reference (11))

a decrease in Dutch-roll damping (ζ_{DR}) (see Figure 8). Further it appears that with $M_{\dot{\beta}} = -1.63$, closure of any or all of the three loops shown in Figure 8 could easily result in an unstable Dutch-roll mode, (Reference (13)). For $M_{\dot{\beta}}$ positive, the migration of the longitudinal short-period and Dutch-roll modes due to the influence of $M_{\dot{\beta}}$ is reversed from that shown in figure 8. That is the longitudinal short-period moves toward the right (unstable) while the Dutch-roll moves to the left.

The concept of aerodynamic cross-coupling (C_{ℓ_q}, C_{m_r}) with respect to dynamic derivatives has only recently been introduced (See Reference (14)). But on the basis of sensitivity studies as described in references (15) and (16), it has been shown that the inclusion in the equations of motion of the dynamic cross-coupling derivative C_{ℓ_q} can cause instabilities in the Dutch-roll and roll subsidence modes of motion. As with any second order effect, it must be kept in mind that the effect of the cross-coupling derivatives is quite dependent on the remaining stability characteristics of the aircraft. The smaller the static margin and the lower the aerodynamic damping, such as represented by C_{ℓ_p}, $C_{\ell_{\dot{\beta}}}$, C_{n_r}, $C_{n_{\dot{\beta}}}$ derivatives, the more sensitive the aircraft motion will be to variations in cross-coupling derivatives and vice versa.

Time-Dependent Effects

In addition to modelling quasi-steady effects such as represented by dynamic derivatives due to angular velocities (C_{ℓ_p}, C_{n_r}, C_{n_p} etc.), the existence and importance of modelling the purely unsteady effects (as represented by derivatives due to the time rate of change of angular deflections, $C_{\ell_{\dot{\beta}}}$, $C_{n_{\dot{\alpha}}}$, etc) at high angles-of-attack is documented in references (17) and (18). The translational derivatives as they are often referred to, constitute part of the dynamic results obtained with standard wind-tunnel techniques of oscillating a model around a fixed-axis. These tests always gives composite derivatives expressed as ($C_{n_r} - C_{n_{\dot{\beta}}} \cos\alpha$) and the like (see Table I). Common practice when formulating this data into the standard Taylor series expansion of the aerodynamic forces and moments is to ignore the $\dot{\alpha}$ and $\dot{\beta}$ effects (or to introduce a simple correction for them) and to use the composite derivatives in place of the purely rotary ones. At low angles-of-attack the errors introduced by this formulation is often small and the simplification is large enough to make it justifiable. At higher angles of attack, however, the $\dot{\alpha}$ and $\dot{\beta}$ effects can become quite substantial

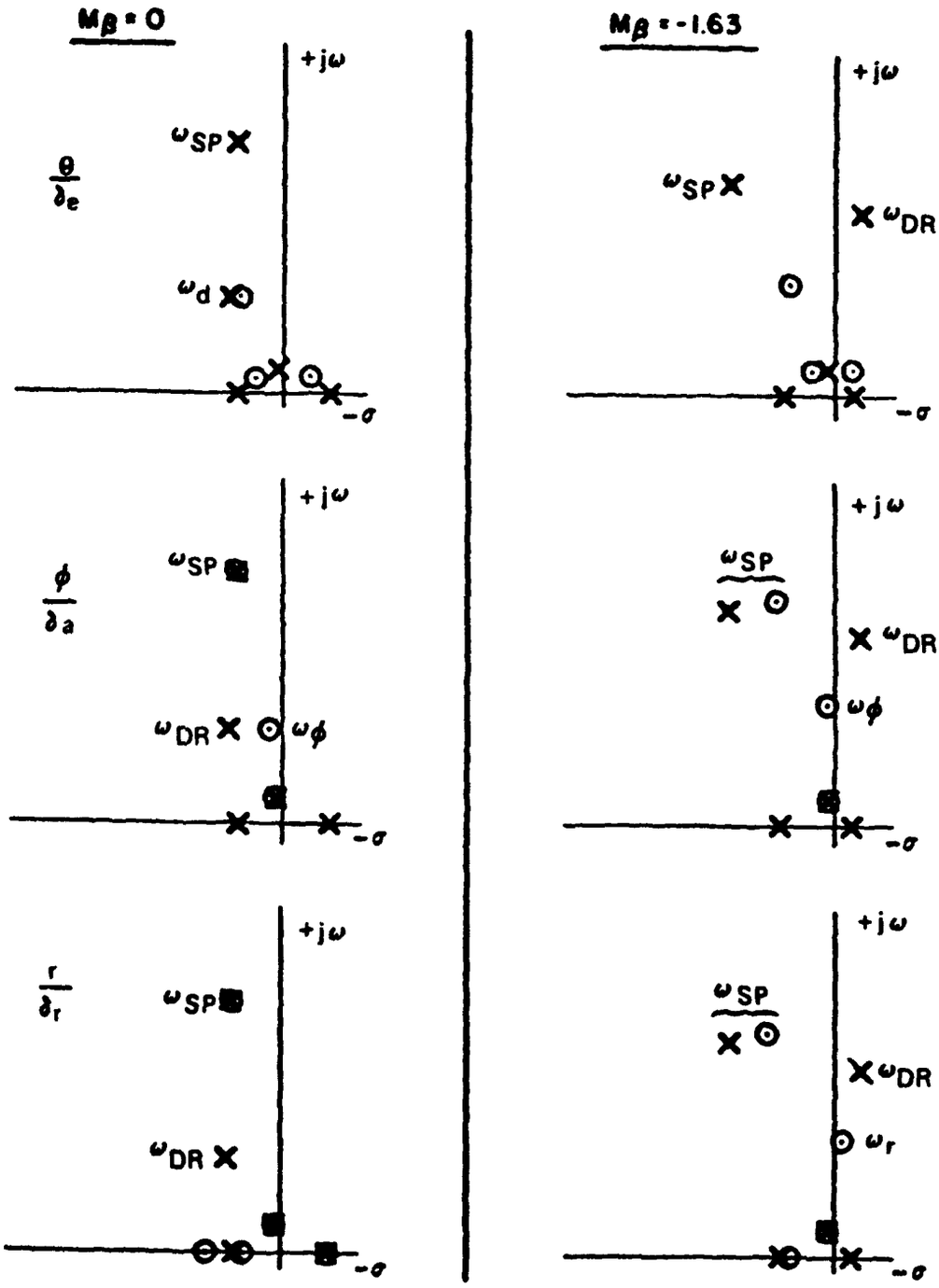

Figure 8 The Effect of the Static Cross-Coupling Derivative M_β on the Pole-Zero Locations for the F-4 Aircraft ($\alpha_0 = 20°$; $\beta_0 = 1°$) (Reference (13))

Table I Dynamic Moment Derivatives (Reference (6))

Pure rotation			Translational acceleration			Oscillation around fixed axis		
						Damping derivatives	Cross derivatives	Cross-coupling derivatives
$C_{l_p} = \frac{\partial C_l}{\partial \frac{pb}{2V_T}}$	$C_{m_p} = \frac{\partial C_m}{\partial \frac{pb}{2V_T}}$	$C_{n_p} = \frac{\partial C_n}{\partial \frac{pb}{2V_T}}$	$C_{l_{\dot{\alpha}}} = \frac{\partial C_l}{\partial \frac{\dot{\alpha}\bar{c}}{2V_T}}$	$C_{m_{\dot{\alpha}}} = \frac{\partial C_m}{\partial \frac{\dot{\alpha}\bar{c}}{2V_T}}$	$C_{n_{\dot{\alpha}}} = \frac{\partial C_n}{\partial \frac{\dot{\alpha}\bar{c}}{2V_T}}$	$C_{lp} + C_{l_q}\sin\alpha$	$C_{l_r} - C_{l_q}\cos\alpha$	$C_{l_q} + C_{l_{\dot{\alpha}}}$
$C_{l_q} = \frac{\partial C_l}{\partial \frac{q\bar{c}}{2V_T}}$	$C_{m_q} = \frac{\partial C_m}{\partial \frac{q\bar{c}}{2V_T}}$	$C_{n_q} = \frac{\partial C_n}{\partial \frac{q\bar{c}}{2V_T}}$	$C_{l_\beta} = \frac{\partial C_l}{\partial \frac{\beta b}{2V_T}}$	$C_{m_\beta} = \frac{\partial C_m}{\partial \frac{\beta b}{2V_T}}$	$C_{n_\beta} = \frac{\partial C_n}{\partial \frac{\beta b}{2V_T}}$	$C_{m_q} + C_{m_{\dot{\alpha}}}$	$C_{n_p} + C_{n_p}\sin\alpha$	$C_{m_r} - C_{m_p}\cos\alpha$
$C_{l_r} = \frac{\partial C_l}{\partial \frac{rb}{2V_T}}$	$C_{m_r} = \frac{\partial C_m}{\partial \frac{rb}{2V_T}}$	$C_{n_r} = \frac{\partial C_n}{\partial \frac{rb}{2V_T}}$				$C_{n_r} - C_{n_\beta}$		$C_{m_p} + C_{m_\beta}\sin\alpha$
								$C_{n_q} + C_{n_{\dot{\alpha}}}$

and may no longer be ignored or corrected for in a simple fashion (Reference (6)). A more detailed discussion on the modelling and significance of the time-dependent effects can be found in reference (19).

Based on a series of experiments conducted in the Tracor Hydronautics Ship Model Basin, the pure longitudinal and lateral rotational and translational derivatives were measured for a 0.19 scale model of a preliminary X-31A configuration operating at a Reynolds number of about 1.28×10^6. From Reference (20) the following results are cited.

1. The measured value of the composite pitch damping derivative ($C_{m_q} + C_{m_{\dot{\alpha}}}$) is equal to the algebraic summation of the individual rotational (C_{m_q}) and translational ($C_{m_{\dot{\alpha}}}$) up to 24 degrees angle-of-attack. Beyond 24 degrees angle-of-attack there is a marked difference between the results. At 70-degrees angle-of-attack the algebraic sum of C_{m_q} and $C_{m_{\dot{\alpha}}}$ is about twice the value of the measured composite derivative derived from the combined pitching motion. This is shown in figure 9.

2. Figure 10 and 11 show the measured values of the composite derivative $(C_{Y_r} - C_{Y_{\dot{\beta}}})_S$ and $(C_{\ell_r} - C_{\ell_{\dot{\beta}}})_S$ compare quite well with the algebraic sum of the individual coefficients for the entire angle-of-attack range.

3. In the case of the composite yaw damping derivative $(C_{n_r} - C_{n_{\dot{\beta}}})_S$ (see Figure 12), agreement with the algebraic sum of $(C_{n_r})_S$ and $(C_{n_{\dot{\beta}}})_S$ is good up to an angle-of-attack of approximately 30 degrees. For angles-of-attack greater than 30 degrees the derivative derived from the algebraic sum of $(C_{n_r})_S$ and $(C_{n_{\dot{\beta}}})_S$ has a much smaller positive (unstable) value than the values obtained from the combined yawing motion. It is apparent that, depending on how the aircraft aerodynamics is mathematically modelled, the predicted behavior of the aircraft dynamic response in the lateral mode could be substantially different.

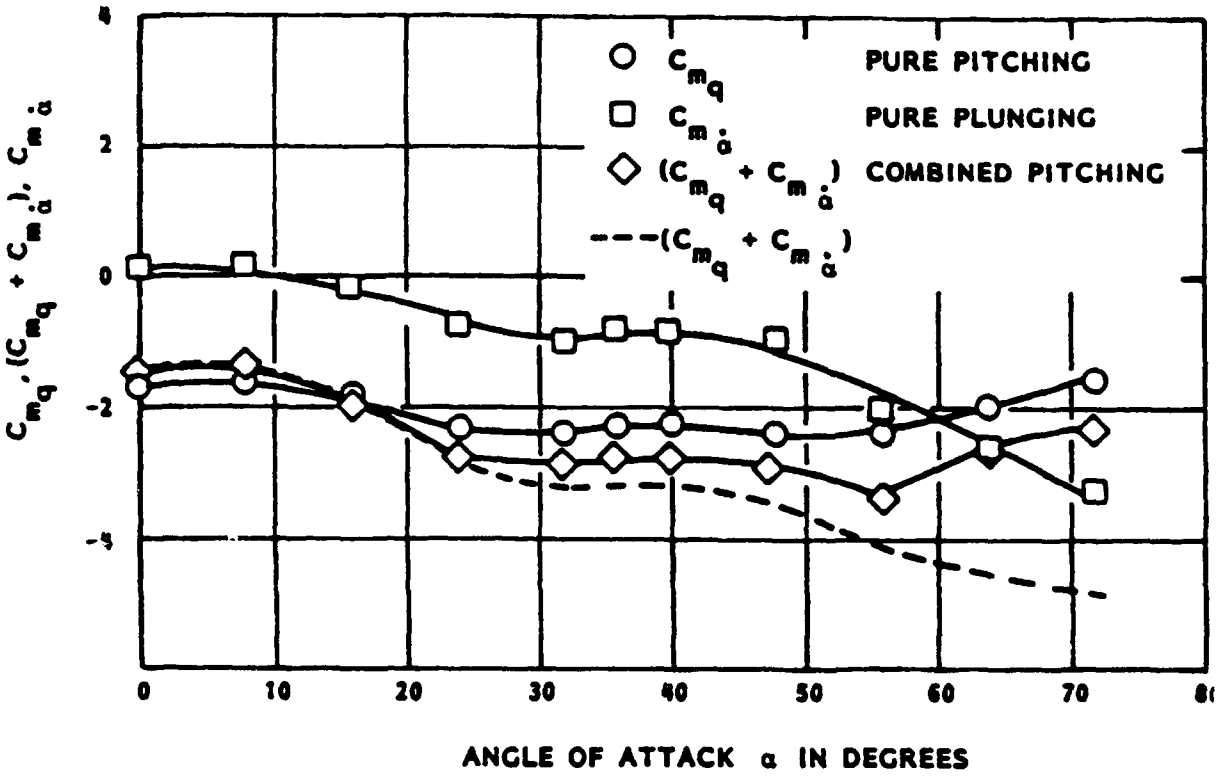

Figure 9 Comparison of the Composite Pitch Damping Derivative ($C_{m_q} + C_{m_{\dot{\alpha}}}$) and the Sum of the Pure Pitching (C_{m_q}) and Pure Plunging ($C_{m_{\dot{\alpha}}}$) Derivatives with Angle-of-Attack for a Preliminary Configuration of the X-31A Aircraft (Reference (20)

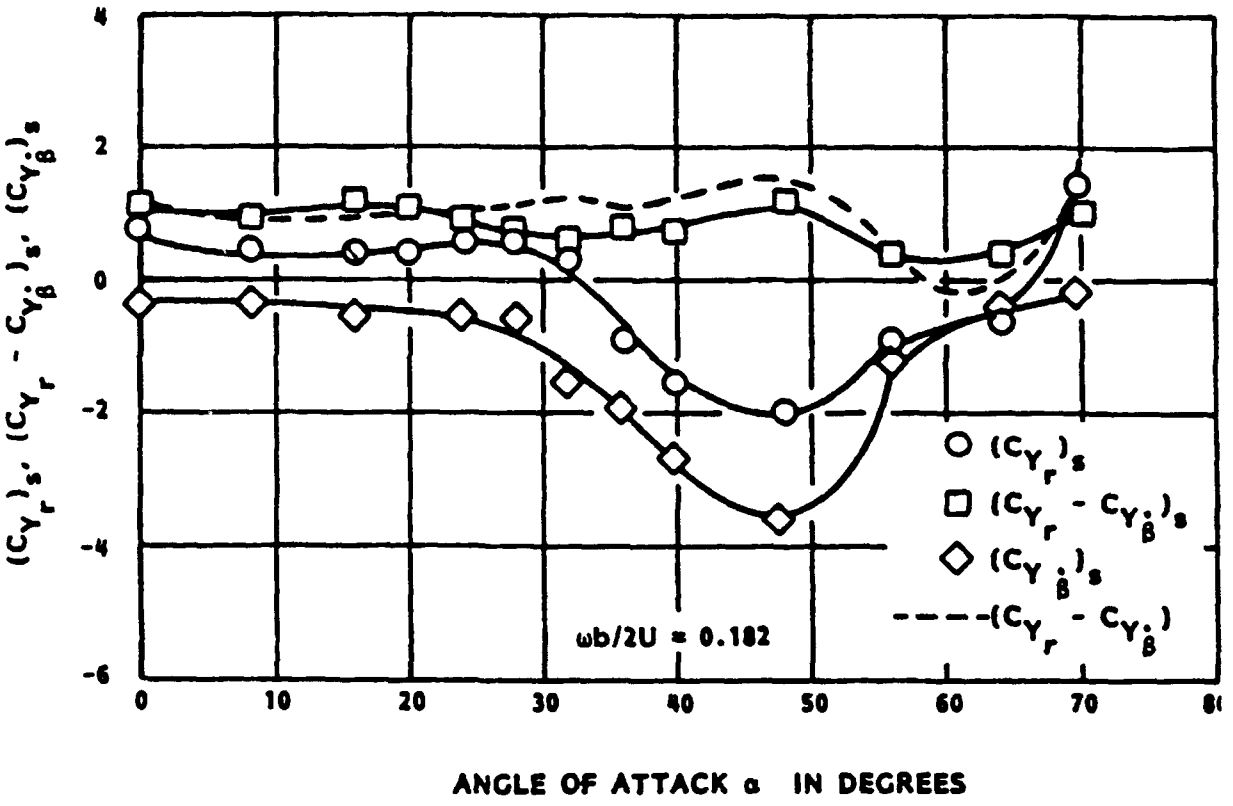

Figure 10 Comparison of the Composite Sideforce Damping Derivative $(C_{Y_r} - C_{Y_{\dot{\beta}}})_s$ and the Sum of the Pure Yawing $(C_{Y_r})_s$ and Pure Sideslipping $(C_{Y_{\dot{\beta}}})_s$ Derivatives with Angle-of-Attack for a Preliminary Configuration of the X-31A Aircraft (Reference (20))

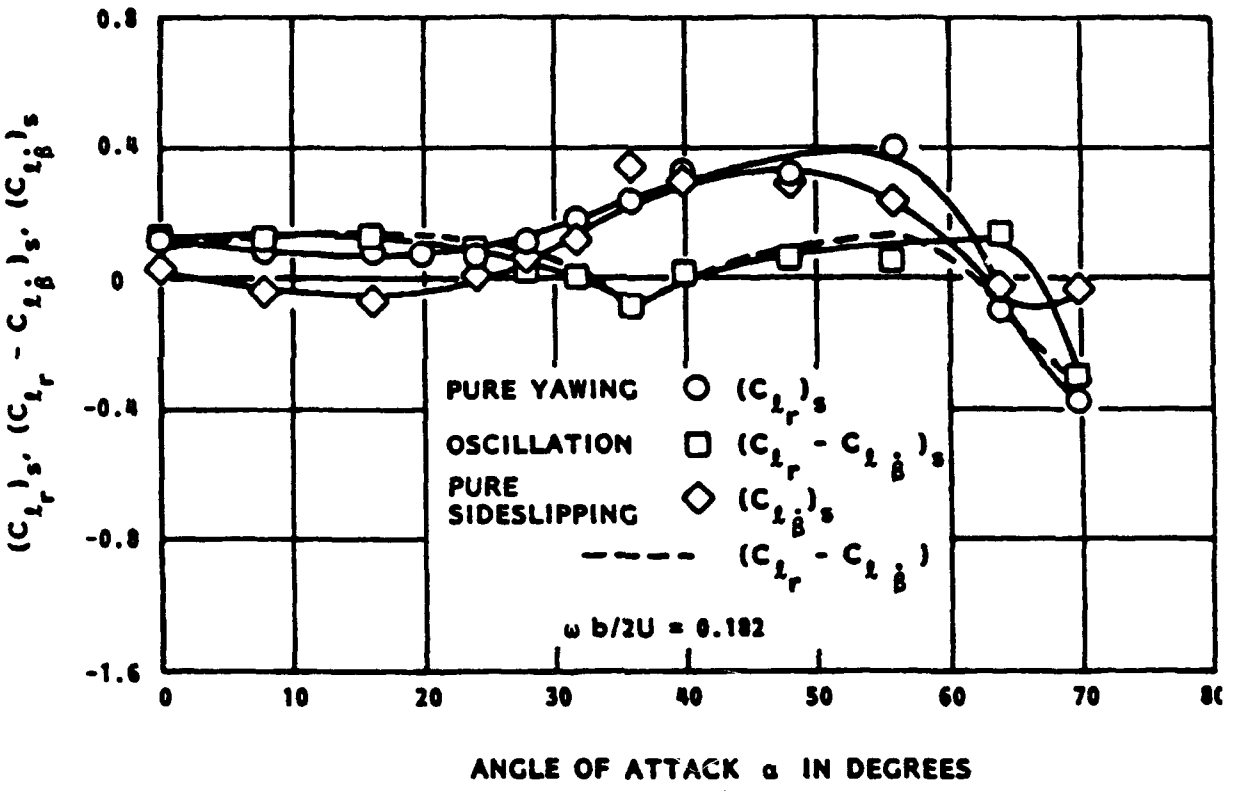

Figure 11 Comparison of the Composite Derivative (C_{ℓ} - $C_{\ell_{\dot{\beta}}}$)$_s$ and the Sum of the Pure Yawing (C_{ℓ_r})$_s$ and Pure Sideslipping ($C_{\ell_{\dot{\beta}}}$)$_s$ Derivatives with Angle-of-Attack for a Preliminary Configuration of the X-31A Aircraft (Reference (20))

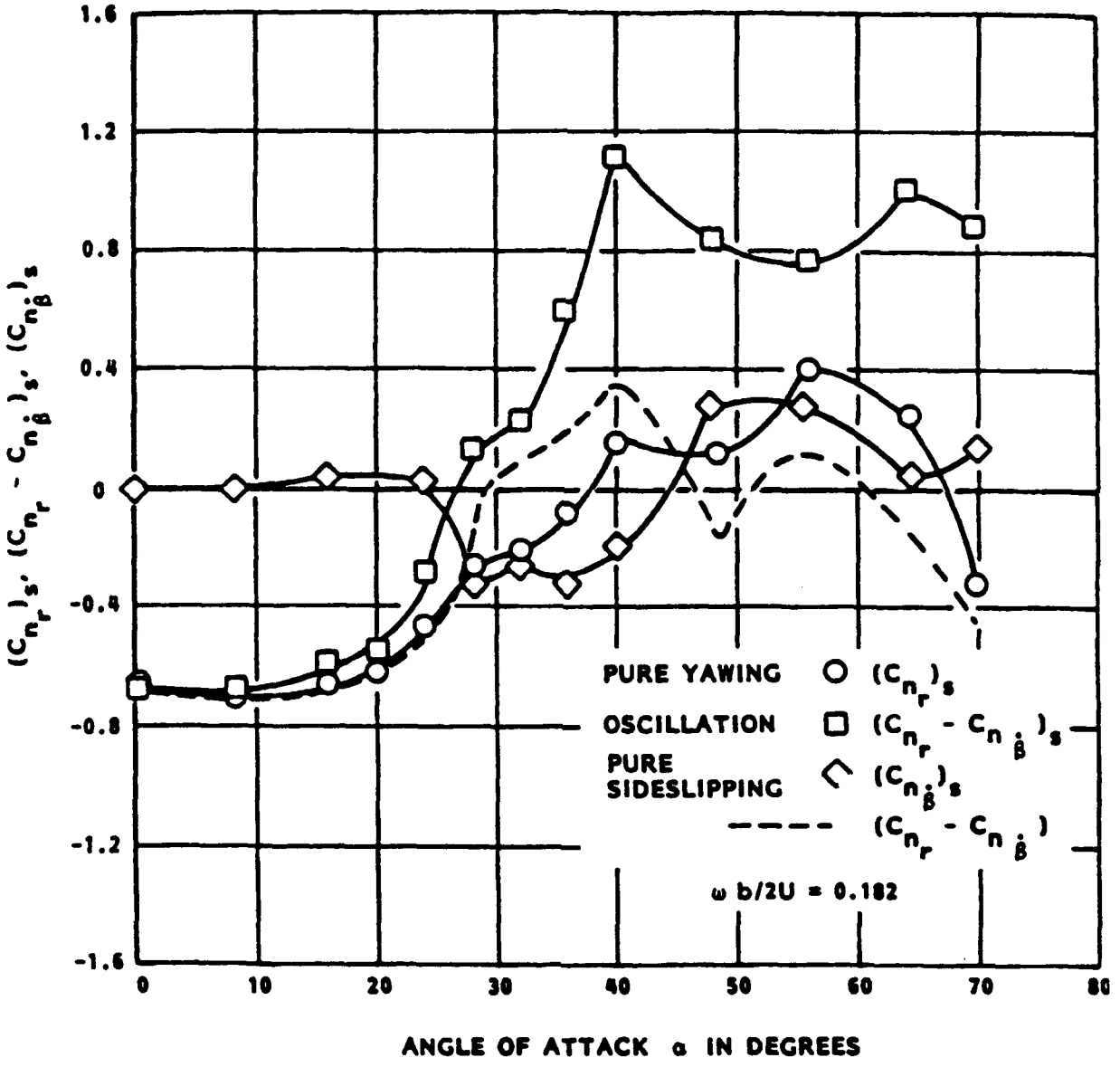

Figure 12 Comparison of the Composite Yaw Damping Derivative $(C_{n_r} - C_{n_{\dot{\beta}}})_s$ and the Sum of the Pure Yawing $(C_{n_r})_s$ and Pure Sideslipping $(C_{n_{\dot{\beta}}})_s$ Derivatives with Angle-of-Attack for a Preliminary Version of the X-31A Aircraft (Reference (20))

Hysteresis Effects

High angle-of-attack flow phenomena such as asymmetric vortex shedding, vortex burst, or periodic separation and reattachment of the flow are frequently responsible for aerodynamic hysteresis effects. Such hysteresis is characterized by a double-valued behavior of the steady-state aerodynamic response to variations in one of the motion variables such as angle-of-attack, angle of sideslip or spin rate. In the presence of hysteresis, the dynamic derivatives measured in large amplitude oscillation experiments may have two distinct components. Namely, one associated with the small-amplitude oscillation, and a second one representing the effect of the hysteresis.

Configuration Dependence

The intricate vortex pattern that exists around an aircraft configuration at high angles-of-attack is very sensitive to even small changes in aircraft geometry. (see References (3), (21) and (22)). The forebody vortices are greatly dependent on the planform and the cross-sectional geometry of the aircraft nose, as well as on the presence of any protuberances on the forebody (such as nose boom, strakes, etc.) that may affect the stability of an existing vortex pattern. Such protuberances give rise to new vortices and create and/or alter conditions of vortex interactions.

The wing leading-edge vortices, in addition to being a strong function of the leading-edge sweep, are also known to be greatly affected by various modifications of the wing itself, such as the addition of wing fences. All of these variations of the geometry of the wing affect not only the position and strength of the wing vortices, but also the all-important location at which these vortices breakdown. Knowledge of the sensitivity of the forebody and wing vortex systems to even small geometric changes, and in turn the strong dominance of aircraft lateral-directional stability at high angles of attack on forebody aerodynamics, is indicative of how carefully one must approach analyzing aircraft open-loop stability at high angles of attack. In reference (6), a preliminary assessment was made of the relative significance of modelling each of the dynamic derivatives for an aircraft at high angles-of-attack. The results of the assessment are given in Table II.

Table II Relative Significance of Dynamic Moment Derivatives at High Angles-of-Attack (Reference (6))

Type of derivative(s)	Derivative(s)	Significant	
		Aircraft	Missiles
Direct	C_{m_q}, C_{n_r}, C_{l_p}	Yes	Yes
Cross	C_{n_p}, C_{l_r}	Yes	Yes
Cross-coupling	C_{l_q}, C_{n_q}	Yes	Yes
Cross-coupling	C_{m_p}	No	Yes
Cross-coupling	C_{m_r}	No	No
Acceleration	$C_{m_{\dot{\alpha}}}$, $C_{l_{\dot{\beta}}}$, $C_{l_{\dot{\alpha}}}$	Yes	?
Acceleration	$C_{n_{\dot{\beta}}}$, $C_{m_{\dot{\beta}}}$, $C_{n_{\dot{\alpha}}}$	?	?

STABILITY AND THE RIGID AIRCRAFT EQUATIONS-OF-MOTION

Before discussing analytical methods/criteria for predicting aircraft departure susceptibility, an up front definition of departure from controlled flight is essential. The term "departure" is generally defined to be a divergent, large amplitude, uncommanded aircraft motion (i.e., pitch-up, nose-slice, roll reversal, etc.). This definition can be further refined and a distinction be made between open-loop and closed-loop departures. Open-loop departures refer to departures from controlled flight that are due to instabilities in the basic aircraft. That is, even if the pilot does not move the controls, small perturbations in the aircraft states build-up until the aircraft can no longer be controlled. In a closed-loop departure, the basic aircraft may or may not be unstable, but the addition of a pilot-loop closure creates an unstable vehicle/pilot system. With the exception of the lateral control departure parameter (LCDP) and $1/T_{\phi_1}$, the departure susceptibility criteria presented in MIL-STD 1797A, solely addressed open-loop instabilities of the basic airframe dynamics.

Analytically predicting the occurrence of an aircraft departure from controlled flight is invariably based on the assumptions of the equations-of-motion (EOM)/math model used to describe the response of the aircraft to initial conditions, pilot control inputs, atmospheric disturbances and system failures (i.e., propulsion, flight control system, etc.). As can already be inferred by the definition presented for an open-loop departure, departure from controlled flight connotes an instability with respect to an initial flight condition. While a closed-loop departure has to do with the stability of the aircraft due to pilot control inputs and loop closures. Like all physical systems, the six degree-of-freedom EOM describing the motion of a rigid aircraft are nonlinear and have time varying parameters to some degree (see Figure 13). Associated with nonlinear systems, the concept of stability is very much different than that of linear systems. For a linear system, stability, or the lack of it, is a property of the linear constant parameter system, and the stability is determined by the eigenvalues (solution of the homogenous EOM) of the system. In addition, the stability of a linear system is unaffected by the initial conditions or the forcing functions (care must be taken when applying this last statement that one does not violate assumptions that permitted the use of a linear model in the first place).

$$\dot{U} = \frac{X}{M} + RV - QW - g\sin\theta \quad (1)$$

$$\dot{V} = \frac{Y}{M} + PW - RU + g\cos\theta\sin\phi \quad (2)$$

$$\dot{W} = \frac{Z}{M} + QU - PV + g\cos\theta\cos\phi \quad (3)$$

$$\dot{P} = \frac{I_z}{I_x I_z - I_{xz}^2}\left[L + \left(\frac{I_{xz}}{I_z}\right) N \right] - QR\left(\frac{I_{xz}^2}{I_z} + I_z - I_y\right) + PQI_{xz}\left(1 - \frac{I_y - I_x}{I_z}\right) \quad (4)$$

$$\dot{Q} = \frac{1}{I_y}\left[M - \left(P^2 - R^2\right) I_{xz} - RP\,(I_x - I_z) \right] \quad (5)$$

$$\dot{R} = \frac{I_x}{I_x I_z - I_{xz}^2}\left[N + \left(\frac{I_{xz}}{I_z}\right) L \right] + PQ\left(\frac{I_{xz}^2}{I_z} + I_z - I_y\right) + QRI_{xz}\left(1 - \frac{I_z - I_y}{I_x}\right) \quad (6)$$

$$\dot{\psi} = (Q\sin\phi + R\cos\phi)\sec\theta \quad (7)$$

$$\dot{\theta} = Q\cos\phi - R\sin\phi \quad (8)$$

$$\dot{\phi} = P + Q\sin\phi\tan\theta + R\cos\phi\tan\theta \quad (9)$$

Note: The force (X,Y,Z) and moment ($\mathcal{L}$,M,N) terms represent the external forces and moments acting on the vehicle other than gravity (i.e., aerodynamic, engine, etc.)

Figure 13 Six Degree-of-Freedom, Nonlinear, Rigid Body Equations-of-Motion (Body-Axis; $I_{yz} = I_{xz} = 0$)

In contrast, a nonlinear system may be stable for one input or initial condition and unstable for another. That is, stability for a nonlinear system is generally not a system property but a property of a particular solution corresponding to a particular initial condition of the nonlinear system. For this reason, there unfortunately exists no convenient method for the determination of the stability of a nonlinear system in general (the Routh, Horwitz, and Nyquist stability criteria are only applicable to linear systems). In most cases this forces attention to focus on the stability of a nonlinear system in the "neighborhood" of a solution. The reformulation of the nonlinear system equations into a "linearized" set of equations about a defined reference point is an effective and widely used technique to begin to understand the stability characteristics of a nonlinear system. This technique is justifiable provided that the magnitudes of the perturbation quantities and the chosen operating point used to define the linear model reproduces the nonlinear system dynamics "accurately" over a "sufficient" time span. When the linearizing assumptions are not justified the analysis of the mathematical model must be carried out by one or more of the nonlinear analysis methods (see Reference (23)). An exception to this exists if the analyst has the capability of deriving multiple linear math models from a nonlinear system math model using a computerized numerical method technique. Each of the models would then provide stability information valid for a particular region of the state space of interest.

A technique, known as the linear approximation theroms of Lyapunov,[1] states that for sufficiently small disturbances, the stability (or instability) of an equilibrium solution of a nonlinear system can be determined in all cases from the linear model if none of the eigenvalves is zero. If one of the eigenvalves is zero than the set of equations is said to be critical according to Lyapunov and the stability of the nonlinear solution is dictated by the discarded nonlinear terms.

Note that this concept of stability addresses the initial states and not the control inputs. Thus this definition is applicable to investigating the potential of an open-loop departure occurring. On the other hand, the stability

---

[1]The reader may wish to review the formal definitions and theroms of the small disturbance stability theory provided in References (24) and (25).

concept in terms of the control inputs (and not the initial conditions) is described by the following concept; A linear system (described by ($\dot{x} = Ax + Bu$; $y = Cx$) whose Laplace transform of the output y(s) is,

$$y(s) = C(sI-A)^{-1} X(o) + C(sI-A)^{-1}Bu(s)$$

has bounded-input bounded-output (BIBO) stability if

$$\left.\begin{array}{c} \| u(t) \| < \infty \\ X(0) = 0 \end{array}\right\} \rightarrow \| y(t) \| < \infty$$

It turns out that time-invariant linear systems are BIBO stable if all eigenvalves of [A] lie in the open left half plane. (Note if the system modes are all completely observable and controllable then Lyapunov and BIBO stability are one in the same.) In some cases the actual response of y(t) may not be BIBO stable if for example an excited observable mode does not appear in the transfer function ($C(sI-A)^{-1}B$) due to pole-zero cancellation implying the uncontrollability of a normal mode.

The existence of a valid "linearized" model of a nonlinear system however is not always assured. Linearized equations have meaning only if the higher order terms (products and cross product terms of the perturbation variables) are "smaller" than the linear terms, otherwise the higher order terms can dominant the system behavior.

As explained earlier, the application of the concept of stability (in terms of Lypanov) to a nonlinear system described by equations (1) to (9) requires studying the behavior of the nonlinear system in the vicinity of a particular solution. The particular solution of interest is the equilibrium solution(s) of the nonlinear system for reasons still to be discussed. Consider now reformulating the nonlinear equation, given by equations (1) to (9) using small-pertubation theory (See figure 14). To do this, the state and input variables are redefined in terms of the sum of a reference state (and input) quantity (subscripted "0") and a perturbed state (and input) quantity (lower case). The result is given by equation (13) of figure 14, where A and B are assumed to be time-invariant matrices and the column matrix h(x) contains all the nonlinear terms as a function of the perturbed states, x.

Given the Nonlinear System,

$$\dot{x} = f(x,u,t) \tag{10}$$

$$y = g(x,u,t)$$

Redefine the state and input variables such that,

$$x = x_0 + x \tag{11}$$

$$u = u_0 + u$$

Equation (10) becomes,

$$\dot{x} = f(x,u,t) \tag{12}$$

$$y = g(x,u,t)$$

or in state-space form equation (12) can be written,

$$\dot{x} = Ax + Bu + h(x) \tag{13}$$

$$y = Cx$$

where : A, B are assumed to be time-invarient matrices defined by

$$A = \left.\frac{\partial f}{\partial x}\right|_{x_0,\, u_0}, \quad B = \left.\frac{\partial f}{\partial u}\right|_{x_0,\, u_0}$$

h(x) = nonlinear terms as a function of the perturbed states, x.

Figure 14 General Formulation of the Linear State Equations for a Nonlinear System

According to the small disturbance stability theory of Lypanov, the stability of the solution x(t) can now be determined if the eigenvalues (λ_A) of [A] are nonzero (positive or negative). This statement holds true provided the two conditions below are satisfied. (Reference (25))

$$1.\ A = \left.\frac{\partial f}{\partial x}\right|_{\bar{x}\ =0} \text{ exists}$$

$$2.\ \lim_{x \to 0} \frac{\| h(x,t) \|}{\| x \|} = 0$$

The second condition above implies that the higher order nonlinear terms of h(x) are negligible compared to the linear terms of A. If an eigenvalue of the derived linear system is zero then the stability characteristics must be determined from the nonlinear equations.

There are two reasons why the reference or nominal state (x_0) used in small perturbation theory is chosen to be a trimmed condition in which all the acceleration terms are zero (i.e., $\dot{\vec{V}} = 0$, $\dot{\vec{\omega}}_B = 0$). The first is that the linear system equations most accurately represent the nonlinear system dynamics. This is shown mathematically by equations (14) through (17).

$$\vec{V}_B = \left(\vec{V}_B\right)_0 + \Delta\vec{V} \tag{14}$$

$$\vec{\omega}_B = \left(\vec{\omega}_B\right)_0 + \Delta\vec{\omega}_B \tag{15}$$

Now if $\left(\dot{\vec{V}}_B\right)_0 = \left(\dot{\vec{\omega}}_B\right)_0 = 0$ is satisfied,

$$\dot{\vec{V}}_B = + \Delta\dot{\vec{V}} \tag{16}$$

$$\dot{\vec{\omega}}_B = \Delta\dot{\vec{\omega}}_B \tag{17}$$

Total State = Perturbation
Rates State Rates

The second reason for choosing the reference state as a trim state is that the total state and control trajectories equate to the sum of the constant nominal values and the linear perturbation time history values.

$$\vec{V}_B(t) \cong (\vec{V}_B)_0 + \Delta\vec{V}_B(t) \tag{18a}$$

$$\vec{\omega}_B(t) \cong (\vec{\omega}_B)_0 + \Delta\vec{\omega}_B(t) \tag{18b}$$

$$\vec{U}(t) \cong (\vec{U})_0 + \Delta\vec{U}(t)$$

At this point, the nonlinear rigid aircraft EOM of Figure (13) have been reformulated in the perturbed state-space form of equation (13) (see Figure 15). The matrix [A] multiplied into [x] along with the [B] matrix multiplied into [u] represents the linear portion of the equations and the column matrix h(x) represents the nonlinear portion. The [A] matrix is commonly referred to as the stability or Jacobian matrix while the [B] matrix is referred to as the control matrix.

For sufficiently small disturbances the product and cross products of the perturbation variables may be considered negligible and the nonlinear portion of the equation, h(x) is eliminated leaving only the matrix equation that describes the six degree-of-freedom linear dynamics for a general reference condition (recall, that this method is utilized based on the premise $\lim_{x \to 0} \frac{\| h(x,t) \|}{\| x \|} = 0$ (Reference (25)).

The [A] matrix given in figure 15 is completely general with the only assumptions being that the aircraft is symmetrical about its xz-plane and that attitude (θ) and bank angle (ϕ) perturbations are approximately less than 15 degrees.

Simplifying assumptions associated with the complete 6 DOF linear EOM are used in many flight dynamic applications to reduce the complexity of the problem and provide engineering insight. The problem of predicting aircraft departure from controlled flight is no exception as will be seen in the development of many of the existing departure susceptibility criteria parameters. The major point of the discussion that follows is to point out when these simplifying assumptions may not be justified and, in other cases, where they are valid.

A-MATRIX

$$\begin{bmatrix} \dot{u} \\ \dot{v} \\ \dot{w} \\ \dot{p} \\ \dot{q} \\ \dot{r} \\ \dot{\psi} \\ \dot{\theta} \\ \dot{\phi} \end{bmatrix} = \begin{bmatrix} X_u & R_0 & X_w - Q_0 & 0 & X_q - W_0 & V_0 & 0 & -g\cos\theta_0 & 0 \\ -AR_0 & A \cdot Y_v & {}^{*}A \cdot P_0 & A[Y_p + W_0] & 0 & A[Y_r - U_0] & 0 & -Ag\sin\phi_0\sin\theta_0 & -A \cdot g\cos\phi_0\cos\theta_0 \\ B[Z_u + Q_0] & -B \cdot P_0 & B \cdot Z_w & -B \cdot V_0 & B[Z_q + U_0] & 0 & 0 & -Bg\cos\phi_0\sin\theta_0 & -Bg\sin\phi_0\cos\theta_0 \\ \begin{matrix} C_1 \cdot \\ [Bz'_u(Z_u + Q_0) \\ (-Az'_uR_0] \end{matrix} & \begin{matrix} C_1 \cdot \\ [z'_v + Az'_uY_v \\ (-Bz'_uP_0] \end{matrix} & \begin{matrix} C_1 \cdot \\ [z'_w + Az'_uP_0 \\ (-Bz'_uZ_w] \end{matrix} & \begin{matrix} C_1 \cdot [z'_p + \\ Az'_u(Y_p + W_0) \\ (-Bz'_uV_0 + C_4P_0] \end{matrix} & \begin{matrix} C_1 \cdot [z'_q \\ +Bz'_u(Z_q + U_0) \\ (+C_4P_0 - C_3R_0] \end{matrix} & \begin{matrix} C_1 \cdot [L'_r + AL'_q(Y_r - U_0) \\ (-C_3Q_0] \end{matrix} & 0 & 0 & 0 \\ \begin{matrix} M_u + \\ B \cdot M_{\dot{w}}(Z_u + Q_0) \end{matrix} & M_v - M_{\dot{w}}P_0 \cdot B & M_w + M_{\dot{w}}Z_w \cdot B & \begin{matrix} -M_{\dot{w}}V_0B + \\ D_1R_0 - 2D_2P_0 \end{matrix} & \begin{matrix} M_q + \\ BM_{\dot{w}}[Z_q + U_0] \end{matrix} & D1P_0 + 2D2P_0 & 0 & -BM_{\dot{w}}g\cos\phi_0\sin\theta_0 & -BM_{\dot{w}}g\sin\phi_0\cos\theta_0 \\ \begin{matrix} E_1 \cdot \\ [BN'_{\dot{w}}(Z_u + Q_0) \\ (-AN'_{\dot{w}}R_0] \end{matrix} & \begin{matrix} E_1 \cdot \\ [N'_v + AN'_{\dot{w}}Y_v \\ (-BN'_{\dot{w}}P_0] \end{matrix} & \begin{matrix} E_1 \cdot \\ [N'_w + AN'_{\dot{w}}P_0 \\ (+BN'_{\dot{w}}Z_w] \end{matrix} & \begin{matrix} E_1 \cdot [N'_p + \\ AN'_{\dot{w}}(Y_p + W_0) \\ (-BN'_{\dot{w}}V_0 + E_3Q_0] \end{matrix} & \begin{matrix} E_1[N_q \\ +BN'_{\dot{w}}(Z_q + U_0) \\ (+E_3P_0 - E_4R_0] \end{matrix} & \begin{matrix} E_1 \cdot [N'_r + AN'_{\dot{w}}(Y_r - U_0) \\ (-E_4Q_0] \end{matrix} & 0 & 0 & 0 \\ 0 & 0 & 0 & 0 & \sin\phi_0\sec\theta_0 & \cos\phi_0\sec\theta_0 & 0 & \begin{matrix} Q_0\sin\phi_0\sec\theta_0\tan\theta_0 \\ +R_0\cos\phi_0\sec\theta_0\tan\theta_0 \end{matrix} & \begin{matrix} Q_0\cos\phi_0\sec\theta_0 \\ -R_0\sin\phi_0\sec\theta_0 \end{matrix} \\ 0 & 0 & 0 & 0 & \cos\phi_0 & \sin\phi_0 & 0 & 0 & -R_0\cos\phi_0 - Q_0\sin\phi_0 \\ 0 & 0 & 0 & 1 & \sin\phi_0\tan\theta_0 & \cos\phi_0\tan\theta_0 & 0 & \begin{matrix} Q_0\sin\phi_0\sec^2\theta_0 \\ +R_0\cos\phi_0\sec^2\theta_0 \end{matrix} & \begin{matrix} Q_0\cos\phi_0\tan\theta_0 \\ -R_0\sin\phi_0\tan\theta_0 \end{matrix} \end{bmatrix} \begin{bmatrix} u \\ v \\ w \\ p \\ q \\ r \\ \psi \\ \theta \\ \phi \end{bmatrix}$$

NOTE: $A = \frac{1}{1-Y_{\dot{v}}}$ $B = \frac{1}{1-Z_{\dot{w}}}$ $C_1 = \frac{I_z}{I_xI_z - I_{xz}^2}$ $C_2 = \frac{I_{xz}}{I_z}$ $C_3 = \frac{I_{xz}^2}{I_z} + I_z - I_y$ $C_4 = I_{xz}\left[1 - \frac{I_y - I_x}{I_z}\right]$

$D_1 = \frac{I_z - I_x}{I_y}$ $D_2 = \frac{I_{xz}}{I_y}$ $E_1 = \frac{I_x}{I_xI_z - I_{xz}^2}$ $E_2 = \frac{I_{xz}}{I_x}$ $E_3 = \frac{I_{xz}}{I_x} + I_z - I_y$ $E_4 = I_{xz}\left[1 + \frac{I_z - I_y}{I_x}\right]$

Figure 15 Nonlinear Rigid Aircraft Equations of Motion in Perturbed State-Space Form (Body-Axis)

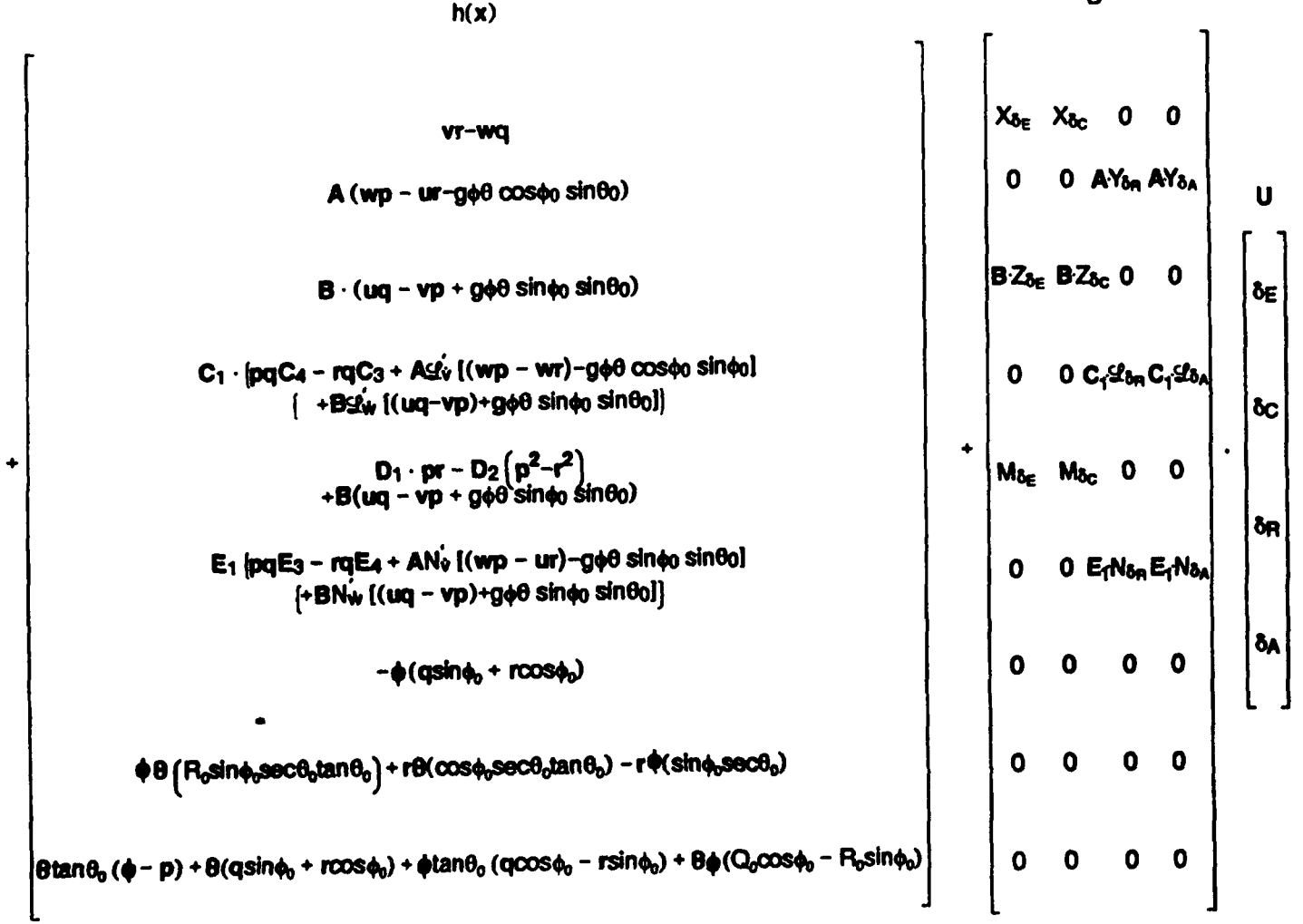

Figure 15 (Concluded) Nonlinear Rigid Aircraft Equations of Motion in Perturbed State-Space Form (Body-Axis)

CHOICE OF THE LINEARIZED REFERENCE FLIGHT CONDITION

Although the A-matrix of Figure 15 is linear, it is still highly complex due to the generality presumed for the reference trim condition. Because of their complexity, application of the equations in their complete form is seldom used. Instead, simpler trim cases that still reveal stability and control problems are more commonly used. Such is the case in the derivation of the departure susceptibility parameters $C_{n_{\beta DYN}}$, LCDP , α-β, and δ_α. The derivation of these parameters assumes steady ($\dot{\vec{V}}, \dot{\vec{\omega}} = 0$), straight ($\dot{\psi}, \dot{\phi} = 0$), symmetric ($\psi_0$, $V_0 = 0$), wings level ($\phi_0 = 0$) flight. There are not many (analysts, pilots, etc.) who would consider steady, straight, symmetric, wings level flight to be important initial conditions practically associated with departure susceptible flight. However the fact remains that $C_{\beta DYN}$ and LCDP are well accepted departure susceptibility parameters that have correlated well with wind tunnel, and flight test data over the last two decades (see References (26) to (28)).

There are significant simplifications and insight to be gained if a reference flight condition ($\bar{X}_0$) is chosen such that V_0 (β_0), P_0, R_0 and ϕ_0 are zero. Namely, the longitudinal ($\dot{u}$, $\dot{w}$ (or $\dot{\alpha}$), $\dot{q}$ and $\dot{\theta}$) and lateral/directional ($\dot{v}$(or $\dot{\beta}$), $\dot{p}$, $\dot{r}$, $\dot{\phi}$) linear EOM sets can be decoupled from the complete linear six degree-of-freedom aircraft EOM (as given by the [A] matrix in Figure 15) and solved independently of each other (see Figures 16 and 17). However, as shown by the authors of References (24) and (29) through (33), these simplifications in many cases may not be justified and often their solution leads to misleading stability information. In the worse case, an assumed stable flight condition may in fact be unstable.

To highlight how the major individual elements of the stability matrix are influenced by asymmetric flight conditions ($\beta, \phi \neq 0$) and nonzero angular rates ($P_0, Q_0, R_0 \neq 0$), the Stability Matrix ([A]) given in Figure 15 has been simplified and presented in Figure 18. Three simplifying assumptions were made. They are, (1) the cross product of inertia, $(I_{xz})_B$, is zero, (2) the $\dot{v}(\dot{\beta})$ and $\dot{w}(\dot{\alpha})$ dynamic translational derivatives

$$\dot{x} = Ax + Bu$$

Where : x = State vector, $x = [u, w, q, q]^T$

A = Jacobian (or Stability) matrix $[\partial f / \partial x]$ evaluated at $x = \bar{X}_o$

Assumptions :

- $(I_{xz})_B = 0$ slug - ft^2
- $V_0 = 0$ ft/s
- $P_0, R_0 = 0$ rad/s
- No Aerodynamic Cross-coupling (i. e., $M_\beta = 0$)
- $\phi_0 = 0$ rad

$$\begin{bmatrix} \dot{u}\left(\frac{ft}{s^2}\right) \\ \dot{w}\left(\frac{ft}{s^2}\right) \\ \dot{q}\left(\frac{rad}{s^2}\right) \\ \dot{\theta}\left(\frac{rad}{s}\right) \end{bmatrix} = \begin{bmatrix} X_u + X_{T_u} & X_w - Q_0 & X_q - W_0 & g\cos\theta_0 \\ Z_u + Q_0 & Z_w & Z_q + U_0 & -g\cos\theta_0 \\ M_u + M_{\dot{w}}\left(Z_u + Q_0\right) & M_w + M_{\dot{w}}Z_w & M_q + M_{\dot{w}}\left(Z_q + U_0\right) & -M_{\dot{w}}g\sin\theta_0 \\ 0 & 0 & 1 & 0 \end{bmatrix} \begin{bmatrix} u\left(\frac{ft}{s}\right) \\ w\left(\frac{ft}{s}\right) \\ q\left(\frac{rad}{s}\right) \\ \theta(rad) \end{bmatrix} + Bu$$

Figure 16 Decoupled Longitudinal Body-Axis Stability Matrix

$$\dot{x} = Ax + Bu$$

Where : x = State vector, $x = [v, p, r, \phi]^T$

A = Jacobian (or Stability) matrix $[\partial f / \partial x]$ evaluated at $x = \bar{X}_0$

Assumptions :

- $(I_{xz})_B = 0$ slug - ft^2
- $V_0 = 0$ ft/s
- $P_0, R_0 = 0$ rad/s
- No Aerodynamic Cross-coupling (i. e. , $N_\alpha = 0$);
- $\phi_0 = 0$ rad
- Translational Rate Derivatives, $Y_{\dot{\beta}}, Z_{\dot{\alpha}} \approx 0$

$$\begin{bmatrix} \dot{v}\left(\frac{ft}{s}\right) \\ \dot{p}\left(\frac{rad}{s^2}\right) \\ \dot{r}\left(\frac{rad}{s^2}\right) \\ \dot{\phi}\left(\frac{rad}{s}\right) \end{bmatrix} = \begin{bmatrix} Y_v & Y_p + W_0 & Y_r - U_0 & g\cos\theta_0 \\ \mathcal{L}'_v & \mathcal{L}'_p & \mathcal{L}'_r & 0 \\ N'_v & N'_p & N'_r & 0 \\ 0 & 1 & \tan\theta_0 & Q_0\tan\theta_0 \end{bmatrix} \cdot \begin{bmatrix} v \\ p \\ r \\ \phi \end{bmatrix} + \begin{bmatrix} Y_{\delta_a} & Y_{\delta_r} \\ \mathcal{L}_{\delta_a} & \mathcal{L}_{\delta_r} \\ N_{\delta_a} & N_{\delta_r} \\ 0 & 0 \end{bmatrix} \cdot \begin{bmatrix} \delta_a \\ \delta_r \end{bmatrix}$$

Figure 17 Decoupled Lateral/Directional Body-Axis Stability Matrix

A-Matrix

$$\begin{bmatrix} \dot{u} \\ \dot{v} \\ \dot{w} \\ \dot{p} \\ \dot{q} \\ \dot{r} \\ \dot{x} \\ \dot{\theta} \\ \dot{\phi} \end{bmatrix} = \begin{bmatrix} X_u & R_0 & X_w - Q_0 & 0 & X_q - w_0 & V_0 & 0 & g\cos\theta_0 & o \\ -R_0 & Y_v & P_0 & Y_p + W_0 & 0 & Y_r - U_0 & 0 & -g\sin\phi_0\sin\theta_0 & g\cos\phi_0\cos\theta_0 \\ Z_u + Q_0 & -P_0 & Z_w & -V_0 & Z_q + U_0 & 0 & 0 & -g\cos\phi_0\sin\theta_0 & -g\sin\phi_0\cos\theta_0 \\ 0 & \mathcal{L}'_v & \mathcal{L}'_w & \mathcal{L}'_p & \frac{I_z - I_y}{I_x} \cdot R_0 & \mathcal{L}'_r - \frac{Q_0(I_z - I_y)}{I_x} & 0 & 0 & 0 \\ \begin{matrix} M_u + \\ M_w(Z_u + Q_0) \end{matrix} & \begin{matrix} M_v \\ -M_wP_0 \end{matrix} & \begin{matrix} M_w + \\ M_wZ_w \end{matrix} & \begin{matrix} -M_wV_0 + \\ \frac{I_z - I_y}{I_x} \cdot R_0 \end{matrix} & \begin{matrix} M_q + \\ M_w[Z_q + U_0] \end{matrix} & \frac{I_z - I_y}{I_x} \cdot P_0 & 0 & -M_wg\cos\phi_0\sin\theta_0 & -M_wg\sin\phi_0\cos\theta_0 \\ 0 & N'_v & N'_w & \begin{matrix} N'_p + \\ \frac{I_x - I_y}{I_z} \cdot Q_0 \end{matrix} & \frac{I_x - I_y}{I_z} \cdot P_0 & N_r & 0 & 0 & 0 \\ 0 & 0 & 0 & 0 & \sin\phi_0\sec\theta_0 & \cos\phi_0\sec\theta_0 & 0 & \begin{matrix} Q_0\sin\phi_0\sec\theta_0\tan\theta_0 \\ + R_0\cos\phi_0\tan\theta_0\sec\theta_0 \end{matrix} & \begin{matrix} Q_0\cos\phi_0\sec\theta_0 \\ - R_0\sin\phi_0\sec\theta_0 \end{matrix} \\ 0 & 0 & 0 & 0 & \cos\phi_0 & \sin\phi_0 & 0 & 0 & \begin{matrix} -R_0\cos\phi_0 \\ -Q_0\sin\phi_0 \end{matrix} \\ 0 & 0 & 0 & 1 & \sin\phi_0\tan\theta_0 & \cos\phi_0\tan\theta_0 & 0 & \begin{matrix} Q_0\sin\phi_0\sec^2\theta_0 \\ +R_0\cos\phi_0\sec^2\theta_0 \end{matrix} & \begin{matrix} Q_0\cos\phi_0\tan\theta_0 \\ - R_0\sin\phi_0\tan\theta_0 \end{matrix} \end{bmatrix} \cdot \begin{bmatrix} u \\ v \\ w \\ p \\ q \\ r \\ \dot{x} \\ \dot{\theta} \\ \dot{\phi} \end{bmatrix}$$

Figure 18 Simplified Linear Stability Matrix Applicable to Asymetric Maneuvering Flight

($\mathcal{L}_{\dot{v}}$, $N_{\dot{v}}$, $\mathcal{L}_{\dot{w}}$, $M_{\dot{w}}$, $N_{\dot{w}}$, $Y_{\dot{v}}$, $Z_{\dot{w}}$) are zero, and (3) the aerodynamic static and dynamic longitudinal - lateral/directional cross-coupling derivatives ($\mathcal{L}_w$, M_v, N_w, $\mathcal{L}_q$, N_q) are zero.

A very thorough discussion on the effects of altitude, h, velocity, V_T, the aerodynamic angles, α_0, β_0 asymmetric flight ($\beta_0 \neq 0$) and steady maneuvering (P_0, Q_0, $R_0 \neq 0$) dynamics on the unaugmented rigid aircraft stability in terms of the eigenvalues and the modal shapes is given by Stengel in References (30) and (32). The general findings[1] of this work are summarized in Table III.

[1] Note, these results were derived for a reference aircraft (small supersonic fighter type designed for air superiority missions) but can be generalized in most cases.

Table III Summary Of The Effects Of Altitude, Velocity, Aerodynamic Angles And Steady Maneuvering On The Unaugmented Rigid Aircraft Stability. (Reference (30) and (32))

I. ALTITUDE EFFECT:

Effects:	Stability Impact:
• Air density (ρ) and thus dynamic pressure (which in turn effects control effectiveness).	With increasing altitude, • $(\omega_n)_{SP}$ and $(\omega_n)_{DR}$ increases • $(\zeta)_{SP}$ and $(\zeta)_{DR}$ increases • T_r increases

II. VELOCITY EFFECT:

Effects:	Stability Impact
• Dynamic pressure (which in turn effects control effectiveness). • Angular rate normalization terms ($b/2V_T$ and $\bar{c}/2V_T$) • Velocity-angular rate cross-product terms	With increasing velocity, • $(\omega_n)_{SP}$ and $(\omega_n)_{DR}$ increase significantly • $(\zeta)_{SP}$ affected only slightly (slight increase). • $(\zeta)_{DR}$ increases • T_r is changed only slightly

Table III (Cont) Summary of the Effects of Altitude, Velocity, Aerodynamic Angles and Steady Maneuvering on the Unaugmented Rigid Aircraft Stability. (References (30) and (32))

III. ANGULAR RATE EFFECTS:

Affect:

- The nominal aerodynamic forces and moments due to steady angular rates.
- Terms due to the cross-product of angular rate with velocity (in the force equations) and with angular momentum (in the moment equation).

Stability Impact

Q_0:

- Appears in both the longitudinal (U, W, Q, θ) and lateral (V, P, R, ϕ) set of equations but does not introduce any coupling between the two sets of equations.

  Is a second order term in the roll damping due to yaw rate term,

  $[\mathcal{L}_r - Q_0 (I_z - I_y)]/I_x$

  Is a second order term in the yaw damping due to roll rate term,

  $[N_p + Q_0 (I_x - I_y)]/I_z$

Table III (Cont) Summary of the Effects of Altitude, Velocity, Aerodynamic Angles and Steady Maneuvering on the Unaugmented Rigid Aircraft Stability. (References (30) and (32))

III. ANGULAR RATE EFFECTS (Cont)

Stability Impact

Q_0 : • The major effect of nonzero Q_0 is destabilizing, especially on the Dutch-roll mode.

- With increasing Q_0 some mode shape changes appear in the roll mode and in the separation of the complex phugoid mode into two real roots.

Control Impact

- Nominal Q_0 has a large effect on the steady state gain, primarily due to the creation, of non-minimum phase zeros and unstable modes.

P_0, R_0 : • Introduces coupling between the longitudinal and lateral/directional equation of motion set.

Couple longitudinal dynamics into the $\dot{P}$ and $\dot{R}$ equation through q.

- $\left[R_0 \cdot \left(\frac{I_z - I_y}{I_x}\right)\right] \cdot q$
- $\left[P_0 \cdot \left(\frac{I_z - I_y}{I_x}\right)\right] \cdot q$

Couple Longitudinal dynamics into the $\dot{v}$ equation through u and w

$\left[-R_0\right]u$ and $\left[P_0\right]w$

Table III (Cont) Summary of the Effects of Altitude, Velocity, Aerodynamic Angles and Steady Maneuvering on the Unaugmented Rigid Aircraft Stability. (References (30) and (32))

III. ANGULAR RATE EFFECTS (Cont)

P_0, R_0 : • Nonzero P_0 has only a small effect on the "fast" modes, primarily the Dutch-roll mode. However the combination of nonzero P_0 and small values of sideslip angle, β_0 of opposite sign destabilizes the Dutch-roll mode for the reference aircraft.

P_0 destabilizes the phugoid mode in general.

Nonzero R_0 has a mild stabilizing effect on the Dutch-roll and spiral modes while short-period and phugoid damping decrease.

Table III (Concluded) Summary of the Effects of Altitude, Velocity, Aerodynamic Angles and Steady Maneuvering on the Unaugmented Rigid Aircraft Stability. (References (30) and (32))

IV EFFECT OF AERODYNAMIC ANGLES (α, β) :

Affect :

- The orientation of the aircraft relative to the velocity vector and to a large extent define the flow field around the aircraft.
- Aerodynamic coefficients are typically a function of α and β and are prime determinants of the aerodynamic forces and moments.

Stability Impact :

- Significant variations in the speeds and shapes of the normal modes occur with variations in α_0 and β_0
  - Mean α_0 variations have significant effect on the eigenvalues (due to variations of the aerodynamic data with α). Mode shape (eigenvector) variations are small relative to other effects.
  - Mean Sideslip ($\beta_0 \neq 0$) introduces lateral/longitudinal coupling; therefore it has a large effect on the mode shapes (eigenvectors) without causing large changes in the eigenvalues.
  - Lateral/longitudinal coupling primarily occurs between modes of similar speed and can lead to a transfer of damping.

CHRONOLOGICAL REVIEW OF THE DEVELOPMENTS OF AIRCRAFT DEPARTURE SUSCEPTIBILITY CRITERIA

Much has been written on the subject of criteria which predict aircraft departure susceptibility. A review of these criteria immediately points out that linearization of the nonlinear rigid body aircraft equations-of-motion (see Figure 13) is common to the derivation of each, with the exception of Bihrle's Design Plots.

Table IV chronologically cites the major departure susceptibility criteria developments along with the associated researcher(s) and the referenced work.

It should be noted that some of the departure susceptibility criteria developments shown in Table IV are more closely classified as "stability" parameters (i.e., $C_{m_{\alpha COP}}$, $C_{n_{\alpha COP}}$, etc.) as opposed to parameters that have been correlated with aircraft departure susceptibility.

This section presents a review of the departure susceptability criteria developements given in Table IV. Each of the criteria will be discussed (in chronological order) in terms of its basic derivation, the impact the criterion has on aircraft design and the advantages and shortcomings of the criterion.

Table IV. Chronology of the Major Aircraft Departure Susceptibility Criteria Developements

DATE	PARAMETER(S)/CRITERION	RESEARCHER(S)/ REFERENCES	DESCRIPTION/ COMMENTS
1950	$C_{n_\beta} > 0$ $C_{l_\beta} < 0$	Unknown References: 24, 34	Lateral/directional body-axis stability derivative requirements for positive static stability.
1958	$C_{n_{BDYN}}$ See equation (19) AADP (or LCDP) > 0 (See equation (20))	Moul & Paulson (NASA, Langley) References: 3, 25, 30, 35, 36, 37, 38, 39, 40, 41	Open-loop, lateral-directional requirements for positive static stability about the velocity vector. Closed-loop, lateral-directional requirements for positive static stability with respect to roll control.
1971	$\alpha-\beta > 0$, $\alpha-\beta > \alpha_\delta$	Jenny (McDonnell Douglas) References: 37, 42, 43	Alternate form of the $C_{n_{BDYN}}$ and LCDP departure parameters. • $\alpha-\beta > 0$ implies $C_{n_{BDYN}} > 0$ • $\alpha-\beta > \alpha_\delta$ implies LCDP > 0 Criterion derived based on the summation of yawing moments about the z-stability axis being positive.
1971	$C_{n_{BDYN}}$ versus LCDP Criterion Plane (See Figure 28, 29 and 30).	Weissman (Wright-Patterson Air Force Base) References: 27, 28, 37, 44, 45, 46 Titiriga/Skow (Northrop) References: 47 Johnston (STI) References: 48	First criterion to correlate types and severity of aircraft departure susceptibility with a cross-plot of the open-loop lateral/directional departure parameter $C_{n_{BDYN}}$ and the closed-loop parameter LCDP.

Table IV (Cont). Chronology of the Major Aircraft Departure Susceptibility Criteria Developements

DATE	PARAMETER(S)/CRITERION	RESEARCHER(S)/ REFERENCES	DESCRIPTION/ COMMENTS
1974	A. Closed-loop Parameter $1/T_{\theta_3}$ and ω_θ, ω_{SR}, ω_ϕ B. Open-loop Parameters • Aerodynamic, $\mathcal{L}'_\alpha$, N'_α • Kinematic, Z_p, Z_r	Johnston (STI) References: 13, 37	Closed-loop stability parameter that indicates the potential of a roll-spiral divergence occurring due to longitudinal-lateral/directional coupling. Aerodynamic cross-coupling terms that manifest themselves in the calculation of $1/T_{\theta_3}$.
1978	$N_{\beta_{COP}} > 0$ $M_{\alpha_{COP}} > 0$ $A^2 - 4B > 0$ (See equations (41) to (47))	Kalviste (Northrop) References: 51, 52	Developed open-loop static stability criterion that accounts for the effects of asymmetric flight ($\beta \neq 0$), aerodvnamic longitudinal-lateral/directional cross-coupling, and nonlinear aerodynamic data
1978	C_{n_β} Versus C_{ℓ_β} Criterion Plane (See Figure 39)	Bihrle (BAR) References: 53	Empirically derived static stability preliminary design guidelines applicable to large angle transient maneuvering flight.
1980	$1/T_{\phi_1} > -0.5$ (Closed-loop, symmetric flight)	Johnston (STI) References: 13, 37, 47, 54	Closed-loop lateral/directional stability criterion that extends the application of LCDP to augmented aircraft.
1983	$C_{n_{\beta_{APP}}} > 0$ (See equation (51))	Pelikan (McDonnell Douglas) References: 55	Open-loop lateral/directional static departure susceptability criterion that extends $C_{n_{\beta_{DYN}}}$ to include the effect of the controls.

Table IV (Concluded). Chronology of the Major Aircraft Departure Susceptibility Criteria Developements

DATE	PARAMETER(S)/CRITERION	RESEARCHER(S)/ REFERENCES	DESCRIPTION/ COMMENTS
1989	$\mathcal{L}_{\beta_{COP}} > 0$ $N_{\dot{\beta}_{COP}} > 0$ $N_{\beta_{COP}} > 0$ $N_{\dot{\alpha}_{COP}} < 0$ $N_{\alpha_{COP}} < 0$ (See equation (69))	Kalviste (Northrop) References: 5	Open-loop longitudinal-lateral/directional dynamic stability parameters applicable to asymmetric, steady maneuvering flight.
1989	$C_{n_r} = \left(\frac{I_z}{I_x}\right)_B C_{l_\phi} > 0$ $C_{n_{BOYN}} > \frac{I_z\left(N_p^* L_r^* - L_p^* N_r^*\right)}{qSb}$ $\frac{I_x}{I_z}\left(\frac{C_{n_\beta}}{C_{l_\phi}}\right) > \frac{\left(N_r^* - N_p^* \tan\theta_0 \cos\phi_0\right)}{\left(L_r^* - L_p^* \tan\theta_0 \cos\phi_0\right)}$ $\frac{I_x}{I_z}\left(\frac{C_{n_\beta}}{C_{l_\phi}}\right) < \frac{\left(N_\Omega V - g\cos\beta_0 \cos\phi_0 \cos\theta_0\right)}{\left(L_\Omega V + g\cos\beta_0 \cos^2\phi_0 \sin\theta_0\right)}$ $LCDP_{CHODY} > \frac{-\left[Y_\beta^*\left[N_r^* - L_r^*\left(\frac{N_{\delta_a}}{L_{\delta_a}}\right)\right] - \left[N_p^* - L_p^*\left(\frac{N_{\delta_a}}{L_{\delta_a}}\right)\right]\tan\theta_0 \cos\phi\right.}{(\cos\alpha_0 + \sin\alpha_0 \tan\theta_0 \cos\phi_0)}$	Chody (Eidetics) Reference: 36	Addresses lateral-directional stability boundaries based on Routh's Stability Criteria for asymmetric, steady maneuvering flight.

(UNKNOWN): C_{n_β}, C_{ℓ_β}

DATE/RESEARCHER :

< 1950; (UNKNOWN): C_{n_β}, C_{ℓ_β}

CRITERIA :

Positive lateral/directional aerodynamic static stability.

$C_{n_\beta} > 0$: Basic static directional weathercock stability

$C_{\ell_\beta} < 0$: Dihedral Effect (lateral static stability)

BASIS OF CRITERIA :

Stable static lateral/directional moment data

TYPE OF CRITERIA :

Open-loop Static Stability Criteria

CRITERION PLOT :

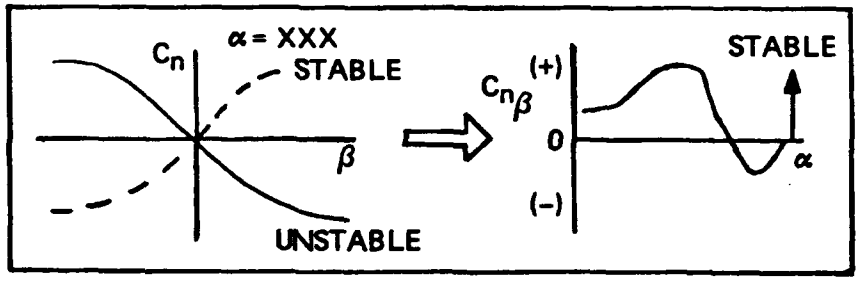

DESIGN IMPACT :

C_{n_β} : - Primarily determines natural frequency of the Dutch-roll mode $(\omega_n)_{DR}$

- factor in determining spiral stability
- prevents excessive sideslip and/or yawing motion while maneuvering and/or in turbulent air.
- aids in turn coordination

C_{ℓ_β} : -Prime factor in damping of the Dutch-roll and spiral mode.
- Good ζ_{DR} — C_{ℓ_β} ≅ small negative (stable) values

- Stable Spiral Stability → C_{ℓ_β} ≅ large negative values

- involved in maneuvering characteristics of the airframe especially with rudder alone controls near stall.

The sketches below illustrate the effect of varying C_{n_β} and C_{ℓ_β} on the lateral/directional characteristic modes.

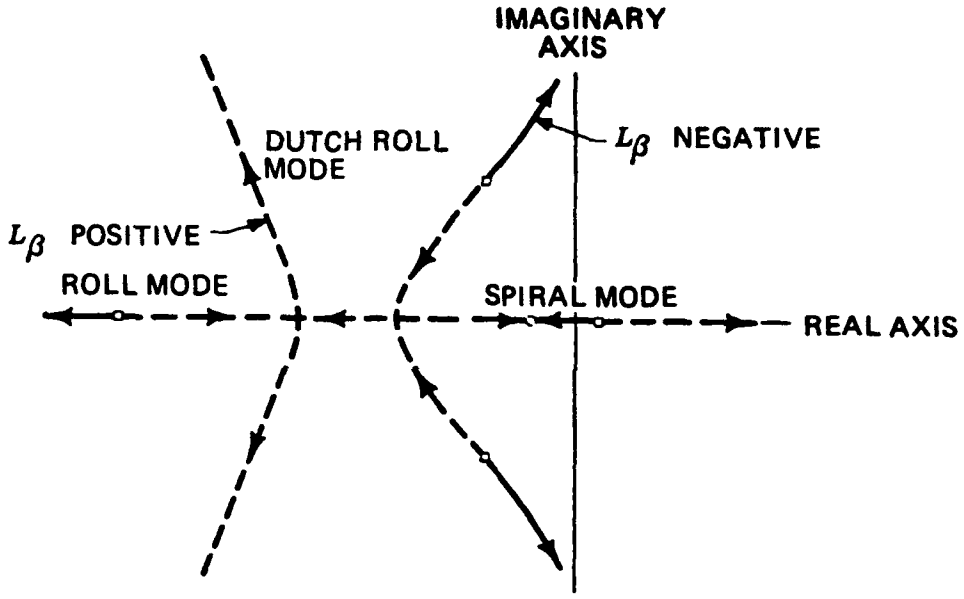

Figure 19 Lateral/Directional Root Locus Plot Varying C_{ℓ_β} (Reference (33))

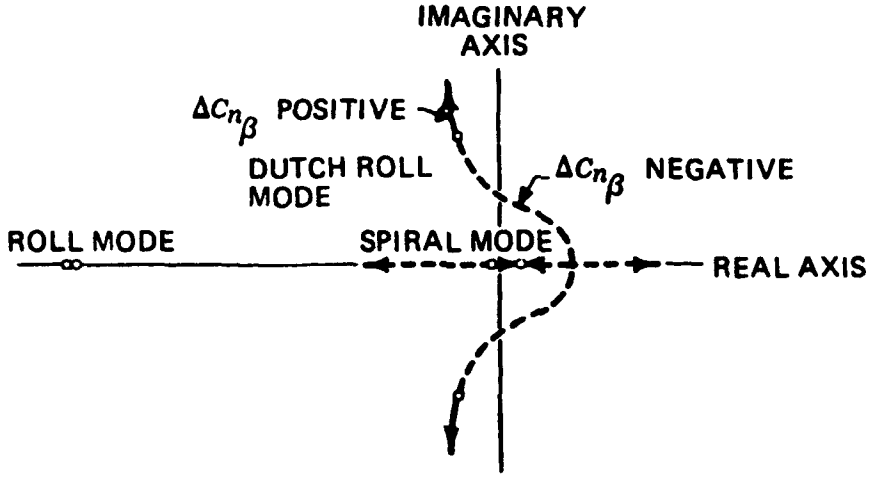

Figure 20 Lateral/Directional Root Locus Plot Varying C_{n_β} (Reference (34))

CRITERION ADVANTAGE(S) :

Data is available early to affect preliminary design phase (i.e., $C_{\ell_\beta} = f$ (AR, $\Lambda_{c/4}$, wing location, C_L, aeroelasticity, wing-fuselage interference; $C_{n_\beta} = f(S_{VT}, \ell_{VT},)$, fuselage/wing contribution).

CRITERION SHORTCOMINGS :

Criterion address only aerodynamic static stability of the unaugmented aircraft with respect to sideslip disturbances. The influence of maneuvering dynamics and aerodynamic cross-coupling are not considered.

MOUL & PAULSON: $Cn_{\beta DYN}$

DATE/RESEARCHER :

1958; Moul & Paulson (NASA, Langley)

CRITERIA :

A. Positive lateral/directional open-loop aircraft static stability about the velocity vector

$$Cn_{\beta DYN} > 0$$

where :

$$Cn_{\beta DYN} \triangleq Cn_{\beta}\cos\alpha - \left(\frac{Iz}{Ix}\right)_B Cl_{\beta}\sin\alpha \qquad (19)$$

B. Aileron Alone Departure Parameter (AADP)/Lateral Control Departure Parameter (LCDP)

Positive closed-loop lateral-directional stability when lateral control is used to provide constant roll rate.

$$\text{LCDP (or AADP)} > 0$$

where :

$$\text{LCDP} \triangleq (Cn_{\beta})_s - (Cl_{\beta})_s \left(\frac{Cn_{\delta_a}}{Cl_{\delta_a}}\right)_s \qquad (20)$$

(Note, LCDP is defined with stability-axis derivatives.)

BASIS OF $Cn_{\beta DYN}$ CRITERIA :

Derived from the general aircraft rigid body equations-of-motion by considering the stability of the linear uncoupled lateral/directional dynamics (i.e.,$\phi_0 = 0$ degrees and $V_o = 0$ ft/sec) and assuming the reference equilibrium state has zero angular rates (i.e., $P_o = Q_o = R_o = 0$ deg/sec and $\dot{\psi}_0 = \dot{\theta}_0 = \dot{\phi}_0 = 0$ deg/sec).

To test for stability, Routh's stability criteria is applied to the characteristic equation, $|(\lambda I - A)| = 0$ (where [A] is given in figure 17, See equation (21a)).

$$A\lambda^4 + B\lambda^3 + C\lambda^2 + D\lambda + E = 0 \qquad (21a)$$

A dynamic system becomes unstable and divergence will occur when one or more of the roots of the characteristic equation (eigenvalues) becomes positive. According to Routh's Stability Criterion, the characteristic equation, described by the quartic above, will have positive eigenvalues if any of the coefficients (A, B, C, D, E) or if the combination of coefficients $BCD-AD^2-B^2E$ (Routh's Discriminant) becomes negative.

Solving for the coefficients of the characteristic equation yields,

$$A = 1$$

$$B = -(Y_v + L'_p + N'_r) \tag{21b}$$

$$C = N'_v (U_o - Y_r) - L'_v (Y_p + W_o) + L'_p (Y_v + N'_r) + (Y_v N'_r - N'_p L'_r) \tag{21c}$$

$$D = N'_r [L_v (Y_p + W_o) - Y_v L'_p] \tag{21d}$$

$$+ N'_v [L'_p (Y_r - U_o) - L'_r (Y_p + W_o)]$$

$$+ N'_p [Y_v L'_r - L'_v (Y_r - U_o)]$$

$$+ g \cos\theta [N'_v \tan\theta_0 - L'_v]$$

$$E = -g\cos\theta \{-L'_v N'_p \tan\theta_0 + N'_v [L_p \tan\theta_0 - L_r] - L'_v N'_r\} \tag{21e}$$

Moul & Paulson concluded that the oscillatory instability that they observed was associated with a change in the sign of the "C" coefficient of the characteristic equation.

Rearranging and simplifying the "C" coefficient above to nondimensional form yields,

$$C = C'_{n_\beta}(\cos\alpha - \frac{\rho Sb}{4m} C_{Y_r}) - \left(\frac{I_z}{I_x}\right)_B \cdot C'_{\ell_\beta}(\sin\alpha + \frac{\rho Sb}{4m} \cdot C_{Y_p}) \qquad (22)$$

$$+ \frac{\rho Sb^3}{8I_x} [C'_{\ell_p} C'_{n_r} - C'_{\ell_r} C'_{n_p}]$$

$$+ \frac{\rho Sb}{4m} \cdot C_{Y_\beta} [C'_{n_r} + \left(\frac{I_z}{I_x}\right)_B \cdot C'_{\ell_p}]$$

The "C" coefficient given in equation (22) is rewritten as shown in equation (23) to aid in a later discussion on recent proposed extensions of the $C_{n_{\beta DYN}}$ concept as well as to help understand its limitations.

$$C = A + B + C \qquad (23)$$

where : $$A = C'_{n_\beta}(\cos\alpha - \frac{\rho Sb}{4m} C_{Y_r}) - \left(\frac{I_z}{I_x}\right)_B \cdot C'_{\ell_\beta}(\sin\alpha + \frac{\rho Sb}{4m} \cdot C_{Y_r})$$

$$B = \frac{\rho Sb^3}{8I_x} [C'_{\ell_p} C'_{n_r} - C'_{\ell_r} C'_{n_p}]$$

$$C = C_{Y_\beta}[C'_{n_r} + \left(\frac{I_z}{I_x}\right)_B \cdot C'_{\ell_p}]$$

To arrive at the expression for $C_{n_{\beta DYN}}$ most often seen in the literature (e.g., Mil Standard-1797A) the terms of equation (23) containing products of derivatives are assumed to be small compared to the other terms (i.e. this drops terms B and C from equation (23)) and the terms $\left(\frac{\rho Sb}{4m} C_{Y_r}\right)$ and $\left(\frac{\rho Sb}{4m} C_{Y_p}\right)$ are assumed small in the A term compared to $\cos\alpha$ and $\sin\alpha$ respectively.

Dropping these terms from equation (23) yields the expression,

$$C = C_{n_\beta} \cos\alpha - \left(\frac{I_z}{I_x}\right)_\beta C_{\ell_\beta} \sin\alpha \qquad (24)$$

$$\triangleq C_{n_{\beta DYN}}$$

Equation (24) is referred to as $C_{n_{\beta DYN}}$ because it has been found to be a good indicator of absolute (not relative) lateral/directional dynamic stability (without directly calculating the aircraft eigenvalves, i.e., $C_{n_{\beta DYN}} < 0$ implies lateral/directional instability) for a host of aircraft (see Reference (26)).

TYPE OF CRITERIA :

Open-loop Dynamic Stability Criteria

CRITERION PLOT :

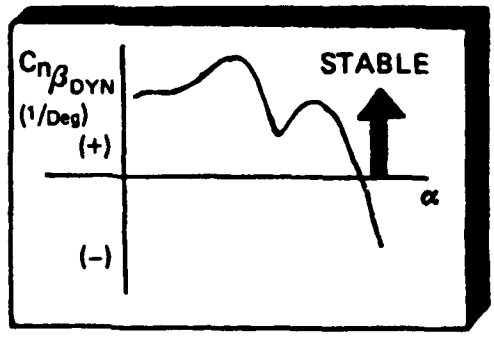

DESIGN IMPACT :

The $C_{n_{\beta DYN}}$ stability parameter shows that the effective directional stiffness is a function not only of the weathercock stability C_{n_β}, but also a function of the dihedral, C_{ℓ_β}, and the product of inertias I_x, I_z, and I_{xz}. The parameter illustrates clearly how at high angle-of-attack, a negative C_{n_β}

value (possibly due to tail immersion in the wing/body wake) can be stabilized by overriding negative (stable) values of $(I_Z/I_X\, C_{\ell_\beta})$.

As an approximation only (it is not very good for most swept wing fighter aircraft which have relatively large values of C_{ℓ_β} and significant I_{XZ} values) the $C_{n_{\beta DYN}}$ term can be related to the Dutch-roll natural frequency as shown in equations (25) to (27) below.

$$\omega_{n_{DR}}^2 \cong N'_{\beta_s} + Y_V N'_{r_s} \tag{25}$$

$$N'_{\beta_s} = \frac{\bar{q}Sb}{I_{Z_B}} C_{n_{\beta DYN}} \tag{26}$$

Provided $Y_V N'_{r_s} << N'_{\beta_s}$, then

$$C_{n_{\beta DYN}} \cong \frac{I_{Z_B}}{\bar{q}Sb}\omega_{n_{DR}}^2 \tag{27}$$

CRITERION ADVANTAGE(S) :

Data is available early to affect preliminary design phase (i.e., C_{ℓ_β} =; f ($AR_{\Lambda_{c/4}}$, wing location, etc) ; $C_{n_\beta} = f(S_{VT}, \ell_{VT}$, etc.))

CRITERION SHORTCOMINGS :

The ability of $C_{n_{\beta DYN}}$ to predict directional divergence can be affected in several ways, all of which are important to understanding its application and limitations. First off, it must be reiterated that the $C_{n_{\beta DYN}}$ parameter is derived purely from application of the Routh Stability Criteria to the "C" coefficient of the linear decoupled lateral/directional equations-of-motion. Other types of instabilities can also occur and have been correlated with departure susceptibility. For example, equation (27) reveals that $C_{n_{\beta DYN}}$ directly relates to the static stability of the Dutch-roll mode. However, $C_{n_{\beta DYN}} > 0$ does not preclude the existence of dynamic instability due to the Dutch roll damping term being negative. This could be revealed by analyzing the

"B-coefficient" of the characteristic equation (see equation (21a)). Still other instabilities associated with longitudinal and lateral/directional dynamic coupling have been associated with departure susceptibility. The properties of these instabilities will be discussed further under the Chody criteria and the $1/T_{\theta_3}$ departure susceptibility criteria.

The factors that directly affect the accuracy of the correlation between the $C_{n_{\beta DYN}}$ parameter and departure susceptibility (i.e., lateral/directional instability/divergence) are:

(1) The terms that were assumed negligible in reducing the C-coefficient of the linear lateral/directional equations-of-motion to $C_{n_{\beta DYN}}$.

In reference (25), calculations were made for two different configurations to compare the values of the C-coefficient (equation (22)) and the $C_{n_{\beta DYN}}$ parameter (equation (24)) to support the simplification. In terms of supporting the simplifications, the reported results were excellent for the two configurations considered. That is, the contribution of the B and C terms of equation (23) were negligible compared to the terms of A (see figure 21). Additionally the C_{Y_p} and C_{Y_r} terms of the A term are also negligible. It is interesting to note that the comparisons of the C- coefficient (unsimplified) and the simplified $C_{n_{\beta DYN}}$ parameter reproduced in figure 21 from reference (26) was considered up to an angle- of-attack of only 35-degrees. In comparison today's high performance fighter aircraft are capable of trimming up to angles-of-attack of 55 degrees (e.g., McDonnell Douglas F/A-18) and experimental aircraft such as the X-31A are being designed to maneuver up to angles-of-attack as large as 70 degrees to achieve maximum performance goals. The

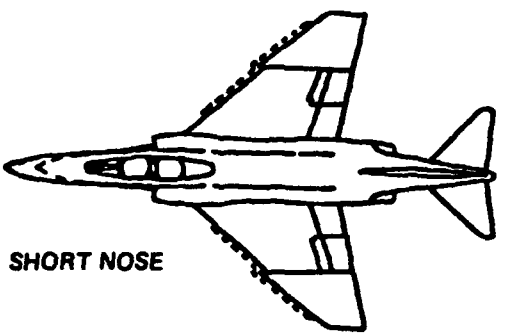

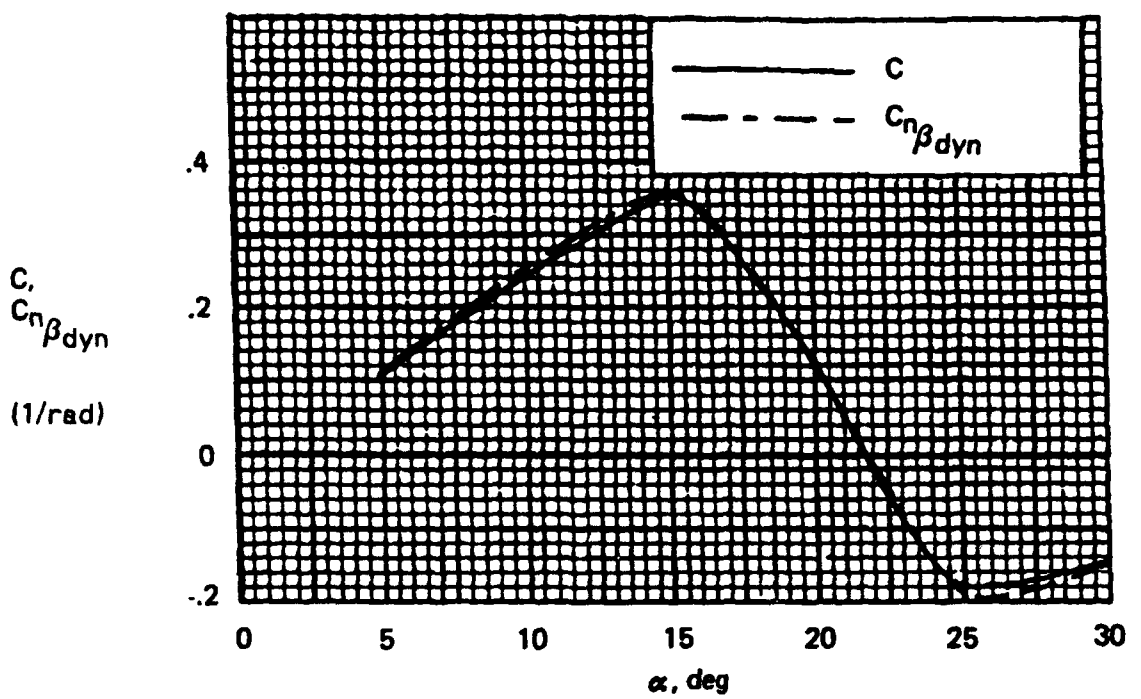

a. Configuration A

Figure 21 Comparison of the Lateral/Directional Characteristic Quartic C-Coefficient with $C_{n_{\beta DYN}}$ for Two Configuratons (Reference (26)).

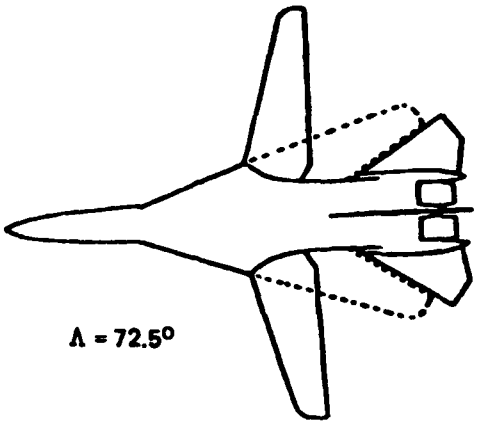

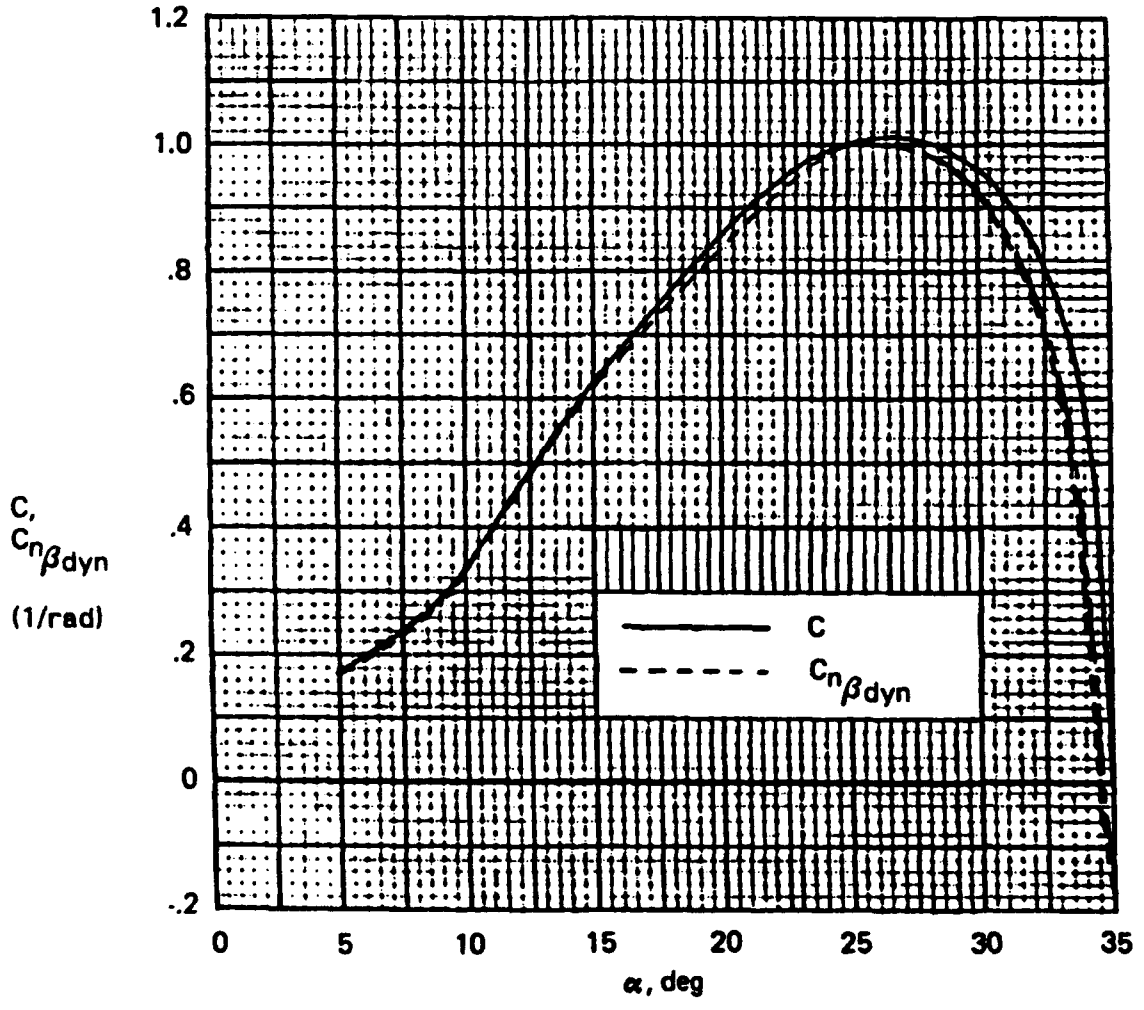

b. Configuration B

Figure 21 (Concluded) Comparison of the Lateral/Directional Characteristic Quartic C-Coefficient for Two Configuratons (Reference (26)).

same comparison of the C-coefficient with the $C_{n_{\beta DYN}}$ parameter has been repeated for a preliminary design of the X-31A aircraft from 20 degrees up to an angle-of-attack of 70 degrees. As illustrated in Figure 22, the X-31A data comparing the values of the C-coefficient and the $C_{n_{\beta DYN}}$ parameter overlay each other. In the case of the X-31A configuration the static characteristics (C_{ℓ_β} , C_{n_β}) entirely washout the second order effects of the dynamic terms. This data further supports use of the simplifying equation described by the $C_{n_{\beta DYN}}$ parameter to approximate the C-coefficient (equation (22)) of the lateral/directional quartic.

As pointed out in Reference (36), the fact that the dynamic derivatives can become important in determining the C-coefficient values of certain aircraft configurations might explain the inconsistency of the empirically derived boundaries for a minimum $C_{n_{\beta DYN}}$ value. As an example, the work of Reference (47) suggested that the design guidelines of Figure 23 be used in lieu of $C_{n_{\beta DYN}} > 0$ when considering the presence of possible aircraft asymmetrics, destabilizing external loads and nonlinear inertial coupling moments during maneuvering flight (Reference (36)). Reference (38) simplifies this even further and suggests that $C_{n_{\beta DYN}} > 0.004$ (1/deg).

(2) The assumption that C_ℓ and C_n are linear with sideslip angle.

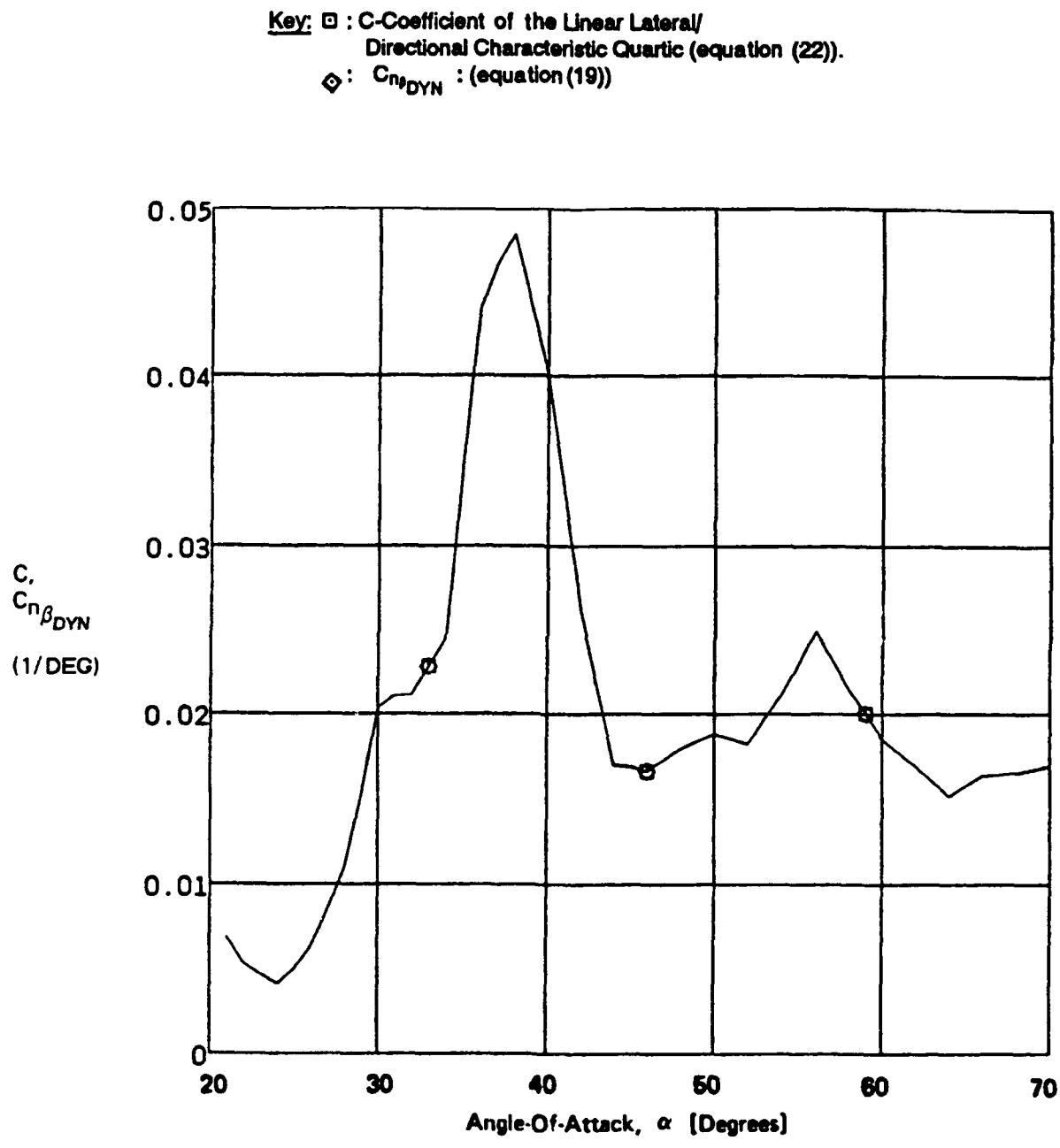

Figure 22 Comparison o f$C_{n_{\beta DYN}}$ and the C-coefficient of the Linear Lateral/Directional Characteristic Quartic for a Preliminary Configuration of the X-31A Aircraft.

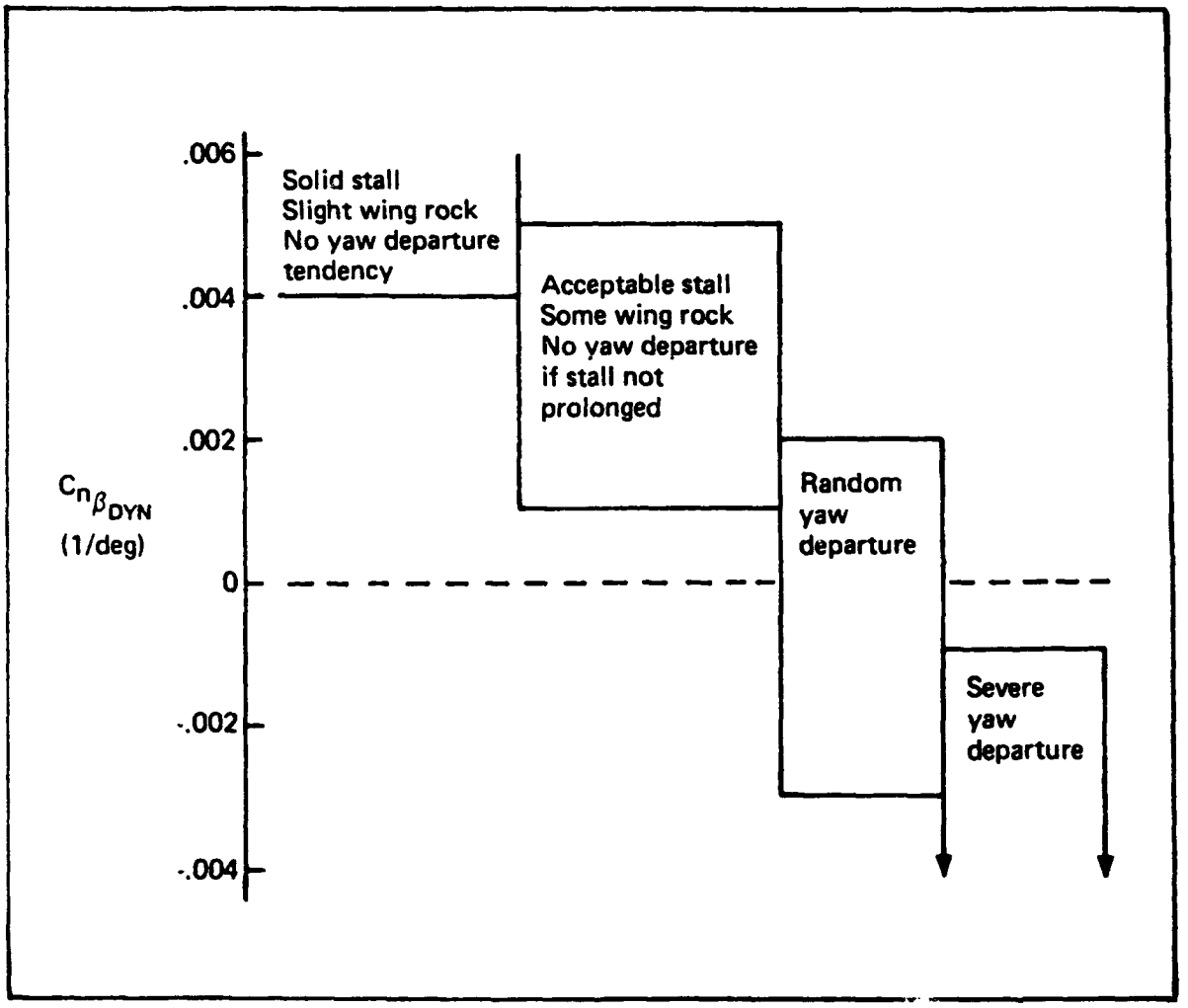

Figure 23 $C_{n_{\beta DYN}}$ Stability Design Guide as Suggested by Reference (47)

As illustrated with F-18 aircraft data in Figure 24, the aerodynamic rolling and yawing moments of many of today's fighter/attack aircraft are nonlinear with sideslip angle at large angles-of-attack.

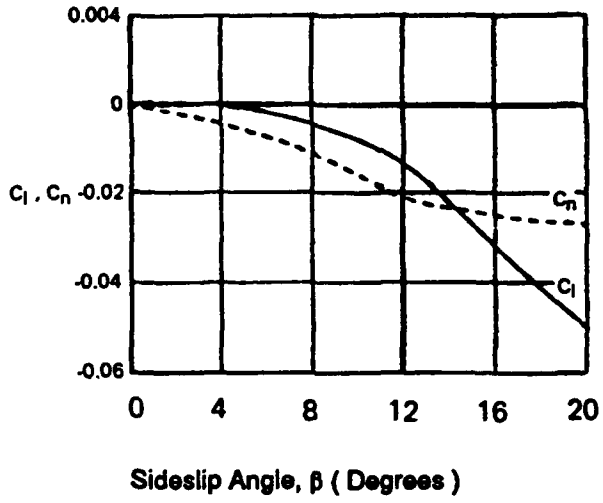

Figure 24 Nondimensional Rolling and Yawing Moment Coefficient Versus Sideslip Angle for the F-18 Aircraft at 30 Degrees Angle-of-Attack (Reference (43))

The analytical technique of linearizing C_ℓ and C_n at zero degrees of sideslip angle in these cases can lead to erroneous stability estimates. Given this fact along with the fact that most fighter/attack aircraft departure susceptibility degrades for asymmetric flight conditions makes asymmetric flight an important consideration in the determination of an aircraft's full envelope departure characteristics. As will be shown later, Pelikan's $C_{n_{\beta_{APP}}}$ criteria utilizes a secant slope technique (as opposed to the tangent slope) to account for the nonlinearity of the data. STI, Kalviste and Chody on the other hand, linearize the equations-of-motion assuming non-zero sideslip and calculate the beta derivatives (C_{ℓ_β}, C_{n_β}, etc) using the local tangent slope (i.e., $\partial C_n/\partial\beta\Big|_{\substack{\alpha o=xxx \\ \beta o=yyy}}$).

(3) The absence of accounting for dynamic maneuvering effects

(i. e. , $\dot{p} = L_p + \cdots + \left(\frac{I_y - I_z}{I_x}\right) \cdot [Q_0 r + R_0 q]$) and the associated longitudinal-lateral/directional cross-coupling as discussed earlier in table III.

(4) The $C_{n_{\rho DYN}}$ parameter can not predict a divergence that is caused by the controls.

At high angles-of-attack it is very common for today's fighter/attack aircraft for the rudder to be in a reduced dynamic pressure area of the wing and forebody wake resulting in reduced directional control effectiveness. Wind tunnel data for a preliminary X-31A configuration examplifies this fact. As shown in figure 25, the rudder control effectiveness essentially reduces to zero above fifty degrees angle-of-attack.

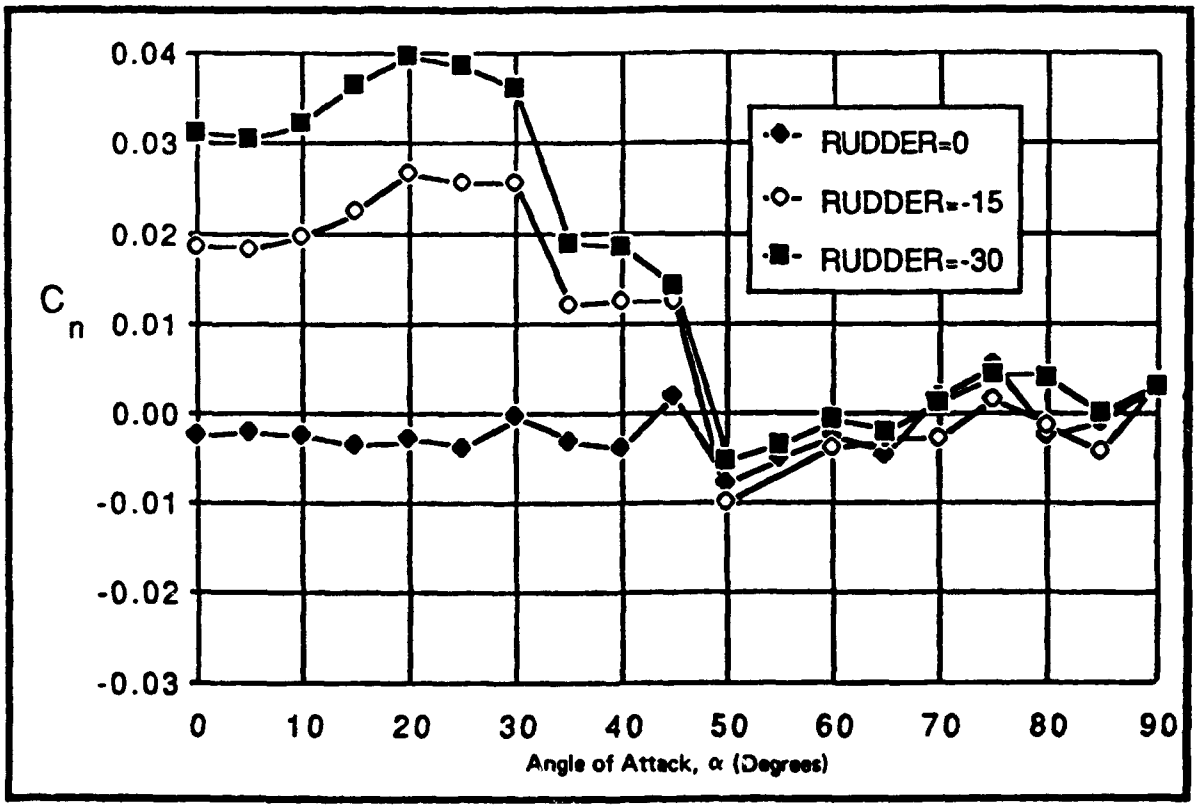

Figure 25 Rudder Control Effectiveness for a Preliminary Configuration of the X-31A Aircraft (Reference (11))

At the same time rudder control effectiveness is degrading with increasing angle-of-attack, the deflection of ailerons at high angles-of-attack often results in large adverse yawing moments. Using the same X-31A configuration as an example, figure 26 shows that differential flap deflection at low angles-of-attack produces proverse yaw, whereas at the higher angles-of-attack, above 60 degrees, full differential trailing-edge flap deflection is very effective in generating adverse yaw.

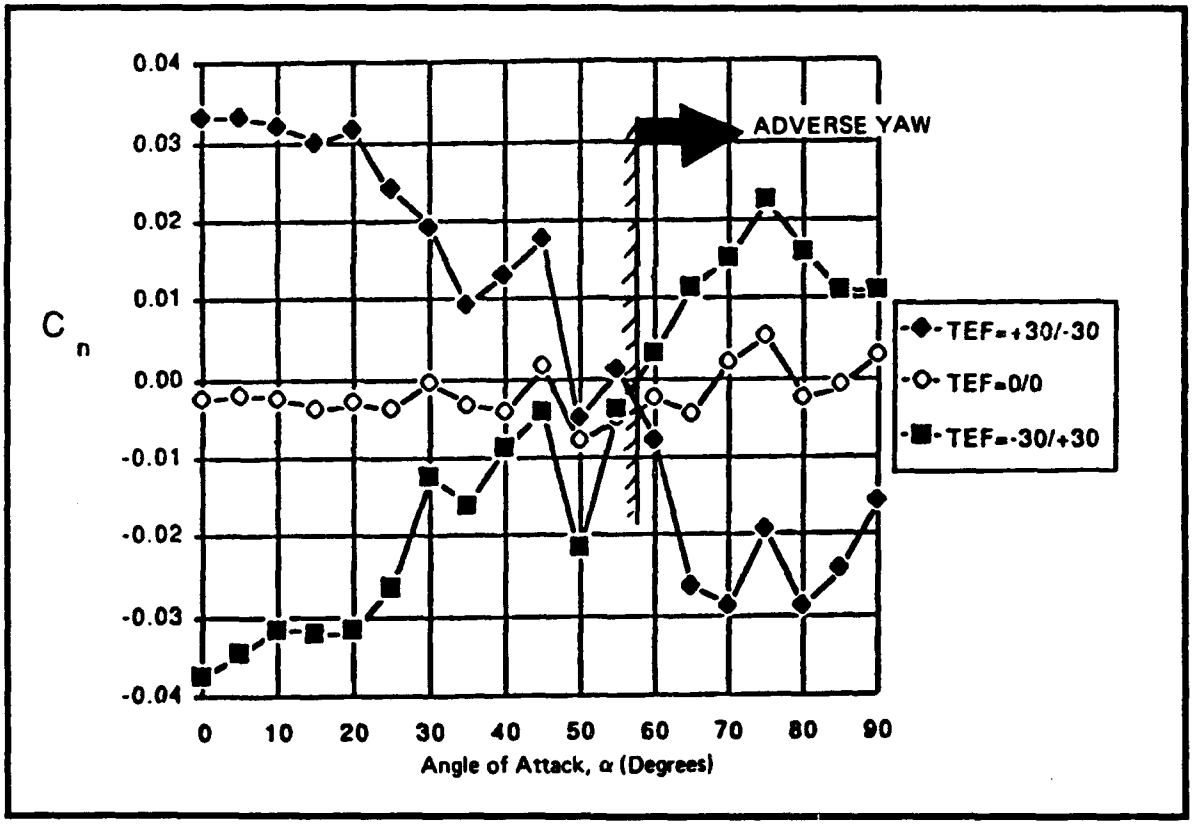

Figure 26 The Effect of Differential Trailing-edge Flap Deflection on the Generation of Adverse Yaw at High Angle-of Attack for a Preliminary Configuration of the X-31A Aircraft (Reference (11)).

This type of divergence can best be revealed by calculating the Lateral Control Departure Parameter (LCDP) discussed next.

(5) One final factor pointed out in Reference (26) which can affect the correlation of the $C_{n_{\beta DYN}}$ parameter with actual in-flight departure is the use of static data which do not accurately match flight conditions in calculating $C_{n_{\beta DYN}}$. The two most influential conditions which may not be matched are control deflections and engine power setting. In some cases these parameters can have substantial effects on the static lateral/directional stability parameters C_{n_β} and C_{ℓ_β}.

BASIS OF LCDP CRITERIA :

The LCDP parameter is derived based on determining conditions for which the roll attitude to aileron control input transfer function ($\phi(s)/\delta_a(s)$) is nonminimum phase (i.e., when the numerator polynominal, $N^{\phi}_{\delta_a}$, contains a zero in the right half plane (RHP) of the root locus). The equations-of-motion utilized are the linear uncoupled lateral/directional dynamics (i.e., rectilinear flight, $\phi_0 = 0$ degrees and $V_o = 0$ ft/sec) assuming the reference equilibrium state has zero angular rates (i.e., $P_o = Q_o = R_o = 0$ deg/sec and $\dot{\psi}_0 = \dot{\theta}_0 = \dot{\phi}_0 = 0$ deg/sec).

Routh's "Stability" Criteria is applied to the polynominal of equation (28) to determine whether the numerator polynominal, $N^{\phi}_{\delta_a}$ of the $\phi(s)/\delta_a(s)$ contains any RHP zeros.

$$N^{\phi}_{\delta_a} = A_\phi s^2 + B_\phi s + C_\phi \tag{28}$$

The numerator polynominal $N^{\phi}_{\delta_a}$ can be determined by taking the determinant of the matrix given by equation (29).

$$N^{\phi}_{\delta_a} = \begin{vmatrix} s-A_{11} & -A_{12} & -A_{13} & Y_{\delta_a} \\ -A_{21} & s-A_{22} & -A_{23} & L_{\delta_a} \\ -A_{31} & -A_{32} & s-A_{33} & N_{\delta_a} \\ -A_{41} & -A_{42} & -A_{43} & 0 \end{vmatrix} \tag{29}$$

A_{nm} = The elements of the decoupled lateral/directional body-axis Stability Matrix given in Figure 17.

According to Routh's Stability Criterion, the quadratic polynominal given by $N^{\phi}_{\delta_a}$ is guaranteed to have no RHP zeros if each of the coefficients, A_ϕ, B_ϕ, and C_ϕ as given in equation (28) have positive values. (Note, in addition to the assumptions of Figure 17, the algebraic expression for A_ϕ, B_ϕ, and C_ϕ assumes $Y_p = Y_r = Y_{\delta_a} = 0$).

$$A_\phi = 1 + \left(\frac{N'_{\delta_a}}{\mathcal{Y}^{\nu}_{\delta_a}}\right) \cdot \tan\theta_0 \tag{30a}$$

$$B_\phi = (N'_p \tan\theta_0 - N'_r - Y_\beta/U_0) + \frac{N'_{\delta_a}}{\mathcal{L}'_{\delta_a}}(\mathcal{L}'_r - \tan\theta_0(\mathcal{L}'_p + Y_v)) \tag{30b}$$

$$C_\phi = U_0[N'_v - \mathcal{L}'_v\left(\frac{N'_{\delta_a}}{\mathcal{L}'_{\delta_a}}\right)] + W_0\tan\theta_0[N'_v - \mathcal{L}'_v\left(\frac{N'_{\delta_a}}{\mathcal{L}'_{\delta_a}}\right)] \tag{30c}$$

$$+ Y_v\left\{N'_r - \mathcal{L}'_r\left(\frac{N'_{\delta_a}}{\mathcal{L}'_{\delta_a}}\right) - [N'_p - \mathcal{L}'_p\left(\frac{N'_{\delta_a}}{\mathcal{L}'_{\delta_a}}\right)]\tan\theta_0\right\}$$

Moul & Paulson found that negative values of the C_ϕ coefficient were associated with lateral/directional departures. In the derivation of the AADP, the condition for C_ϕ having a positive value was simplified to the expression given in equation (31a) by assuming that the Y_v term was second order and simplifying the first term by assuming the use of stability axis (where $U_0 = V_T$; $W_0 = 0$, and $\theta_0 = \gamma_0$ which is assumed to be zero. Also recall, $N'_\beta = N'_v \cdot V_T$; $\mathcal{L}'_\beta = \mathcal{L}'_v \cdot V_T$) yields,

$$C_{\phi_s} \cong (N'_\beta)_s - (\mathcal{L}'_\beta)_s\left(\frac{N'_{\delta_a}}{\mathcal{L}'_{\delta_a}}\right)_s > 0 \tag{31a}$$

$$\triangleq \text{AADP} > 0$$

or expressed in nondimensional terms,

$$\text{AADP} = (C'_{n_\beta})_s - (C'_{\ell_\beta})_s\left(\frac{C'_{n_{\delta_a}}}{C'_{\ell_{\delta_a}}}\right)_s \tag{31b}$$

Moul and Paulson extended the concept of the AADP departure susceptibility parameter to also be applicable to aircraft with an aileron-to-rudder interconnect (ARI). This expression is given by equation (32).

$$\text{LCDP}_{\text{ARI}} = -C'_{\ell_\beta}\frac{C'_{n_{\delta_a}} + KC'_{n_{\delta_r}}}{C'_{\ell_{\delta_a}} + KC'_{\ell_{\delta_r}}} > 0 \tag{32}$$

DaForno (Reference (41)) offers an alternative form of the ARI-LCDP parameter that allows for a more direct determination of the δ_a/δ_r crossfeed necessary to maintain LCDP positive (Reference (37)). This expression is given by equation (33).

$$C'_{n_\beta} - C'_{\ell_\beta}\frac{C'_{n\delta a}}{C'_{\ell_{\delta a}}} + [C'_{n_\beta} - C'_{\ell_\beta}\frac{C'_{n\delta r}}{C'_{\ell_{\delta r}}}]\cdot\frac{C_{\ell_{\delta r}}}{C_{\ell_{\delta a}}}\cdot\frac{\delta_r}{\delta_a} > 0 \qquad (33)$$

(Note, all derivatives are defined in the stability-axis)

Additionally, Weissman, in Reference (27) provides an expression for LCDP that addresses systems augmented with aileron plus rudder proportional to sideslip angle. This expression is given by equation (34).

$$C_{n_\beta} - C_{\ell_\beta}\left(\frac{C_{n_{\delta a}}}{C_{\ell_{\delta a}}}\right) + K_1\left(\frac{C_{n_{\delta a}}}{C_{\ell_{\delta a}}}C_{\ell_{\delta r}} - C_{n_{\delta r}}\right) > 0 \qquad (34)$$

where: $K_1 = -\frac{\delta_r}{\beta}$

(Note, all derivatives are defined in the stability-axis)

TYPE OF CRITERIA :

Closed-loop Lateral/Directional Static Stability Criteria with respect to roll control.

CRITERION PLOT:

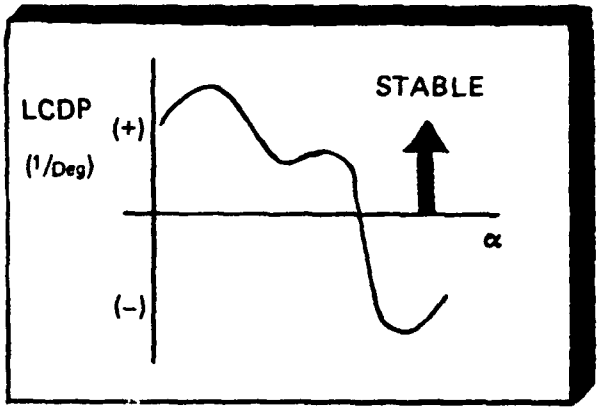

LCDP DESIGN IMPACT :

The LCDP departure susceptibility parameter primarily indicates conditions under which roll reversal (roll is in the opposite direction to that commanded) is likely to occur and divergence or

departure from controlled flight is likely to follow. This can be discerned from equation (31). The typical condition for LCDP having a negative value arises when yaw due to "aileron" (or lateral control) becomes sufficiently adverse (negative) that the second term overpowers moderately positive values of C_{n_β} (Reference (37)).

A dynamic system becomes unstable in a closed-loop sense when open-loop system poles (airframe or flight control system) are driven toward open-loop zeros located in the RHP (called nonminimum phase zeros) of the $\sigma - j\omega$ root locus plane. Nonminimum phase zeros can have a significant influence on an aircraft's transient response. Typical of nonminimum phase systems is the associated control reversal of the initial response as illustrated in figure (27).

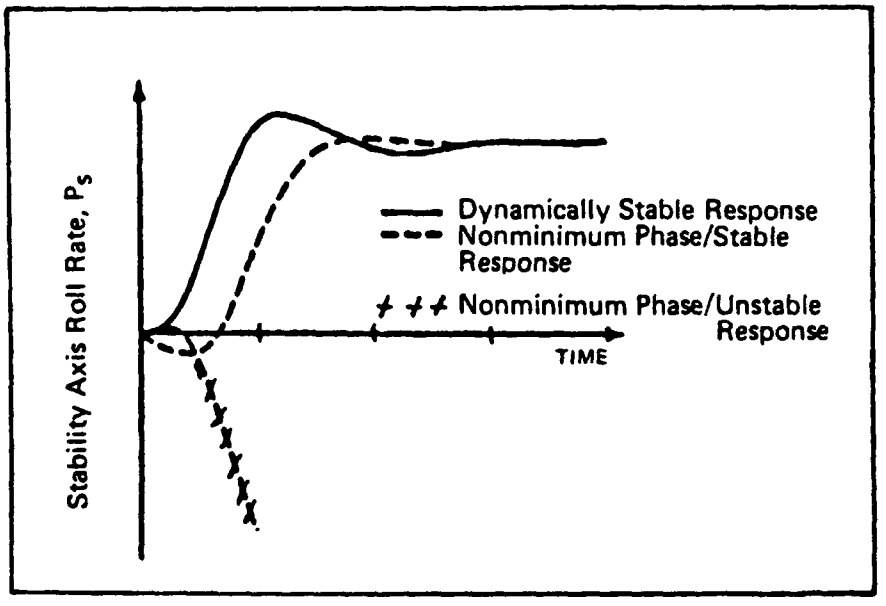

Figure 27 Typical Step Responses for Nonminimum Phase Systems

The nonminimum-phase type of response is undesirable (i.e., the magnitude and sign of the motion is not predictable) because closed-loop pilot control is difficult to the point where the system can be driven unstable.

As mentioned earlier, aircraft departure susceptibility is both an open-loop and a closed-loop phenomena. As with most flying qualities criteria, emphasis should be placed on the development of closed-loop parameters and relate them to open-loop parameters. In the study of Reference (13) one of the chief findings was that departure is "severely aggravated if not caused by closed-loop pilot/vehicle interaction". Along these lines, the LCDP is the most rudimentary and most widely accepted closed-loop departure susceptibility parameter.

WEISSMAN: $C_{n_{\beta DYN}}$ vs LCDP

DATE/RESEARCHER :

1971; WEISSMAN

CRITERION :

$C_{n_{\beta DYN}}$ versus LCDP Departure Susceptibility Criterion Plane as shown in Figure 28.

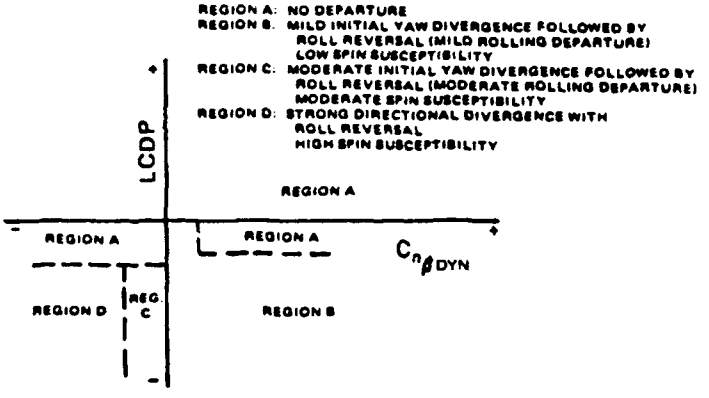

Figure 28 Weissman $C_{n_{\beta DYN}}$ Versus LCDP Departure Susceptibility Criterion Plane

BASIS OF CRITERION :

Weissman developed the criterion from analyzing time history sensitivity studies to lateral/directional static stability derivatives in a digital six degree-of-freedom off-line simulation. Based on these time history traces, Weissman empirically identified regions of increasing roll departure severity and spin susceptibility (see Reference (44)). Weissman later correlated flight test data (F-8, F-102, F-106 and SAAB 37) with his previously defined boundaries (Reference (45)) and found good agreement. The work of Titiriga (Reference (47)) modified Weissman's original criterion plane by adding boundaries for regions E and F. These two regions delineate susceptibility of an aircraft to depart controlled flight in yaw rather than roll (see Figure 29).

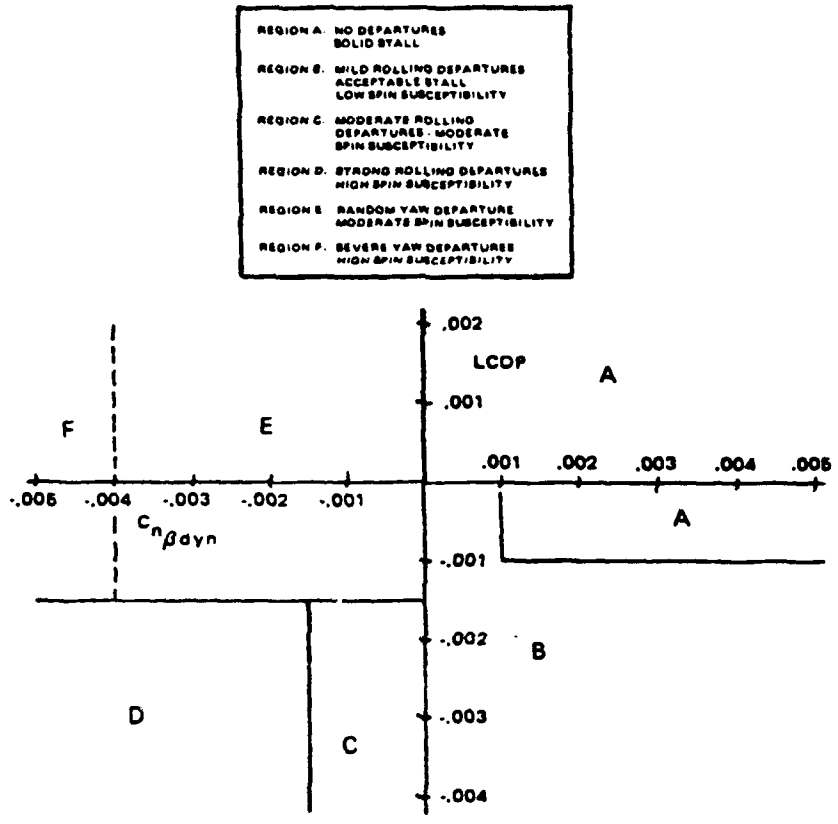

Figure 29 Weissman LCDP Versus $C_{n_{\beta_{DYN}}}$ Departure Susceptibility Criterion Plane as Modified by Skow and Titiriga of Reference (37)

STI has in turn suggested further modifications to the Northrop Modified Weissman Departure and Spin Susceptibility Criterion Plane. The modifications involved shifting the E/F boundary to coincide with the C/D boundary; raising the boundary between the E/F and C/D regions; and extending the A/B boundary to the LCDP axis. These changes were supported by the piloted simulation documented in Reference (48). The STI Modified Weissman Departure and Spin Susceptibility Criterion is shown in Figure 30.

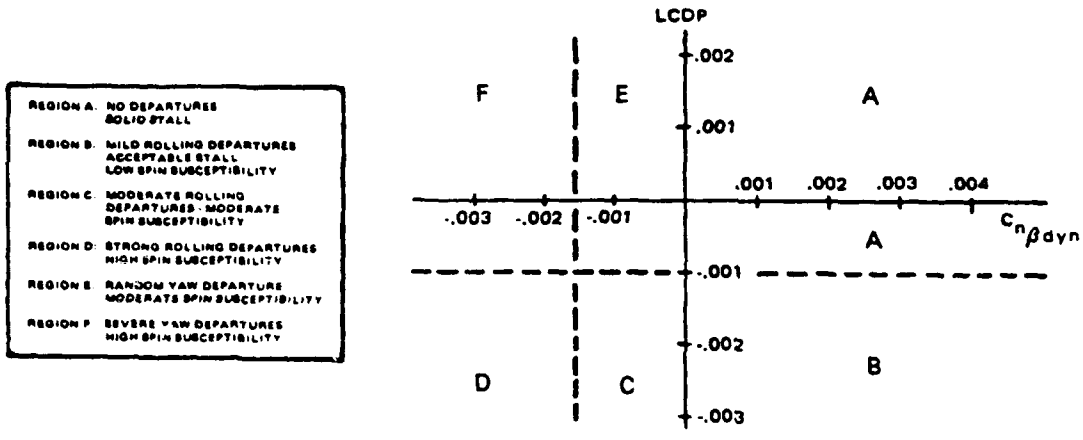

Figure 30 Weissman LCDP Versus $C_{n_{\beta DYN}}$ Departure Susceptibility Criterion Plane as Modified by STI (Reference (48))

TYPE OF CRITERION :

Combined Open and Closed-loop Lateral/Directional Departure/Spin Susceptibility Criteria.

CRITERION PLANE :

See Figure 28, 29 and 30.

DESIGN IMPACT :

The authors of References 37 and 46 offer an insightful design interpretation of the $C_{n_{\beta DYN}}$ versus LCDP criterion plane based on the assumption that active roll control[1] is being attempted by the pilot (and/or flight control system) and that the $C_{n_{\beta DYN}}$ and LCDP departure parameters can be

[1] Note that for augmented aircraft the use of any feedback to rudder/aileron, with the exception of roll or roll rate, will alter the roll- numerator roots, ω_ϕ, and hence the effective LCDP value (Reference (37)).

approximated by the simplified Dutch-roll pole-zero frequency relationships of equations (35) and (36).

$$\omega_{n_{DR}}^2 \simeq \frac{\bar{q}Sb}{I_{z_B}} C_{n_{\beta DYN}} \tag{35}$$

$$\omega_{\phi}^2 \simeq \frac{\bar{q}Sb}{I_{z_S}} LCDP \tag{36}$$

Figure 31 shows the pole-zero relationships associated with each of the $C_{n_{\beta DYN}}$ versus LCDP criterion plane quadrants. The arrows show the direction of the closed-loop root migration with increased loop gain.

Region A depicts three cases all of which are open-loop stable and closed-loop stable at high gain. The differences between the three cases is as follows:

(1) For $\omega_{\phi}/\omega_{n_{DR}}$ greater than one the locus beginning at the Dutch-roll pole will proceed counterclockwise into the zero in a roughly circular arc. Note that if ζ_{ϕ} and ζ_{DR} are lightly damped (i.e., close to the $j\omega$-axis) the locus may pass very close, or even into the unstable RHP.

(2) For $\omega_{\phi}/\omega_{n_{DR}}$ equal to one the Dutch-roll mode is not excited by the effective lateral control law and is thus decoupled.

(3) For $\omega_{\phi}/\omega_{n_{DR}}$ less than one the locus proceeds counterclockwise from the Dutch-roll pole to the zero, as a result the Dutch-roll damping increases slightly.

Region B indicates that roll control reversal exists and that with increasing pilot or FCS gain the Dutch-roll mode will eventually go unstable.

Regions C and D indicate an airframe instability ($C_{n_{\beta DYN}} < 0$) that can not be stabilized by roll control; and Regions E and F indicate an airframe instability that can be compensated via roll control. To summarize, when LCDP (ω_{ϕ}^2) is negative, closing the roll loop may lead to

$$\frac{\phi}{\delta_a} = \frac{L'_{\delta_a}[\zeta_\phi, \omega_\phi]}{(1/T_S)(1/T_R)[\zeta_{DR}, \omega_{n_{DR}}]}$$

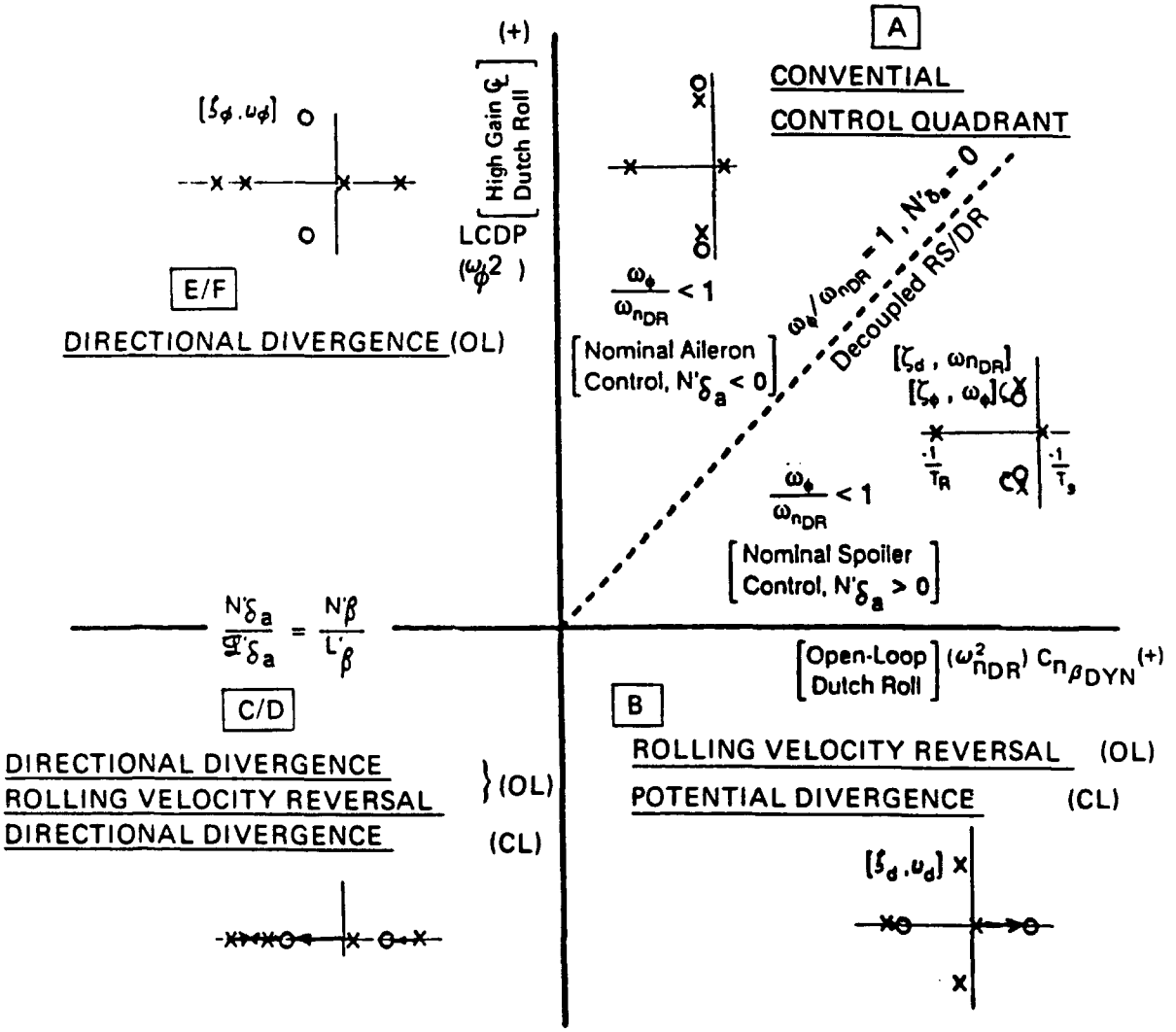

Figure 31 Generalized Pole-Zero Relationships Associated With Quadrants Of The LCDP Versus $C_{n_{\beta_{DYN}}}$ Criterion Plane (Reference (46))

divergent motions or if $\zeta_{DR}, \zeta_{\phi} << 1$ and $\omega_{\phi}/\omega_{n_{DR}} > 1$ closing the roll loop may lead to oscillatory instabilities. When LCDP is negative, the possibility of stabilizing the Dutch-roll mode with aileron control vanishes and other means must be utilized such as an a_y or β feedback to rudder control is required.

This points out that, when designing for "good" closed-loop flying qualities, modifications to basic airframe dynamics as well as the FCS design to obtain favorable zero locations (*i. e.*, $\omega_{\phi}^2 \cong$ LCDP) is just as important, if not more important than, the open-loop eigenvalues.

From a configuration perspective, low or negative values of LCDP can be improved by reducing the effective dihedral, C_{ℓ_β} and or utilizing a blended spoiler/aileron control to mitigate adverse yaw ($C_{n_{\delta_a}}$) characteristics.

Additionally, via flight control system augmentation, directional stability can be improved by augmenting C_{n_β} and adverse yaw can be reduced by use of an aileron-to-rudder interconnect control law scheme. Both of these means of augmentation require the availability of sufficient directional control power, which is not typically available at high angles-of-attack using conventional aerodynamic controllers. The X-31A aircraft is a good example of this. As illustrated in Figure 25, the aerodynamic rudder effectiveness is effectively zero above 45 degrees angle-of-attack. Above 45 degrees angle-of-attack the yaw thrust vectoring controller must be relied upon to provide all the directional control power necessary to maintain stability and control to prevent the possibility of departing controlled flight.

Besides thrust vectoring control, another alternative means of providing directional control power that is beginning to show some promise at high angles-of-attack is the use of active forebody

strakes. The strakes are used to control the relatively powerful, forebody, vortices that eminate from the apex of the sharp forebodies of most current fighter type aircraft. Reference (49) and (50) are good sources to gain more information concerning current research advances of this new configuration design technology.

$C_{n_{\beta DYN}}$ versus LCDP CRITERION ADVANTAGES :

The use of the $C_{n_{\beta DYN}}$ versus LCDP Departure Susceptibility Criterion Plane provides two major advantages over either of the two departure parameters $C_{n_{\beta DYN}}$ or LDCP independently. First off it provides both open and closed-loop lateral/directional stability information on a single criterion plane and secondly the two parameters have been correlated with flight test data to identify regions of the criterion plane in terms of the type and severity of departure that can be expected. A third and important advantage of this criterion is that the parameters can be calculated early enough in the design phase to affect the final configuration.

SHORTCOMINGS OF THE $C_{n_{\beta DYN}}$ versus LCDP CRITERION :

As pointed out earlier under the sections that discussed the $C_{n_{\beta DYN}}$ and LCDP departure parameters, their derivations are based on the assumptions of uncoupled longitudinal and lateral/directional dynamics for rectilinear, steady state flight conditions. Additionally, both parameters neglect second order terms that can be significant for certain aircraft configurations. This section briefly summarized the evolution of the $C_{n_{\beta DYN}}$ versus LCDP Departure Susceptibility Criterion and one should observe (as pointed out by MIL-STD-1797A) that using the same "static-based" parameters, independent investigations have proposed different criterion boundaries and not a common one. This points out that one must clearly understand the assumptions and limitations of the parameters and the criterion planes based on these parameters when applying them to "new" aircraft configurations and flight conditions that violate the underlying assumptions and data base used to develop the criterion.

JOHNSTON: $1/T_{\theta_3}$

DATE / RESEARCHER :

1974 ; Johnston (STI)

CRITERION :

No departure susceptibility criterion was proposed but open- and closed-loop departure parameters were identified for the A-7 aircraft considering the effects of nonzero sideslip angle and the coupled (longitudinal-lateral/directional) equations-of-motion. The closed loop nose-slice departure parameter was identified as $1/T_{\theta_3}$ which is the nonminimum phase zero of the $N^{\theta}_{\delta_e}/\Delta$ transfer function of the complete six degree-of-freedom bare airframe system as given in equation 37.

$$\frac{\theta}{\delta_e} = \frac{N^{\theta}_{\delta_e}}{\Delta} = \frac{K_{\theta}(-1/T_{\theta_3})(1/T_{\theta_2})\left[\zeta_{\theta_1}, \omega_{n_{\theta_1}}\right]\left[\zeta_{\theta_2}, \omega_{n_{\theta_2}}\right]}{[\zeta_p, \omega_{n_p}]\,[\zeta_{RS}, \omega_{n_{RS}}]\,[\zeta_{DR}, \omega_{n_{DR}}]\,[\zeta_{SP}, \omega_{n_{SP}}]} \qquad (37)$$

The nose slice departure parameter was found to be strongly related to the open-loop aerodynamic parameters N'_{α} and $\mathcal{L}'_{\alpha}$ and the kinematic terms $Z_p(\tilde{=} \beta_0 \cos\alpha_0)$ and $Z_r(\tilde{=}\beta_0 \sin\alpha_0)$ as given in Figure 32.

In trying to understand and predict the nose-slice departure characteristics of the A-7 aircraft which evolve from unsymmetrical flight (directional mistrim or miscoordination during maneuvering), Johnston concluded that although pilot ratings (from a fixed base simulation) could not be correlated with any single flying quality parameter, the A-7 departure characteristics were most dependent upon the coupled longitudinal-lateral/directional closed-loop parameter, $1/T_{\theta_3}$. At the A-7's departure angle-of- attack the parameter $1/T_{\theta_3}$ is located in the RHP of the root locus and with "normal" pilot pitch attitude control activity the aircraft/pilot system is driven unstable.

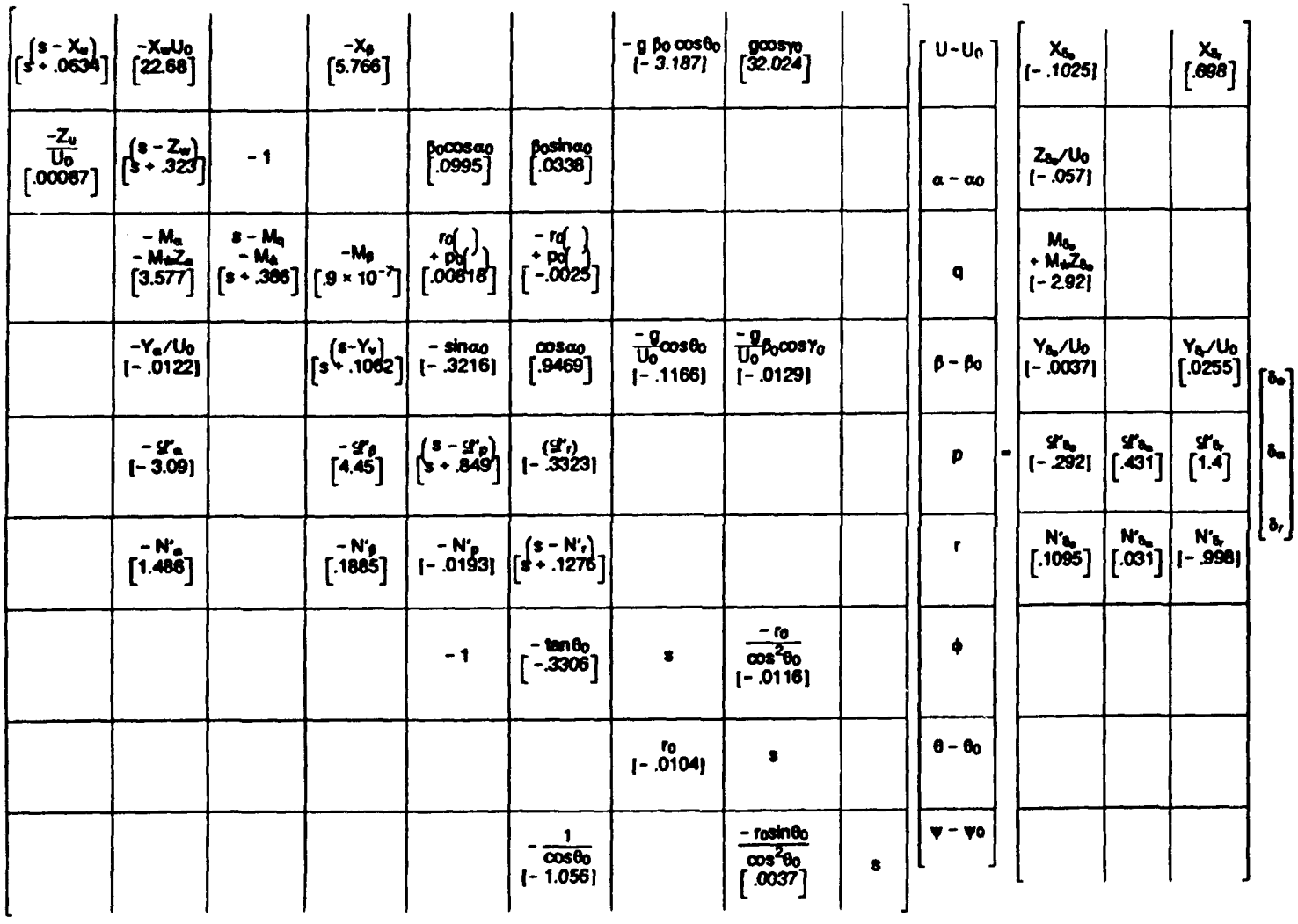

Figure 32 Linear, Rigid, Six Degree-of-Freedom Coupled ($\beta \neq 0$)Equations-of-Motion for the Unuaugmented A-7 Aircraft (Data For $\alpha_0 = 18.8°$; $\beta_0 = 6°$) (Reference (13))

Figure 33 shows a comparison between the bare airframe pole-zero locations of the uncoupled and coupled $N^{\theta}_{\delta_e}/\Delta$ transfer function for the A-7 aircraft near its stall angle-of-attack.

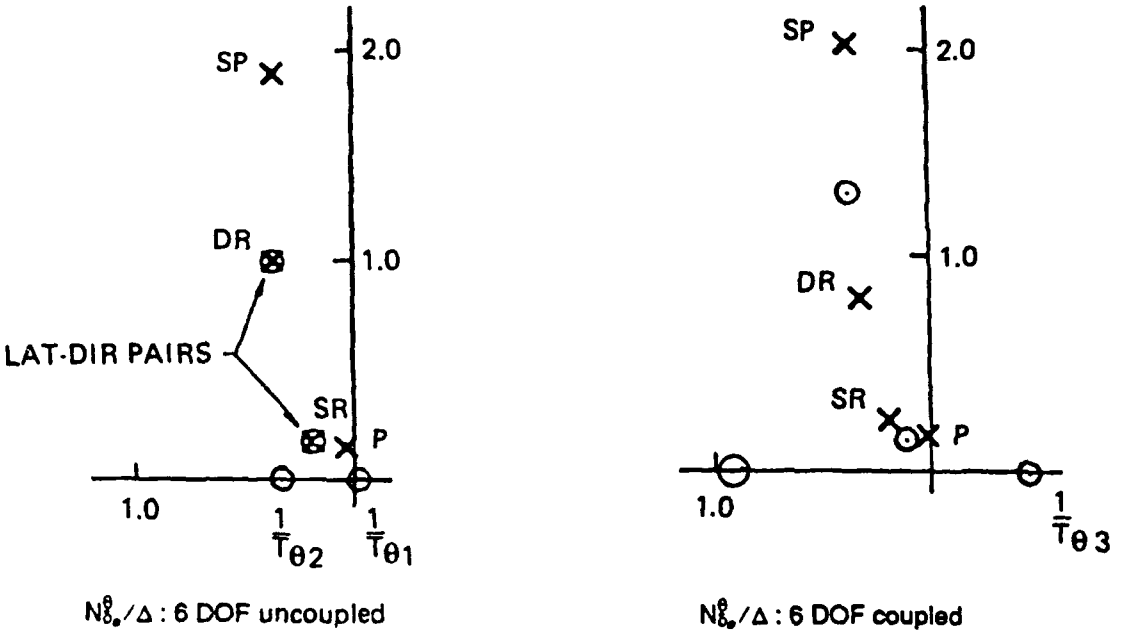

$N^{\theta}_{\delta_e}/\Delta$: 6 DOF uncoupled

$N^{\theta}_{\delta_e}/\Delta$: 6 DOF coupled

Figure 33 Comparison Between the Pole-Zero Locations of the N_{δ_e}/Δ Transfer Function for the Uncoupled and Coupled 6 DOF Equation-of-Motion for the A-7 Aircraft ($\alpha_0 = 18.8^{\circ}$, $\beta_0 = 6^{\circ}$) (Reference (13))

In the uncoupled six degree-of-freedom case the two lateral-directional modes ($\omega_{n_{DR}}$, $\omega_{n_{SR}}$) have cancelling pole-zero dipoles; the longitudinal zero $1/T_{\theta_2}$ is small and positive (LHP); and as might be expected near stall, $1/T_{\theta_1}$ is slightly negative (RHP). For the completely coupled six

degree-of-freedom case, the coupling has a relatively small effect on the eigenvalues[1] compared to a major shift it produces on the zero locations. Of primary concern is the shift of the $1/T_{\theta_1}$ zero into the RHP. Also of concern is the increased separation of the Dutch-roll dipole pair which indicates considerable Dutch roll modal response excitation exists via the elevator controller.

After eliminating the $\dot{U}$ equation from the complete equations-of-motion and observing that the zeros identified as $1/T_{\theta_1}$ and $1/T_{\theta_2}$ remained unchanged (the $1/T_{\theta_1}$ zero is usually eliminated) in location from the complete six degree-of-freedom case (see Figure 34), Johnston deduced that the nonminimum phase zero is a result of the lateral-longitudinal coupling and thereafter identified it as $1/T_{\theta_3}$ (as opposed to $1/T_{\theta_1}$).

A root locus showing a pure gain closure of pitch attitude to elevator is shown in Figure 35 for the six degree-of-freedom coupled airframe in nonsymmetric flight.

Equation 38 provides a simplified expression for $1/T_{\theta_3}$ after all the damping derivatives are neglected.

$$1/T_{\theta_3} \cong \frac{\mathcal{Y}'_\alpha N_\beta - \mathcal{Y}'_\beta N'_\alpha}{\mathcal{Y}'_\alpha \cos\alpha_0 + N'_\alpha \sin\alpha_0} \qquad (38)$$

To avoid a potential closed-loop "spiral" divergence, $1/T_{\theta_3}$ must remain positive.

---

[1] Nonzero sideslip angle has little effect on the longitudinal eigenvalues. The major shift is on the lateral/directional modes in which increasing sideslip causes the roll subsidence and spiral modes to couple into a lateral oscillation (i.e., lateral phugoid). Typically with increased sideslip angle, the Dutch-roll and lateral phugoid modes interchange damping. That is, with increasing sideslip angle, damping of the Dutch-roll mode increases while the damping of the lateral phugoid mode decreases.

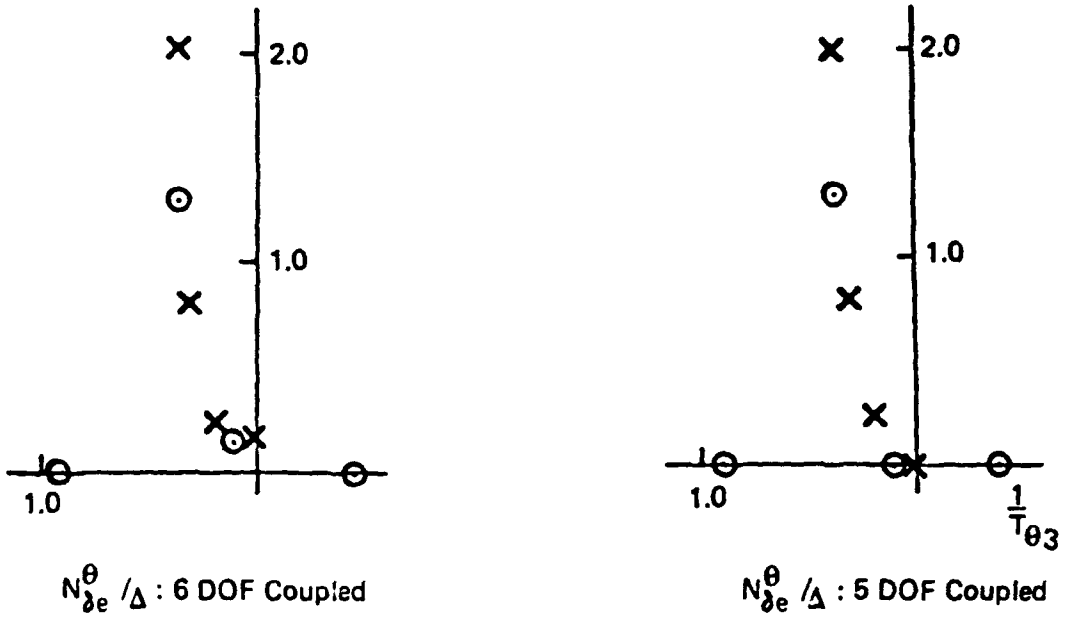

$N^{\theta}_{\delta e}/\Delta$: 6 DOF Coupled

$N^{\theta}_{\delta e}/\Delta$: 5 DOF Coupled

Figure 34 Comparison between the Pole-Zero Locations of the $N^{\theta}_{\delta_e}/\Delta$ Transfer Function for the 6 DOF Equations-of-Motion and the 5 DOF Equations-of-Motion (No Ù-equation) for the A-7 Aircraft ($\alpha_0 = 18.8^{\circ}$, $\beta_0 = 6^{\circ}$) (Reference (13))

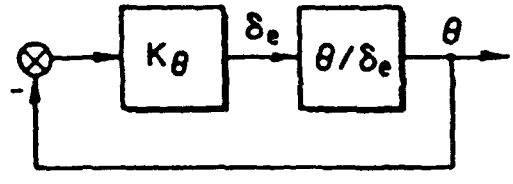

$$\frac{\theta}{\delta_e} = \frac{-2.9(-.3)(.866)[.28,.185][.27,1.4]}{[.163,.167][.71,.29][.36,.88][.185,2.1]}$$

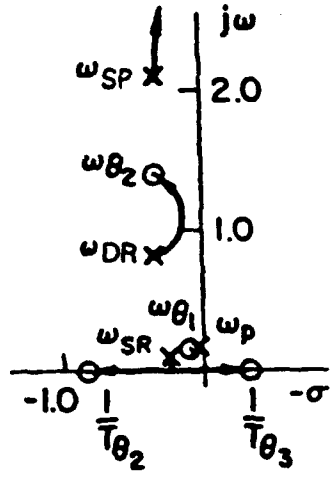

Figure 35 Root Locus Plot for the Six Degree-of-Freedom Coupled ($\beta \neq 0$) θ/δ_e Transfer Function (Data for the A-7 Aircraft; $\alpha_0 = 18.8^{\circ}$, $\beta_0 = 6^{\circ}$) (Reference (13))

The root locus plot shows how the roots starting at ω_{nSR} rapidly move to the real-axis and then split into two real roots, one of which moves towards the $1/T_{\theta_2}$ zero; the other moves toward the nonminimum phase zero, $1/T_{\theta_3}$.

Figure 36 shows the system time response when the pitch attitude loop is closed with unity gain and a step attitude command, θ_c, of 0.01 radians is introduced. The aircraft is initially trimmed for steady flight at α_0 = 18.8 degrees, β_0 = 6 degrees, and ϕ_0 = 5 degrees. The predicted first-order divergence is shown to start immediately and to dominate the r, ψ, ϕ, θ and α traces.

The cause of the RHP zero, $1/T_{\theta_3}$, was traced back through the 9 x 9 equations of motion matrix (see Figure 32) to the dominant coupling terms $\mathcal{L}'_\alpha$, N'_α, Z_p and Z_r. $\mathcal{L}'_\alpha$ and N'_α are the dimensional aerodynamic cross-coupling stability derivatives as given by equations 39 and 40.

$$\mathcal{L}'_\alpha = \frac{\partial \dot{p}}{\partial \alpha} = \frac{\bar{q}Sb}{I_xI_z - I_{xz}^2} \cdot \left(I_z\frac{\partial C_\ell}{\partial \alpha} + I_{xz}\frac{\partial C_n}{\partial \alpha}\right) \tag{39}$$

$$N'_\alpha = \frac{\partial \dot{r}}{\partial \alpha} = \frac{\bar{q}Sb}{I_xI_z - I_{xz}^2} \cdot \left(I_{xz}\frac{\partial C_\ell}{\partial \alpha} + I_x\frac{\partial C_n}{\partial \alpha}\right) \tag{40}$$

Wind tunnel tests and tuft studies performed on the A-7 aircraft revealed that the decrease in directional stability is attributed to the vortex activity from the fuselage and wing center panel impinging on the downward side of the vertical tail (Reference (13)). It is surmised by the authors of Reference (13) that this aerodynamic phenomena is related to the $\mathcal{L}'_\alpha$ and N'_α stability derivatives and hence $1/T_{\theta_3}$. The effect of not including the $\mathcal{L}'_\alpha$ and N'_α in the complete linear six degree-of-freedom equations of motion of the A-7 can be inferred from Figure 37 which compares the pole-zero locations of the coupled six degree-of-freedom $N_{\delta_e}^{\theta}/\Delta$ transfer function with and without the $\mathcal{L}'_\alpha$ and N'_α terms.

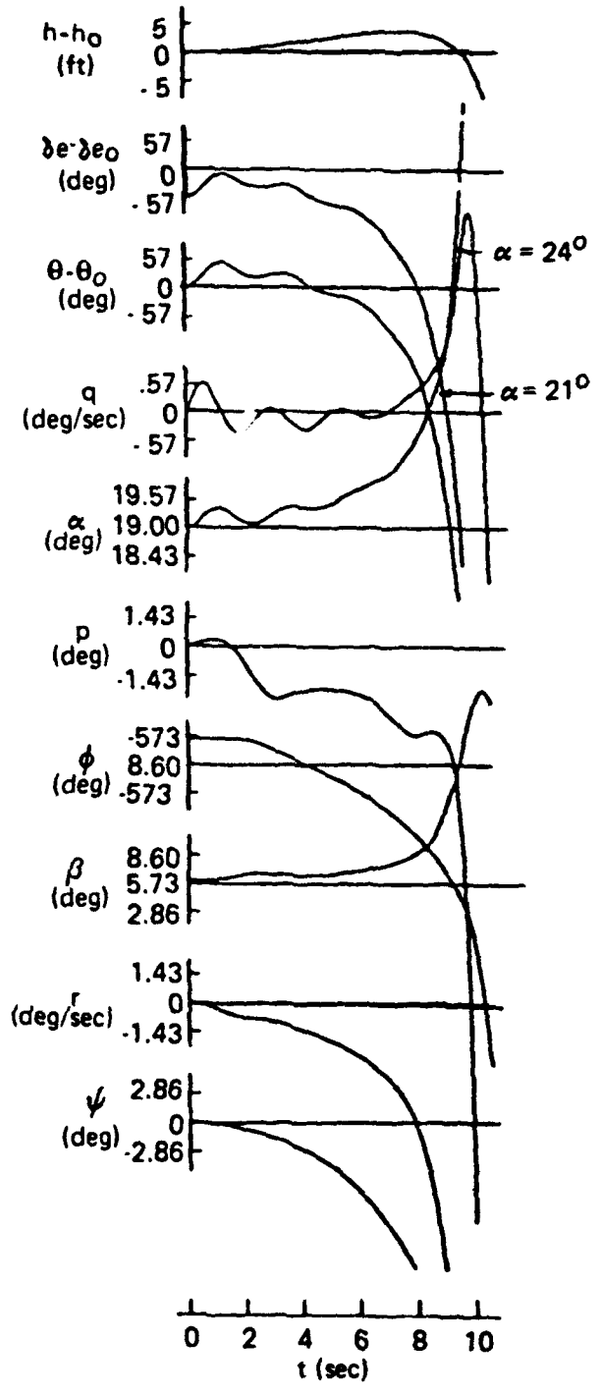

Figure 36 Digital Simulation of a Closed-Loop A-7 Departure to a Step Pitch Attitude Command ($\alpha_0 = 18.8^\circ$, $\beta = 6^\circ$) (Reference (13))

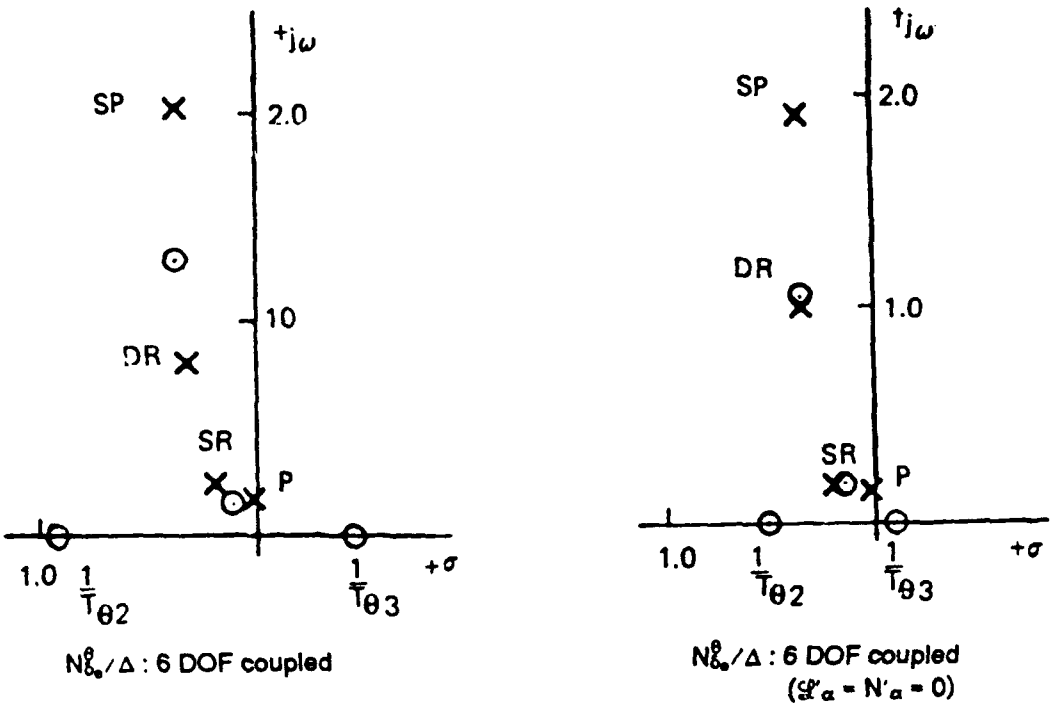

$N^{\delta}_{\delta_e}/\Delta$: 6 DOF coupled

$N^{\delta}_{\delta_e}/\Delta$: 6 DOF coupled ($\mathcal{Y}'_\alpha = N'_\alpha = 0$)

Figure 37 Effect of Not Including the $\mathcal{Y}'_\alpha$ and N'_α Terms (in the 6 DOF Equations-of-Motion) on the Pole-Zero Locations of the $N^{\delta}_{\delta_e}/\Delta$ Transfer Function of the A-7 Aircraft (Data for $\alpha_0 = 18.8^\circ$; $\beta_0 = 6^\circ$). (Reference (13))

The Z_p and Z_r terms represent the nonlinear kinematic coupling between the sideslip and yawing/rolling motion of the aircraft in the Z-equation-of-motion. The effect of not including these two terms in the six degree-of-freedom equations-of-motion is shown in the pole-zero plots of figure 38.

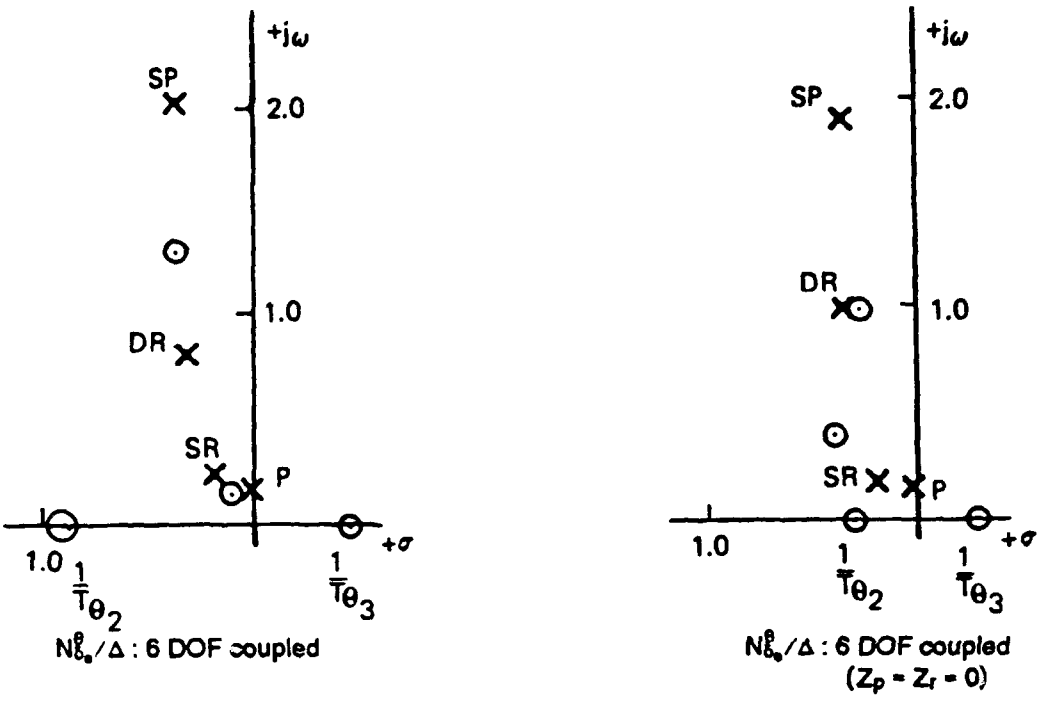

Figure 38 Effect of Not Including the Z_p and Z_r Terms (in the 6 DOF Equations-of-Motion) on the Pole-Zero Locations of the θ/δ_e Transfer Function of the A-7 Aircraft (Data for $\alpha_0 = 18.8^\circ$; $\beta_0 = 6^\circ$). (Reference (13))

TYPE OF CRITERION :

Values for the closed-loop parameter, $1/T_{\theta_3}$ and the open loop parameters $\mathcal{L}'_\alpha$, N'_α, Z_p and Z_r have not been correlated directly with departure susceptibility boundaries to be considered a "Criterion". However, the design impact and influence these parameter have in choosing a methodology to predict under which flight conditions an aircraft will depart controlled flight is substantial.

CRITERION PLANE :

The nose slice departure parameter, $1/T_{\theta_3}$ is a closed-loop stability parameter. If the value of $1/T_{\theta_3}$ is positive a roll-spiral divergence (as described) cannot occur. However, positive value

boundaries have not been correlated with aircraft departure susceptibility. Conservatively the value of $1/T_{\theta_3}$ should be positive.

DESIGN IMPACT :

From a design and analysis perspective the nose-slice departure parameter points out that there are cases in which aerodynamic (longitudinal-lateral/directional) coupling becomes a significant influencing factor in causing an aircraft to depart controlled flight. The influence of these terms is not discernable in departure parameters/criteria that are derived based on uncoupling the longitudinal and lateral/directional equations of motion (i.e., $C_{n_{\beta DYN}}$ and LCDP).

In fact, for the A-7 aircraft, the authors of Reference (13) found that although low departure parameter values of $C_{n_{\beta DYN}}$ and LCDP may contribute to the departure of the A-7, neither is a primary factor. However, when $C_{n_{\beta DYN}}$ and LCDP were negative at the same time at which $1/T_{\theta_3}$ was nonminimum phase, the rapidity and/or severity of the nose slice departure is increased (Reference (13)).

ADVANTAGES OF CRITERION :

The $1/T_{\theta_3}$ closed-loop stability parameter provides stability information concerning the potential of a closed-loop divergence occurring due to coupling (both aerodynamic and kinematic) between the longitudinal and lateral/directional modes of motion. This is the first stability parameter presented that can predict the existence of such an instability.

Derivation of the departure parameter $1/T_{\theta_3}$ recognizes the importance of the effects of sideslip (either intentionally, i.e., rudder maneuvering or unintentionally, i.e., adverse aileron yaw, mistrim, etc.) with respect to aircraft stability and control at high angles-of-attack. In addition, the influence of the aerodynamic cross-coupling (M_β, N'_α, $\mathcal{L}'_\alpha$) and the dynamic derivatives (C_{n_r}, C_{l_p}, etc.) is accounted for in the calculation of $1/T_{\theta_3}$.

CRITERION SHORTCOMINGS :

The $1/T_{\theta_3}$ stability parameter was derived and used to explain the departure characteristics of the A-7 aircraft. It is not meant to be used as a departure parameter exclusive of other parameters such as $C_{n_{\beta DYN}}$, LCDP, etc. Rather it should be used to compliment departure parameters derived based solely on the decoupled equations-of-motion to determine the potential for closed-loop instabilities arising due to longitudinal-lateral/directional dynamic coupling.

KALVISTE: $C_{m_{\alpha COP}}$, $C_{n_{\beta COP}}$, K

DATE/RESEARCHER :

1978; Kalviste

CRITERION :

Coupled Parameters Criteria,

$$N_{\beta COP} > 0$$

$$M_{\alpha COP} > 0$$

$$K < 1$$

Kalviste's coupled parameters, $C_{n_{\beta COP}}$, $C_{m_{\alpha COP}}$ and K, are stability parameters that indicate the open-loop static rotational stability of an aircraft. The "cop" subscript stands for "coupled" indicating that the parameters are derived from the coupled equations-of-motion and thus are applicable to asymmetric flight conditions.

BASIS OF CRITERION :

Kalviste's stability parameters are derived based on solving for the "necessary" conditions for aircraft static rotational stability (note, the aircraft may still be dynamically unstable) for the coupled six degree-of-freedom equations of motions by applying the Routh Stability Criterion. A detailed development of Kalviste's parameters from the equations-of-motion is given in Reference (51) and will not be repeated here. Instead the implications and understanding of these parameters will be elaborated on.

The nondimensional coupled stability parameters are defined in equations (41) to (47).

$$N_{\beta COP} = \frac{1}{2}\left[\left(N_{\beta DYN} - M_{\alpha DYN}\right) + \left(N_{\beta DYN} + M_{\alpha DYN}\right)\cdot\sqrt{1 - \frac{4\left(M_{\beta}N_{\alpha}\right)_{DYN}}{\left(N_{\beta DYN} + M_{\alpha DYN}\right)^2}}\right] \qquad (41)$$

$$M_{\alpha_{COP}} = \frac{1}{2}\left[-\left(N_{\beta_{DYN}} - M_{\alpha_{DYN}}\right) + \left(N_{\beta_{DYN}} + M_{\alpha_{DYN}}\right)\cdot\sqrt{1 - \frac{4\left(M_\beta N_\alpha\right)_{DYN}}{\left(N_{\beta_{DYN}} + M_{\alpha_{DYN}}\right)^2}}\right] \tag{42}$$

$$K \triangleq \frac{4\left(M_\beta N_\alpha\right)_{DYN}}{\left(N_{\beta_{DYN}} + M_{\alpha_{DYN}}\right)^2} \tag{43}$$

where,

$$M_{\alpha_{DYN}} \triangleq M_\alpha - (\mathcal{L}_\alpha \cos\alpha_0 + N_\alpha \sin\alpha_0)\tan\beta_0 \tag{44}$$

$$M_{\beta_{DYN}} \triangleq M_\beta - (\mathcal{L}_\beta \cos\alpha_0 + N_\beta \sin\alpha_0)\tan\beta_0 \tag{45}$$

$$N_{\alpha_{DYN}} \triangleq N_\alpha \cos\alpha_0 - \mathcal{L}_\alpha \sin\alpha_0 \tag{46}$$

$$N_{\beta_{DYN}} \triangleq N_\beta \cos\alpha_0 - \mathcal{L}_\beta \sin\alpha_0 \tag{47}$$

The equations-of-motion used in the derivation of the Kalviste stability parameters differ in two major ways from those used to derive $Cn_{\beta_{DYN}}$:

1. The aerodynamic cross-coupling between the longitudinal and lateral/directional equations-of-motion are modelled (i.e., $\mathcal{L}_\alpha$, N_α, M_β)
2. The kinematic cross-coupling terms are modelled by the $(\cos\alpha_0\tan\beta_0)$ and $(\sin\alpha_0\tan\beta_0)$ terms.

If the sideslip angle is zero then $M_{\alpha_{DYN}}$ reduces to M_α . Furthermore if the aerodynamic cross-coupling terms are zero then the parameters $N_{\alpha_{DYN}}$ and $M_{\beta_{DYN}}$ are both zero and the Kalviste Stability Parameters simplify to $N_{\beta_{DYN}} = N_{\beta_{COP}} > 0$ and $M_\alpha = M_{\alpha_{COP}} < 0$.

Analogous to $N_{\beta_{DYN}}$ and $M_{\alpha_{DYN}}$ being equal to the square of the Dutch-roll and short period natural frequencies respectively (assuming zero damping; see equation (48), the coupled expression for these two parameters, $N_{\beta_{COP}}$ and $M_{\alpha_{COP}}$, can be equated to the coupled Dutch-roll and short period natural frequencies (see equation 49).

$$\text{UNCOUPLED } (M_{\beta_{DYN}} N_{\alpha_{DYN}} = 0) \tag{48}$$

$$N_{\beta_{DYN}} \cong \omega^2_{n_{DR}}$$

$$N_{\alpha_{DYN}} \cong \omega^2_{n_{SP}}$$

$$\text{COUPLED } \left(M_{\beta_{DYN}} N_{\alpha_{DYN}} \neq 0\right) \tag{49}$$

$$N_{\beta_{cop}} \cong (\omega^2_{n_{DR}})_{COP}$$

$$N_{\alpha_{cop}} \cong (\omega^2_{n_{SP}})_{COP}$$

To predict aircraft departure susceptibility for a particular aircraft, Kalviste makes use of contour mapping techniques as shown in Figure 39 to define three regions of unaugmented aircraft instability as a function of angle-of-attack and sideslip angle. These three regions of instability are:

1. $K < 1$ Coupled (α, β) Oscillatory Instability
2. $M_{\alpha_{COP}} > 0$ Coupled Longitudinal Divergence (i.e., Short Period on RHP σ-axis)
3. $N_{\beta_{COP}} < 0$ Coupled Lateral-Directional Divergence (i.e., Dutch-roll root on RHP σ-axis)

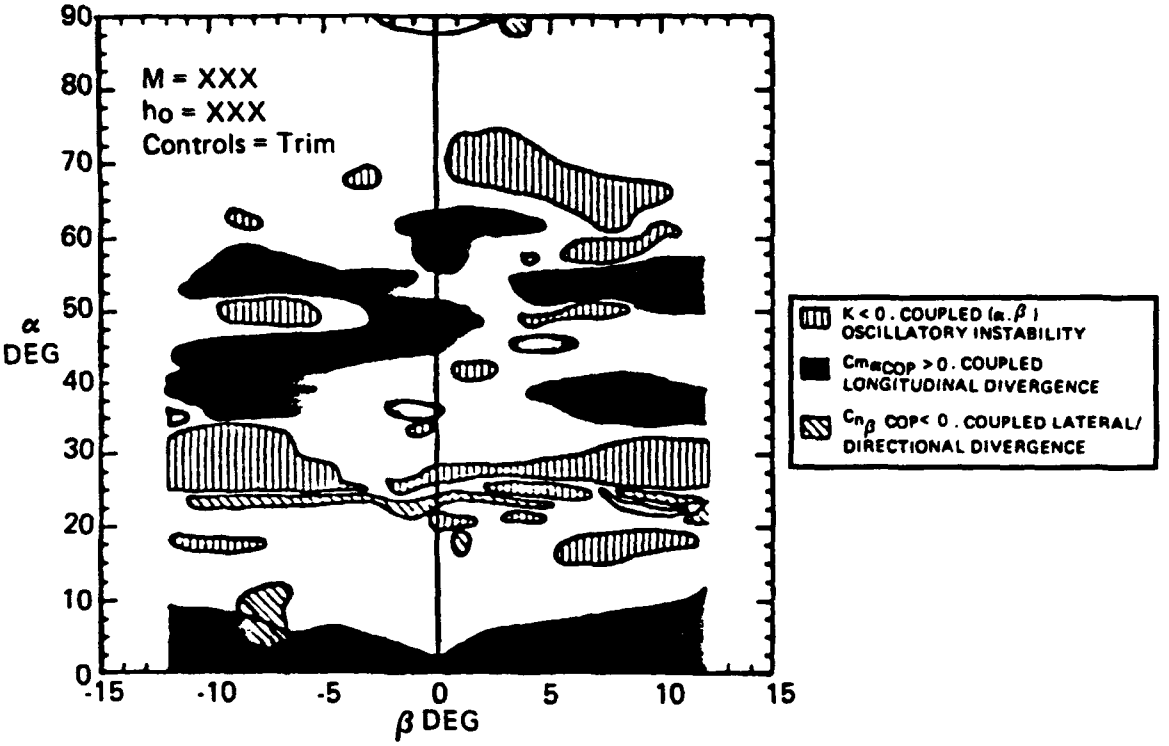

Figure 39 Kalviste α versus β Static Stability Plot (Reference (51))

If the angle-of-attack and sideslip traces of an aircraft in maneuvering flight pass through regions of instability it indicates that the aircraft will have a tendency to depart; it does not necessarily mean that the aircraft will depart controlled flight. There are two possible effects of an unstable region on aircraft motion. They are: (1) if the unstable region is small it can diverge into a stable region; (2) if the unstable region is large, the divergence can cause the aircraft rates to build-up into a developed post-stall gyration or spin.

It is important to realize that regions of the "Kalviste stability plane" that are not identified as regions of instability do not imply that departure cannot occur in these regions. Aircraft departure from controlled flight due to dynamic instability (i.e., as a result of inertial coupling effects, or

negative roll and/or yaw damping) or closed-loop instabilities due to pilot or flight control system loop closures are not addressed by the Kalviste open-loop Coupled Stability Parameters.

TYPE OF CRITERION :

Open-loop longitudinal-lateral/directional static stability criterion.

CRITERION PLANE :

See α - β Stability Plane of Figure 38.

DESIGN IMPACT :

Kalviste's stability parameter analysis technique can be pursued after nonlinear static wind tunnel data becomes available. To make the analysis feasible requires the use of digital computer programming and automatic plotting capability. The computer is used to perform nonlinear interpolations of tabular function (i. e., $C_\ell = f((\alpha, \beta, \delta_a,)$, $C_m = f((M, \alpha, \beta, \delta_c))$ that have continuous first derivatives through the α, β range desired. An iteration procedure is then used to compute the stability contour lines.

CRITERION ADVANTAGES :

The advantage of Kalviste's Coupled Static Stability Parameters criterion is that it extends the open-loop, symmetric, static $C_{n_{\beta DYN}}$ stability parameter to asymmetric flight (which, as shown, can be a prime driver in initiating an aircraft departure) and includes the effects of highly nonlinear aerodynamic data typical of high angle-of-attack flight conditions.

CRITERION SHORTCOMINGS :

The Coupled Static Stability Parameters criterion does not address the potential for departure due to dynamic instabilities (i.e., aerodynamic, inertial coupling, etc.), nor does it address aspects of potential departures due to closed-loop pilot control.

DATE/RESEARCHER :

1978; Bihrle

CRITERION :

C_{ℓ_β} versus C_{n_β} and $C_{n_{\delta_a}}$ Design Boundaries for Departure Susceptibility and Roll Reversal (see Figure 40)

BASIS OF CRITERION :

Experience led Bihrle to believe that there are three aircraft characteristics primarily responsible for departure susceptibility. These characteristics are static directional stability (C_{n_β}), dihedral effect (C_{ℓ_β}) and lateral control ($C_{\ell_{\delta_a}}$, $C_{n_{\delta_a}}$). To determine boundaries for aircraft departure susceptibility and roll reversal, Bihrle conducted a digital simulation of a severe open-loop rolling pull-up maneuver while parametrically varying the C_{n_β} and C_{ℓ_β} aerodynamic parameters for three cases of yaw due to aileron control (i.e., proverse, neutral and adverse). The digital simulation utilized the complete 6 degree-of-freedom rigid body equations-of-motion incorporating the use of nonlinear aerodynamics with angle-of-attack and, if appropriate, control deflection and/or sideslip angle. The choice of the severe rolling pull-up maneuver for the digital simulation is based on the fact that most fighter aircraft departures from controlled flight occur while maneuvering. The particular maneuver chosen is also severe in terms of the amount of kinematic and inertial coupling generated.

By examining the resulting time history associated with each of the matrix variations of C_{n_β} and C_{ℓ_β} the boundaries shown in Figure 40 were empirically determined. Bihrle defined roll reversal as roll opposite in direction to what was commanded by lateral control input. Departure was considered to have occurred when the angle-of-attack was sustained above the maximum trim angle-of-attack value.

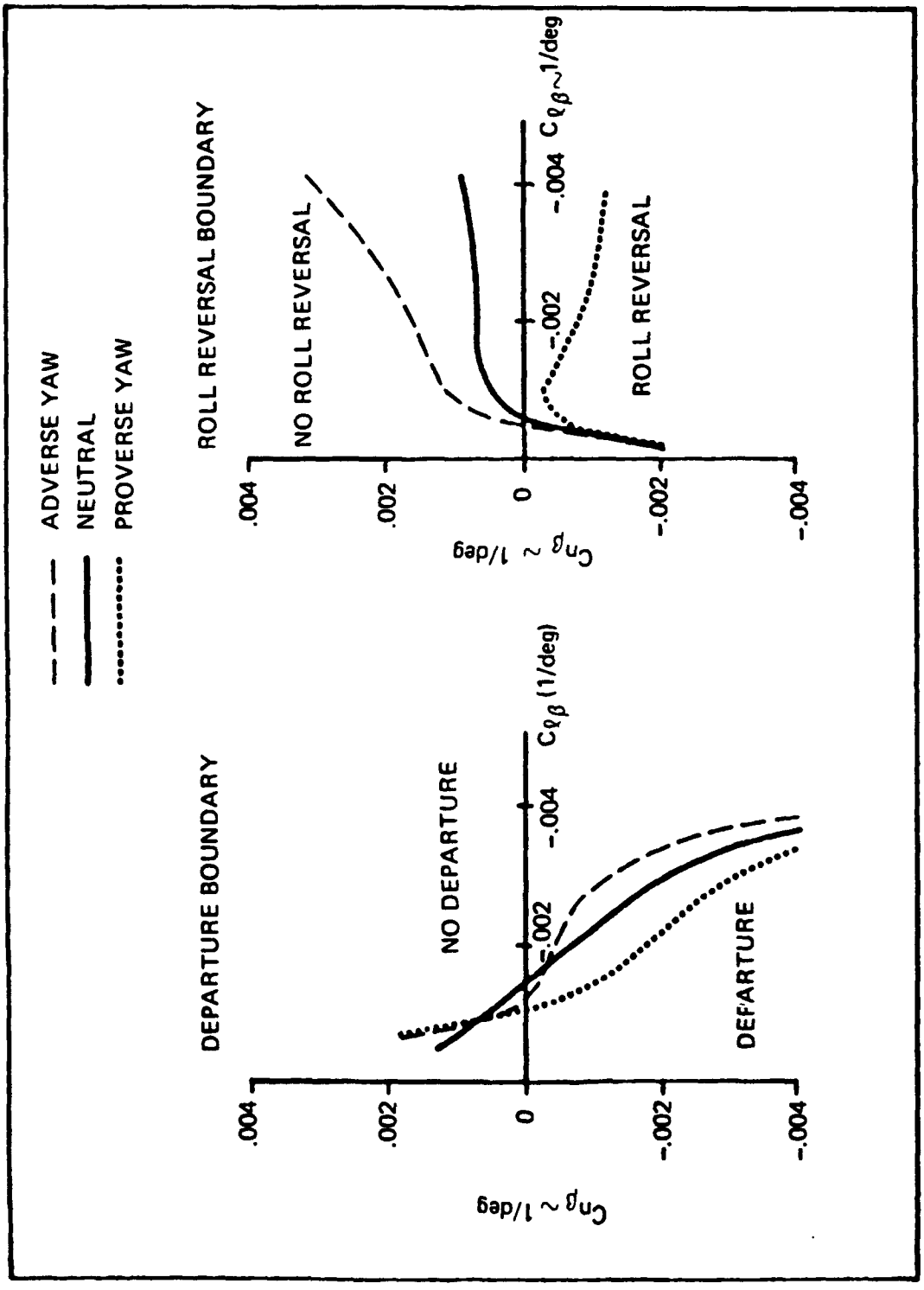

Figure 40 Bihrle Applied Research Design Guidelines for Departure Susceptibility and Roll Reversal (Reference (53))

Some of the noteworthy assumptions that influenced the results of the design charts of Figure 40 are as follows:

1. The parametric variation of C_{n_β} and C_{ℓ_β} (nonlinear with angle-of-attack) was based on data representative of current high performance fighter/attack aircraft at the time, such as the F-4, F-111, F-14 and F-15.
2. The ratio $(I_Z/I_X)_B$ was fixed at a value of 6.2 and $(I_{xz})_B$ was assumed to be zero.
3. The boundaries were developed for longitudinally stable aircraft only.
4. There was no limitation placed on the longitudinal control authority.

TYPE OF CRITERION :

Empirical (based on current high performance fighter/attack aircraft data of the time) static stability design charts applicable to large angle transient maneuvering flight.

CRITERION PLANE :

See Figure 40.

DESIGN IMPACT :

With respect to departure resistant aircraft design and positive roll control, Bihrle's empirical based "design charts" provide similar information to the Weissman Criteria in terms of desired aircraft static stability characteristics. That is, the "ideal" aircraft static characteristics are a combination of positive effective dihedral (negative C_{ℓ_β}) along with positive static directional stability (positive C_{n_β}) and low adverse yaw lateral control characteristics. Bihrle's design charts show that smaller values of positive effective dihedral can be offset by increased directional stability. On the other hand, static directionally unstable aircraft configurations can still be made departure resistant if the effective dihedral is sufficiently large. However, for this situation the occurrence of roll reversal is more likely.

CRITERION ADVANTAGES :

The principal advantage that the Bihrle Departure and Roll Reversal Design Charts have to offer is that they are based on maneuvering flight conditions and thus address maneuvering stability. By proceeding in this manner the effects of kinematic and inertial coupling, as well as the effects of nonlinear aerodynamics, are addressed.

CRITERION SHORTCOMINGS :

The primary shortcoming of the Departure and Roll Reversal Boundaries developed by Bihrle is that they are both a function of the open-loop large angle nonlinear maneuver simulated and the aerodynamic data base and aircraft configuration (i.e., $(I_Z/I_X)_B = 6.2$, etc.) modelled. The author's of Reference (37) comment that they believe the Bihrle Departure and Roll Reversal Boundaries are conservative based on the severity of the dynamics associated with the rolling pull-up maneuver simulated. The Bihrle design boundaries have been correlated with the A/D sectors of the empirically derived Weissman Criterion Plane in Reference (37). However Reference (37) cautions against comparing the two criteria because the Bihrle boundaries are based on fixed ratios of inertias (I_Z/I_X) and aileron moments ($C_{l_{\delta_a}}/C_{n_{\delta_a}}$), where as the $C_{n_{\beta DYN}}$ and LCDP parameters that comprise the Weissman Criteria are not restricted in this manner.

DATE/RESEARCHER :

1980; Johnston (STI)

CRITERION :

$1/T_{\phi_1}$ or $\zeta_{\phi}\omega_{n_{\phi}} > -0.5$ for Departure Resistance where $1/T_{\phi_1}$ is the non-minimum phase zero of the $N^{\phi}_{\delta_a}/\Delta$ (3 DOF) transfer function typical of fighter aircraft at high angle-of-attack flight conditions.

BASIS OF CRITERION :

When the conditions are satisfied that permit the longitudinal and lateral/directional equations of motion to be decoupled, the 3 degree-of-freedom $N^{\phi}_{\delta_{STK}}/\Delta$ transfer function can be represented by equation 50 given below.

$$\frac{N^{\phi}_{\delta_{STK}}}{\Delta} = \frac{K_{\phi_{STK}}\left[s^2 + 2\zeta_{\phi}\omega_{n_{\phi}}\, s + \omega^2_{n_{\phi}}\right]}{(s + 1/T_s)(s + 1/T_R)\left[s^2 + 2\zeta_{DR}\omega_{n_{DR}}\, s + \omega^2_{n_{DR}}\right]} \qquad (50)$$

Typically for low angle-of-attack flight conditions the numerator zeros are a complex pair located in the neighborhood of the Dutch-roll poles (i.e., $\zeta_{\phi}\omega_{n_{\phi}} \cong \zeta_{DR}\omega_{n_{DR}}$ and $\omega_{n_{\phi}} = \omega_{n_{DR}}$) as shown in Figure 41.

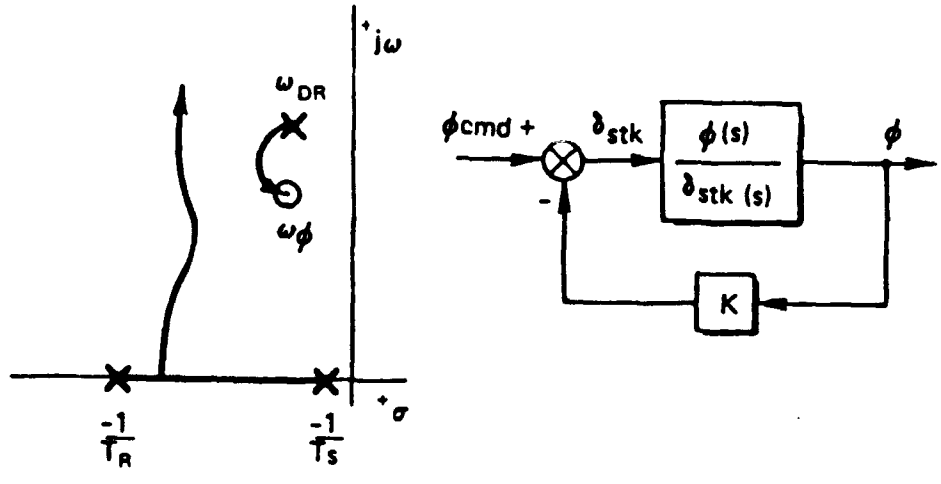

Figure 41 Typical Low Angle-of-Attack $\phi(s)/\delta_{STK}(s)$ Root Loci (Reference (13)).

However, with increasing angle-of-attack the $\omega^2_{n_\phi}$ or C-coefficient $\left(N^{\phi}_{\delta_{STK}} = As^2 + Bs + C\right)$ of the $N^{\phi}_{\delta_{STK}}$ numerator polynominal decreases and can become negative. When this occurs the numerator polynominal can be expressed as given in equation 51 where one root is positive (by definition the $1/T_{\phi_1}$ root) and one root is negative.

$$N_{\delta_{STK}} = K_{\phi_{STK}}(s + 1/T_{\phi_1})(s + 1/T_{\phi_2}) \qquad (51)$$

In this case the root locus of Figure 42 shows that a roll command loop closure will drive the spiral root ($-1/T_s$) toward the RHP (nonminimum phase zero) and a first order divergence results. (Note: the shift in the open-loop denominator roots is common at high angles-of-attack).

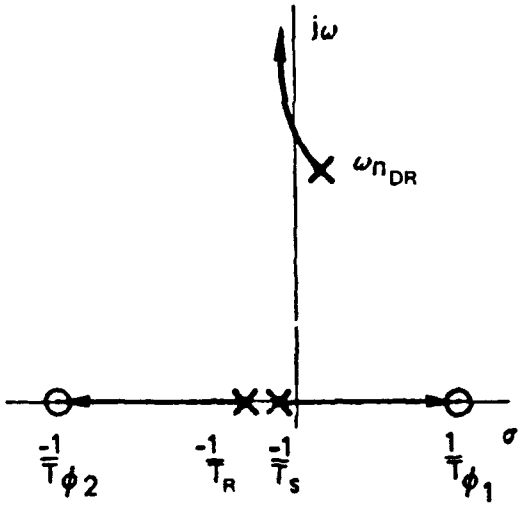

Figure 42 Typical High Angle-of-Attack $\phi(s)/\delta_{STK}(s)$ Root Loci (Reference (13))

The rate of divergence depends upon how far the zero lies in the RHP and how tightly the roll loop is closed (i.e., pilot technique, aggressiveness, etc.). In Reference (13) the closed-loop parameters $\omega^2_{n_\phi}$ and $(2\zeta_\phi\omega_{n_\phi})$ or $(1/T_{\phi_1}, 1/T_{\phi_2})$ were plotted versus angle-of-attack for the F-4J aircraft as shown in Figure 43.

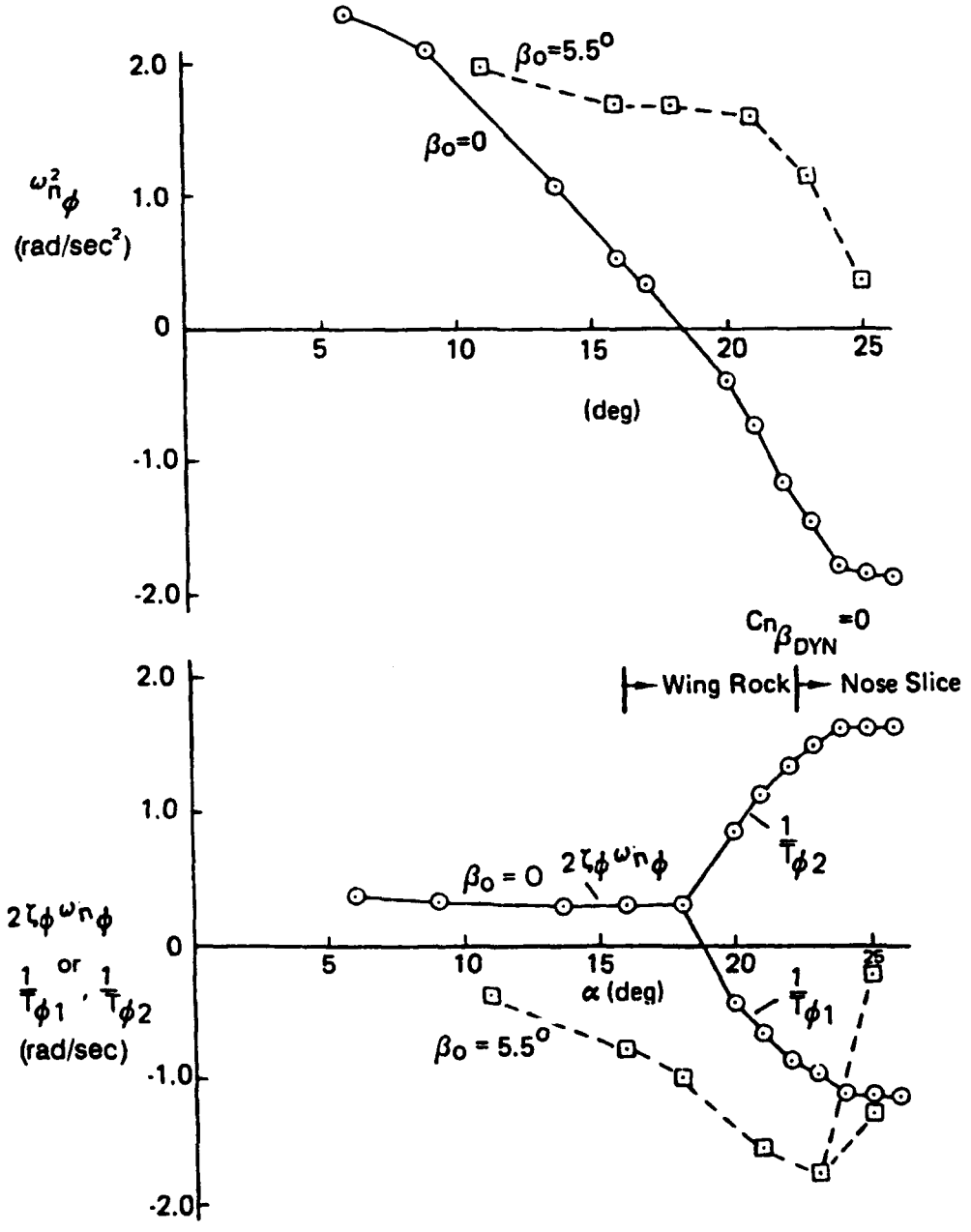

Figure 43 $N^{\phi}_{\delta STK}$ Root Migration with Angle-of-Attack for the F-4J Aircraft (Reference (13)).

This figure illustrates two important points. First, note (as mentioned above) that negative values of $\omega^2_{n_\phi}$ (which the roll reversal parameter LCDP is an approximation of) implies the numerator zeros can now be represented by two real roots, one of which is nonminimum phase. The first point the authors of Reference 13 make, is that for the F-4J aircraft (at zero sideslip angle) wing rock and eventual nose slice characteristics are correlated with small/negative values of $\omega^2_{n_\phi}$ and nose slice correlates with large negative values of $(1/T_{\phi_1})$.

The second point illustrated is the effect of nonzero sideslip angle (i.e., 5.5°) on these parameters. For this F-4 configuration, aerodynamic cross-coupling causes $\omega^2_{n_\phi}$ (i.e., LCDP) to remain positive and close to the Dutch-roll mode. However the damping ratio (ζ_ϕ) becomes negative causing two nonminimum phase zeros to exist in the form of a complex pair as sketched in Figure 43. This points out one case in which LCDP fails to predict the existence of a nonminimum phase zero due to the affects of significant aerodynamic cross-coupling. In this case the parameters $1/T_{\phi_1}$ or $\zeta\omega_{n_\phi}$ correlate more closely to the departure characteristics of the F-4J aircraft.

In the piloted simulation reported in Reference (48), four configurations were evaluated in terms of their departure susceptibility in an attempt to isolate the influence of the open-loop dynamics only (i.e., $C_{n_{\beta DYN}}$), closed-loop dynamics only (i.e., LCDP, $1/T_{\phi_1}$, $\zeta\omega_{n_\phi}$) and the combination of degraded open and closed-loop dynamics. The results of the simulations as supported by the data of Figure 44 shows the division between "departure resistant" (R), and "departure susceptible" (S) ratings to lie at an approximate $1/T_{\phi_1}$ value of -0.5.

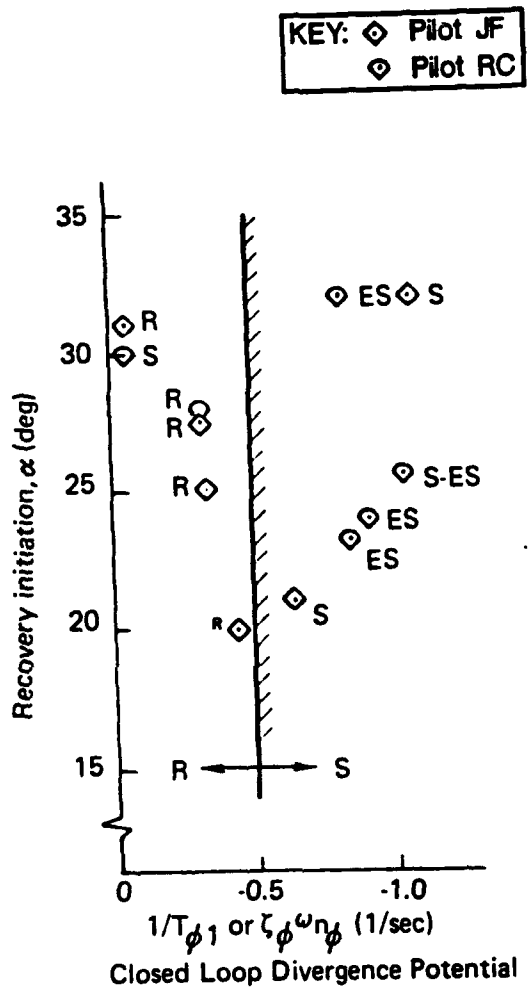

Figure 44 Departure Susceptibility Ratings Versus Lateral Closed-Loop Divergence Potential, $1/T_{\phi_1}$ or ζ_ϕ, ω_{n_ϕ} (R = Departure Resistant; S = Departure Susceptible; ES = Extremely Departure Susceptible) (Reference (48)).

This corresponds to a time to double amplitude of approximately 1.4 seconds. The authors reasoned that zeros which lie to the left of this line apparently limit the first order divergence to a rate slow enough for pilots to respond and prevent departure from controlled flight. Zeros to the right of the -0.5 boundary apparently allow divergence rates so fast that the pilots can not prevent departure. Interestingly, for the flight conditions, inertias, etc., employed in this simulation a $1/T_{\phi_1}$ value of -0.5 corresponds to an LCDP value of -0.001. This coincides with Weissman's LCDP boundary between regions A and B for positive $C_{n_{\beta DYN}}$ (see Figure 28), however it is a little more conservative at negative $C_{n_{\beta DYN}}$ values (Reference (13)).

TYPE OF CRITERION :

The $1/T_{\phi_1}$ criterion is intended as a closed-loop departure parameter in terms of preventing uncommanded motion via roll control inputs. Unlike the LCDP parameter, $1/T_{\phi_1}$ is directly applicable to augmented aircraft.

CRITERION PLANE :

$1/T_{\phi_1} > -0.5$

DESIGN IMPACT :

The design implication is that if the combined aerodynamics and FCS design is such that the value of $1/T_{\phi_1}$ (and/or $\zeta_\phi \omega_{n_\phi}$) does not exceed -0.5 (negatively) throughout the achievable angle-of-attack and sideslip range, the aircraft is predicted to be free of roll reversal characteristics. The $1/T_{\phi_1}$ departure parameter addresses the influence of the FCS on departure and can be used to aid in the design of departure prevention flight control system architecture. This is particularly important for departure design of future fighter aircraft which will very likely have reduced open-loop directionally stability (i.e., vertical tailless, low observable configuration designs). Note that this criterion places no restrictions on open-loop (i.e., $C_{n_{\beta DYN}}$) stability.

CRITERION ADVANTAGES :

Unlike application of the closed-loop departure parameter, LCDP, the $1/T_{\phi_1}$ parameter is not restricted to the three degree-of-freedom lateral/directional equation-of-motion assumptions. The parameter can be applied to completely coupled six degree-of-freedom airframe dynamics with FCS augmentation.

CRITERION SHORTCOMINGS :

Admittedly the researchers make clear that the simulation results used to develop the $1/T_{\phi_1}$ criterion are based on variations of a single nonlinear aerodynamic model (F-4J) representing an α, β region dominated by phenomena that are highly configuration dependent. Therefore, further substantiation of this criterion is desired.

PELIKAN: $Cn_{\beta APP}$

DATE/RESEARCHER :

1984; Pelikan (McDonnell Douglas)

CRITERION :

$Cn_{\beta APP}$(i.e., $Cn_{\beta DYN\,.\,CONTROLS}$) > 0

$$\text{where, } Cn_{\beta APP} = \frac{(\Delta Cn)_\beta + (\Delta Cn)_\delta}{\beta}\cos\alpha - \frac{(\Delta Cl)_\beta + (\Delta Cl)_\delta}{\beta}\sin\alpha\left(\frac{I_z}{I_x}\right)_B \tag{51}$$

This parameter has been used to assess the effect of different control inputs (i.e., neutral controls, lateral stick, coordinated controls, cross controls, rudder alone) on the basic airframe static lateral/directional stability.

BASIS OF CRITERION :

The $Cn_{\beta APP}$ departure parameter is based on whether the initial stability-axis yawing moment acting on the aircraft due to both sideslip and control inputs is either restoring or propelling. The expression for $Cn_{\beta APP}$ given in equation (51) can be derived by transforming the body angular accelerations (N/I_{z_B}, $\mathcal{L}/I_{x_B}$) from either body or principal axis into stability axis using a secant slope linearization technique. One development of the equation that defines the $Cn_{\beta APP}$ parameter is given in equations (52) to (54).

$$\dot{R}_s = \dot{R}_B\cos\alpha - \dot{P}_B\sin\alpha \tag{52a}$$

$$= \frac{N}{I_{z_B}}\cos\alpha - \frac{\mathcal{L}}{I_{x_B}}\sin\alpha \tag{52b}$$

$$= \frac{Cn\bar{q}Sb}{I_{z_B}}\cos\alpha - \frac{Cl\bar{q}Sb}{I_{x_B}}\sin\alpha \tag{52c}$$

$$\frac{I_{z_B}}{\bar{q}Sb}\cdot\dot{R}_s = Cn\cos\alpha - \left(\frac{I_z}{I_x}\right)_B Cl\sin\alpha \tag{52d}$$

Defining the nondimensional body-axis yawing and rolling moment coefficients with regard to the static terms due to sideslip (β)and control deflections (δ) yields,

$$\frac{I_{z_B}}{\bar{q}Sb} \cdot \dot{R}_s = [(\Delta C_n)_\beta + (\Delta C_n)_\delta] \cdot \cos\alpha - \left[\frac{I_z}{I_x}\right]_B \cdot [(\Delta C_\ell)_\beta + (\Delta C_\ell)_\delta] \cdot \sin\alpha \qquad (53)$$

To arrive at Pelikan's final expression for $C_{n_{\beta_{APP}}}$, equation (53) is divided through by the sideslip angle,

$$C_{n_{\beta_{APP}}} \triangleq \frac{\dot{R}_s}{\beta}\left(\frac{I_{z_B}}{\bar{q}Sb}\right) \triangleq \left[\frac{(\Delta C_n)_\beta + (\Delta C_n)_\delta}{\beta}\right] \cdot \cos\alpha - \left(\frac{I_z}{I_x}\right)_B \left[\frac{(\Delta C_\ell)_\beta + (\Delta C_\ell)_\delta}{\beta}\right] \cdot \sin\alpha \qquad (54)$$

Pelikan's motivation for dividing equation (54) by the sideslip angle is to use a secant slope linearization method (as opposed to the local tangent slope linearization method, i.e., stability derivatives) to determine "static stability" in a "global" sense as a function of sideslip angle (see Figure 45).

Note that the $C_{n_{\beta_{APP}}}$ parameter derivation is based on the same concept as Moul and Paulson's $C_{n_{\beta_{DYN}}}$ parameter. That is, the summation of yawing moments about the Z-stability axis must be positive (i.e., $\sum_i N'_{s_i} > 0$) (Reference (37)). The difference lies in the inclusion of yawing and rolling moments due to nonzero control deflections and the use of a secant slope linearization technique.

Tangent Slope ($M = \frac{\partial C_i}{\partial \beta}$, $i = \ell, n$) :_____

Secant Slope ($M' = \frac{Y(\beta) - Y_0}{X(\beta) - X_0}$) :_____

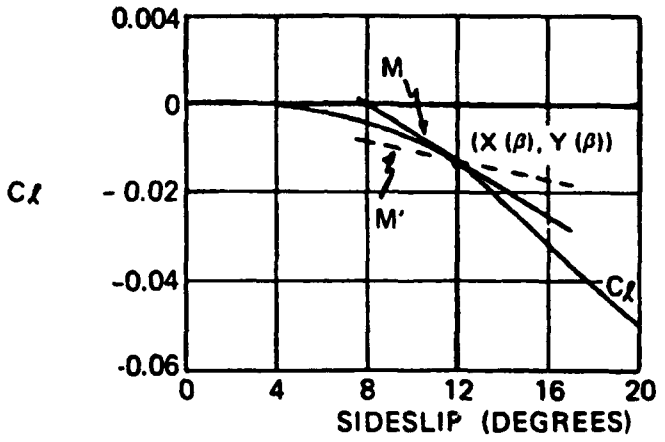

Figure 45 Illustration of the Tangent and Secant Slope Linearization Techniques

From F/A-18 flight test data Pelikan observed open-loop instabilities predicted by the $C_{n_{\beta DYN}}$ departure susceptibility parameter ($C_{n_{\beta DYN}} < 0$) that were never realized in flight. Based on this observation, Pelikan felt that the association of local open-loop instabilities (small/negative values of $C_{n_{\beta DYN}}$) with departure susceptibility should be revised to use the secant slope method of calculating$C_{n_{\beta DYN}}$ when nonlinear lateral-directional characteristics are exhibited. In the F-18 case the local region of instability occurring at approximately 30 degrees tends to slide the aircraft out to a stable region between 6 and 8 degrees sideslip angle and prevents the aircraft from departing controlled flight (although directional controllability is sloppy in this region).

TYPE OF CRITERION:

Open-loop lateral/directional static departure susceptibility criterion that includes the static effect of the controls.

CRITERION PLANE:

$$Cn_{\beta APP} > 0$$

DESIGN IMPACT:

The intent of the $Cn_{\beta APP}$ criterion is to extend the application of the $Cn_{\beta DYN}$ parameter to include nonlinear aerodynamic characteristics with sideslip angle and the effect of different control inputs. Use of this criterion is useful in preliminary control law design architecture for departure prevent portions of the flight control laws.

CRITERION ADVANTAGES:

(See Design Impact)

CRITERION SHORTCOMINGS:

The $Cn_{\beta APP}$ parameter/criterion does not address the potential for departures due to dynamic instabilities, (i.e., aerodynamic, inertial coupling, etc.) nor does it address aspects of potential departures due to closed-loop pilot control. Additionally, the parameter exclusively considers departure only in the lateral directional axis, precluding the possibility of any longitudinal axis departures or longitudinal-lateral/directional coupling that might induce a departure. It is also believed that further validation/correlation with flight test data is needed to support use of the secant slope method of linearization that is the basis of the $Cn_{\beta APP}$ parameter derivation.

KALVISTE: DYNAMIC STABILITY PARAMETERS

DATE/RESEARCHER :

1989; Kalviste (Northrop)

CRITERION :

No departure susceptibility criterion was proposed. Rather, "new" stability parameters are *derived (given in equation (55) below) which relate directly to the "fast" aircraft stability modes* (pitch short period, Dutch-roll and roll subsidence).

$$\mathcal{L}_{\dot{\mu}_{COP}} < 0, \tag{55}$$

$$N_{\dot{\beta}_{COP}} > 0$$

$$N_{\beta_{COP}} > 0$$

$$M_{\dot{\alpha}_{COP}} < 0$$

$$M_{\alpha_{COP}} < 0$$

Failure to satisfy the stability conditions of equation (55) reveals regions of local instability which result in degraded unaugmented flying qualities such as unpredictable control response and the *inability to transition to and maintain certain trim conditions (Reference (5)). The local in-*stabilities however may not necessarily represent conditions where the aircraft will depart from controlled flight.

These five parameters are related directly to the three (roll subsidence, Dutch-roll, and pitch short period) unaugmented stability modes (the six eigenvalues) of the aircraft in terms of three new independent variables ($\dot{\mu}_{COP}$, β_{COP} and α_{COP}) as a function of $\dot{\mu}$, β and $\dot{\alpha}$. As yet, Kalviste has not developed a unique transformation between the uncoupled variables ($\dot{\mu}$, β and $\dot{\alpha}$) and the coupled variables ($\dot{\mu}_{COP}$, β_{COP} and $\dot{\alpha}_{COP}$) for the general case involving both static and *dynamic stability. A transformation between the uncoupled variables (β and α) and the coupled* variables (β_{COP} and α_{COP}) has been derived in Reference (4) for the reduced problem involving static stability only.

The necessary condition for aerodynamic stability is to have the roots of the coupled equations in the left half of the complex plane.

BASIS OF CRITERION :

The five stability parameters given in equation (55) define aircraft stability based on the aircraft's aerodynamic and inertial properties and include both static and dynamic aerodynamic effects, inertial coupling and kinematic coupling effects. These parameters are an extension of the previously developed Coupled Stability Parameters based only on static aerodynamic effects (see Reference (48)). Kalviste defines stability in terms of the rotational motion relative to the flight path. The aerodynamic moments and forces are functions of the aerodynamic angles, α and β, aircraft body axis rates, P, Q, and R, and translational acceleration terms, $\dot{\alpha}$ and $\dot{\beta}$, at a fixed flight condition (Mach, altitude). To derive expressions for the stability parameters of equation 55, the rotational equations of motion are first expressed in the dynamic stability axis system (i.e., the coordinate system about which α, β, and μ are defined). These are shown in equations 56 to 67[1].

$$\ddot{\mu} = \mathcal{L}_{\dot{\mu}DYN}\dot{\mu} + \mathcal{L}_{\dot{\beta}DYN}\dot{\beta} + \mathcal{L}_{\beta DYN}\beta + \mathcal{L}_{\dot{\alpha}DYN}\dot{\alpha} + \mathcal{L}_{\alpha DYN}\alpha \quad (56)$$

$$\ddot{\beta} = -N_{\dot{\mu}DYN}\dot{\mu} - N_{\dot{\beta}DYN}\dot{\beta} - N_{\beta DYN}\beta - N_{\dot{\alpha}DYN}\dot{\alpha} - N_{\alpha DYN}\alpha \quad (57)$$

$$\ddot{\alpha} = M_{\dot{\mu}DYN}\dot{\mu} + M_{\dot{\beta}DYN}\dot{\beta} + M_{\beta DYN}\beta + M_{\dot{\alpha}DYN}\dot{\alpha} + M_{\alpha DYN}\alpha \quad (58)$$

where :

$M_{\alpha DYN}$, $M_{\beta DYN}$, $N_{\alpha DYN}$ and $N_{\beta DYN}$ are defined in equations 44 to 47, respectively, and

$$\mathcal{L}_{\dot{\mu}DYN} = N_r\sin^2\alpha_0 + \mathcal{L}_p\cos^2\alpha_0 + (N_p + \mathcal{L}_r)\sin\alpha_0\cos\alpha_0 + (N_q\sin\alpha_0 + \mathcal{L}_q\cos\alpha_0)\tan\beta_0 \quad (59)$$

$$\mathcal{L}_{\dot{\beta}DYN} = \left[N_p\sin^2\alpha_0 - L_r\cos^2\alpha_0\right] + (L_p - N_r)\sin\alpha_0\cos\alpha_0]\sec\beta_0 \quad (60)$$

$$\mathcal{L}_{\dot{\alpha}DYN} = (\mathcal{L}_q\cos\alpha_0 + N_q\sin\alpha_0)\sec\beta_0 \quad (61)$$

[1] Note this is a simplified equation set used by Kalviste to illustrate computation of the stability parameters. The complete equation set is given in Reference (5).

$$M_{\dot{\mu}_{DYN}} = [\, M_q - N_r\sin^2\alpha_0 - \mathcal{L}_p\cos^2\alpha_0 - (N_p + \mathcal{L}_r)\sin\alpha_0\cos\alpha_0 \quad (62)$$

$$- (\mathcal{L}_q\cos\alpha_0 + N_q\sin\alpha_0)\tan\beta_0]\sin\beta_0 + (M_r\sin\alpha_0 + M_p\cos\alpha_0)\cos\beta_0$$

$$M_{\dot{\beta}_{DYN}} = M_p\sin\alpha_0 - M_r\cos\alpha_0 - [N_p\sin^2\alpha_0 - L_r\cos^2\alpha_0 + (L_p - N_r)\sin\alpha_0\cos\alpha_0]\tan\beta_0 \quad (63)$$

$$M_{\dot{\alpha}_{DYN}} = M_q - (\mathcal{L}_q\cos\alpha_0 + N_q\sin\alpha_0)\tan\beta_0 \quad (64)$$

$$N_{\dot{\mu}_{DYN}} = [\, - \mathcal{L}_r\sin^2\alpha_0 + N_p\cos^2\alpha_0 + (N_r - \mathcal{L}_p)\sin\alpha_0\cos\alpha_0]\cos\beta_0 \quad (65)$$

$$+ (N_q\cos\alpha_0 - \mathcal{L}_q\sin\alpha_0)\sin\beta_0$$

$$N_{\dot{\beta}_{DYN}} = - \mathcal{L}_p\sin^2\alpha_0 - N_r\cos^2\alpha_0 + (N_p + \mathcal{L}_r)\sin\alpha_0\cos\alpha_0 \quad (66)$$

$$N_{\dot{\alpha}_{DYN}} = N_q\cos\alpha_0 - \mathcal{L}_q\sin\alpha_0 \quad (67)$$

Taking the Laplace transform of equations 56 to 58 and placing them in matrix form yields,

$$\begin{bmatrix} s - \mathcal{L}_{\dot{\mu}_{DYN}} & - \mathcal{L}_{\dot{\beta}_{DYN}}s - \mathcal{L}_{\beta_{DYN}} & - \mathcal{L}_{\dot{\alpha}_{DYN}}s - \mathcal{L}_{\alpha_{DYN}} \\ N_{\dot{\mu}_{DYN}} & s^2 + N_{\dot{\beta}_{DYN}}s + N_{\beta_{DYN}} & N_{\dot{\alpha}_{DYN}}s + N_{\alpha_{DYN}} \\ - M_{\dot{\mu}_{DYN}} & - M_{\dot{\beta}_{DYN}}s - M_{\beta_{DYN}} & s^2 - M_{\dot{\alpha}_{DYN}}s - M_{\alpha_{DYN}} \end{bmatrix} \begin{Bmatrix} \dot{\mu} \\ \beta \\ \alpha \end{Bmatrix} = 0 \quad (68)$$

If the off-diagonal terms (coupling terms) of the above matrix equation are zero, then the diagonal terms represent the roll subsidence, Dutch-roll and pitch short period stability modes, respectively (Reference (5)). Taking advantage of the fact that a square matrix with distinct eigenvalues can always be diagonalized ($\Lambda = \text{diag}\,[\lambda_1, \lambda_2, \lambda_3, \ldots\lambda_n]$)by a similarity transformation (see Reference (24)), Kalviste rearranges equation (68) as shown in equation (69) with the five new stability parameters (in dimensional form) on the matrix diagonal.

$$\begin{bmatrix} s - \mathcal{L}_{\dot{\mu}_{COP}} & 0 & 0 \\ 0 & s^2 + N_{\dot{\beta}_{COP}}s + N_{\beta_{COP}} & 0 \\ 0 & 0 & s^2 - M_{\dot{\alpha}_{COP}}s - M_{\alpha_{COP}} \end{bmatrix} \begin{Bmatrix} \dot{\mu}_{COP} \\ \beta_{COP} \\ \alpha_{COP} \end{Bmatrix} = 0 \qquad (69)$$

To relate the new stability parameters to the conventional aircraft modes of motion Kalviste developed a method of integrating the characteristic roots ($s=\delta+j\omega$)from the uncoupled equations to the coupled equations. To account for coupling between the conventional modes of motion, multipliers K_1 and K_2 are placed on the off-diagonal coupling terms as shown in equation (70).

$$\begin{bmatrix} s - \mathcal{L}_{\dot{\mu}_{DYN}} & -\mathcal{L}_{\dot{\beta}_{DYN}}s - \mathcal{L}_{\beta_{DYN}} & -\mathcal{L}_{\dot{\alpha}_{DYN}}s - \mathcal{L}_{\alpha_{DYN}} \\ K_2(N_{\dot{\mu}_{DYN}}) & s^2 + N_{\dot{\beta}_{DYN}}s + N_{\beta_{DYN}} & N_{\dot{\alpha}_{DYN}}s + N_{\alpha_{DYN}} \\ K_2(M_{\dot{\mu}_{DYN}}) & K_1(-M_{\dot{\beta}_{DYN}}s - M_{\beta_{DYN}}) & s^2 - M_{\dot{\alpha}_{DYN}}s - M_{\alpha_{DYN}} \end{bmatrix} \begin{Bmatrix} \dot{\mu} \\ \beta \\ \alpha \end{Bmatrix} = 0 \qquad (70)$$

The migration of the characteristic equation roots due to coupling can be tracked by integrating the characteristic roots with respect to these multipliers from zero to one as shown in Reference 5. Integrating the characteristic roots with respect to K_1 accounts for coupling between the longitudinal and lateral/directional modes and integrating the characteristic roots with respect to K_2 accounts for coupling between the roll subsidence and the Dutch-roll modes. In this manner the migration of the eigenvalues can be tracked, adding insight to the effects of lateral/directional as well as longitudinal-lateral/directional coupling.

The coupled stability parameters given in equation (69) were derived from the equations-of-motion that included the linearized aerodynamic derivatives (both static and dynamic) and the kinematic coupling of these derivatives. To define an aircraft's aerodynamic stability for maneuvering flight, Kalviste includes the inertial effects (see equations (71) to (73)) due to steady rotation rates in the equations-of-motion.

$$\dot{P}_I = \left(\frac{I_{yy}-I_{zz}}{I_{xx}}\right)\cdot\left[Q_0R + R_0Q\right] \tag{71}$$

$$\dot{Q}_I = \left(\frac{I_{zz}-I_{xx}}{I_{yy}}\right)\cdot\left[R_0P + P_0R\right] \tag{72}$$

$$\dot{R}_I = \left(\frac{I_{xx}-I_{yy}}{I_{zz}}\right)\cdot\left[P_0Q + Q_0P\right] \tag{73}$$

To accomplish this, the appropriate aerodynamic derivatives are modified to account for the inertial coupling effects such as:

$$(\mathcal{L}_r)_I = \mathcal{L}_r + \left(\frac{I_{yy} - I_{zz}}{I_{xx}}\right)\cdot Q_0$$

$$(\mathcal{L}_q)_I = \mathcal{L}_q + \left(\frac{I_{yy} - I_{zz}}{I_{xx}}\right)\cdot R_0$$

TYPE OF CRITERION :

The five stability parameters developed by Kalviste relate directly to the stability of the natural aircraft stability modes (i.e., the pitch short period, roll subsidence and Dutch-roll). The parameters can thus be used to predict open-loop stability of an aircraft in steady maneuvering flight (i.e., dynamic aerodynamic effects and kinematic and inertial coupling terms are included in the parameter formulation). Failure to satisfy the stability criterion of one of the five stability parameters has not been correlated with aircraft departure susceptibility. However, regions of the α-β plane for which one of the stability criterion is not satisfied reveals a region of local

instability which results in degraded flying qualities of the unaugmented aircraft and possible departure prone characteristics.

CRITERION PLANE :

No departure susceptibility criterion has been correlated with the Kalviste Coupled Stability Parameters. Figure 46 shows how the five stability parameters can be plotted on an α-β plane to determine whether any regions of instability exist.

DESIGN IMPACT :

The formation of new dynamic modes due to the effects of coupling between the conventional aircraft modes can be identified using the root integration technique presented by Kalviste in Reference (5). The significance of this method is that it applies even in highly coupled, dynamic conditions.

CRITERION SHORTCOMINGS :

Kalviste's formulation of the equations-of-motion is such that the effects of trajectory stability (defined in terms of aircraft translational motion due to aerodynamic and propulsive forces and the force of gravity) are not included. This excludes the possible coupling effects between the "fast" modes and the slow trajectory modes consisting of the conventional phugoid, spiral and altitude stability modes. Kalviste admittedly notes that inclusion of the trajectory effects can either stabilize or destabilize the aerodynamic stability characteristics predicted by the developed stability parameters of equation (69). Kalviste has already incorporated the trajectory effects in the parameter development by including the μ, γ, velocity and altitude equations in the formulation of the equations-of-motion. This results in a ninth order system that fully encompasses all coupling effects of the trajectory into the already developed aerodynamic stability parameters.

Levels of instability/stability of each of the parameters still needs to be further investigated to determine whether they can be correlated with aircraft departure susceptibility.

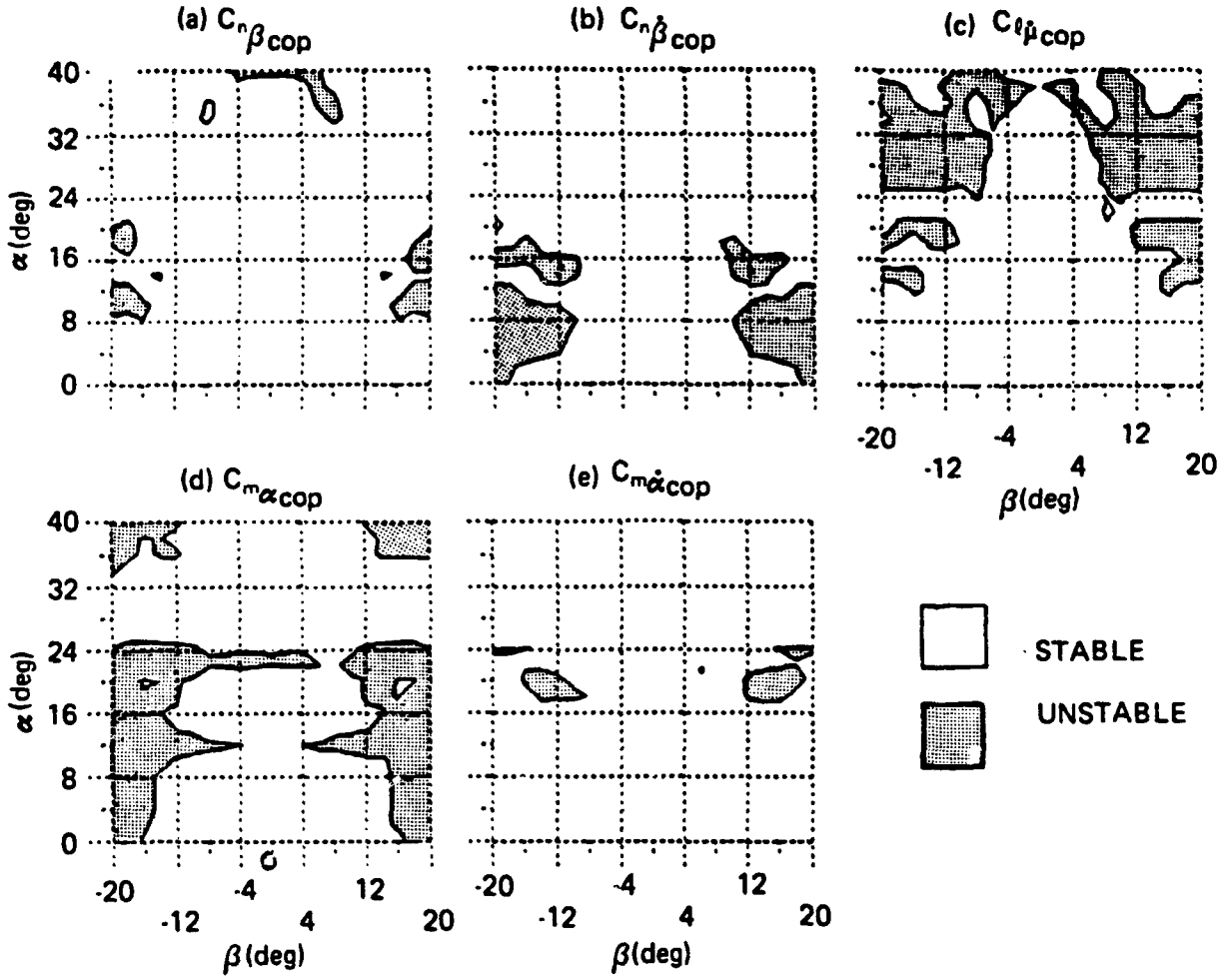

Figure 46 Kalviste Stability Parameters Plotted Versus Angle-of-Attack and Sideslip Angle (Reference (5))

CHODY: ROUTH CRITERION PARAMETERS

DATE/RESEARCHER:

1989; Chody (Eidetics)

CRITERION:

Extension of the $C_{n_{\beta DYN}}$ and LCDP stability concepts to address asymmetric ($\beta_0 \neq 0$; but $\phi_0 = 0$) steady maneuvering flight. Figure 47 illustrates the suggested open-loop stability criteria planes and Figure 48 illustrates the suggested closed-loop stability criteria that refines the classical definition of the LCDP parameter.

BASIS OF CRITERION:

Motivated by inconsistent correlation of recent departure experience with the $C_{n_{\beta DYN}}$ stability parameter, Chody chose to linearize the lateral/directional equations-of-motion and apply Routh's Stability Criteria to the resulting quartic polynominal charactaristic equation with as little simplification as possible (see equation (21)). As was shown in the $C_{n_{\beta DYN}}$ stability criterion section the expression for $C_{n_{\beta DYN}}$ (see equation (22)) now contains two additional terms, the second of which (i.e., $\frac{\rho Sb^3}{8I_x}[C'_{\ell_p}C'_{n_r} - C'_{\ell_r}C'_{n_p}]$) was shown in Figure 22 to be significant at least for the case of the preliminary configuration of the X-31A aircraft. Note that equation (22) is a refinement of the original expression derived from $C_{n_{\beta DYN}}$ to now include higher order terms that with today and future aircraft configuration concepts appear to be important. The modified expression for $C_{n_{\beta DYN}}$ is still a "Routh Stability Test" on the s^2 - coefficient (or "C"-coefficient; see equation (22)) of the uncoupled lateral/directional characteristic equation.

In addition to applying Routh's Stability Criteria to the "C" - coefficient to determine minimum levels of $C_{n_{\beta DYN}}$, Chody proposes that Routh's criteria also be applied to the other coefficients of the lateral/directional characteristic equation as shown in Figure 47a through 47c. (Note, Chody omits addressing the Routh discriminant, $D(BC-AD)-B^2E$; Negative values of the discriminant

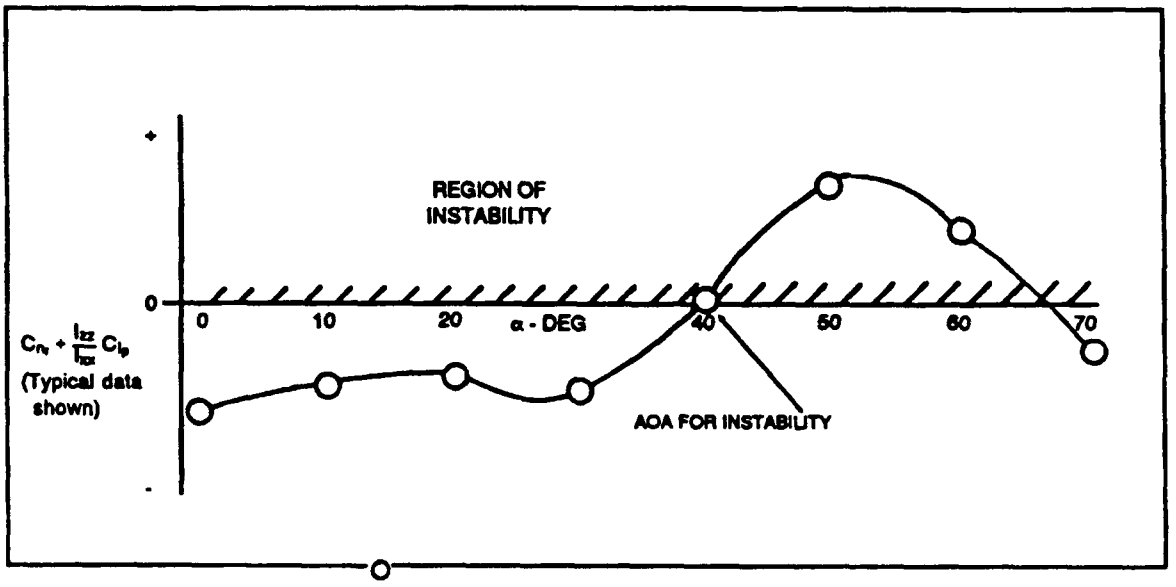

(a) Lateral/Directional Damping for Stability Based on the s^3("B") Characteristic Equation Coefficient

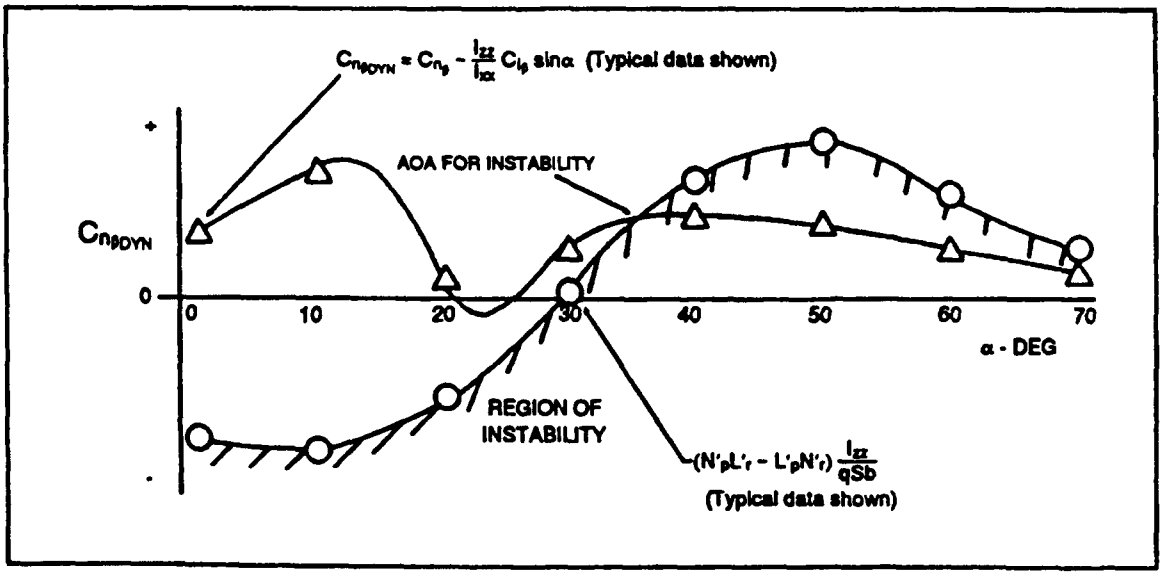

(b) Minimum Value of $C_{n_{\beta DYN}}$ for Stability Based on the s^2 ("C") Characteristic Equation Coefficient

Figure 47 Open-Loop Lateral/Directional Stability Boundaries of Chody Based on the Routh Stability Criteria (Reference (33))

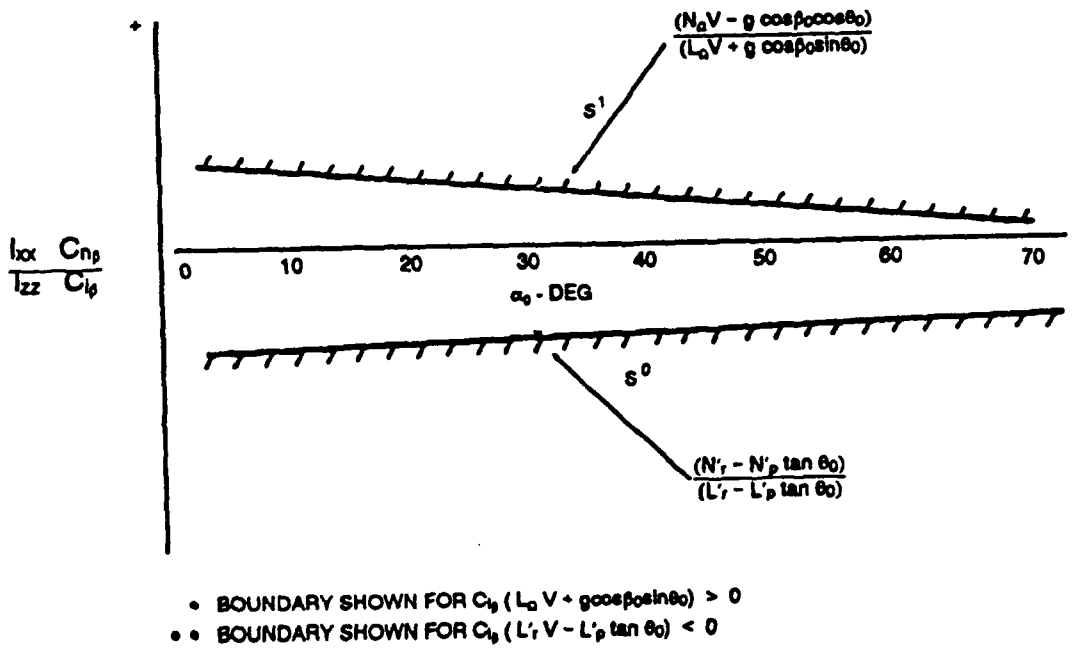

(c) Lateral-Directional Stability Boundaries Based on s^1 and s^0 ("D" and "E") Characteristic Equation Coefficients.

Figure 47 (Concluded). Open-Loop Lateral/Directional Stability Boundaries of Chody Based on the Routh Stability Criteria (Reference (33))

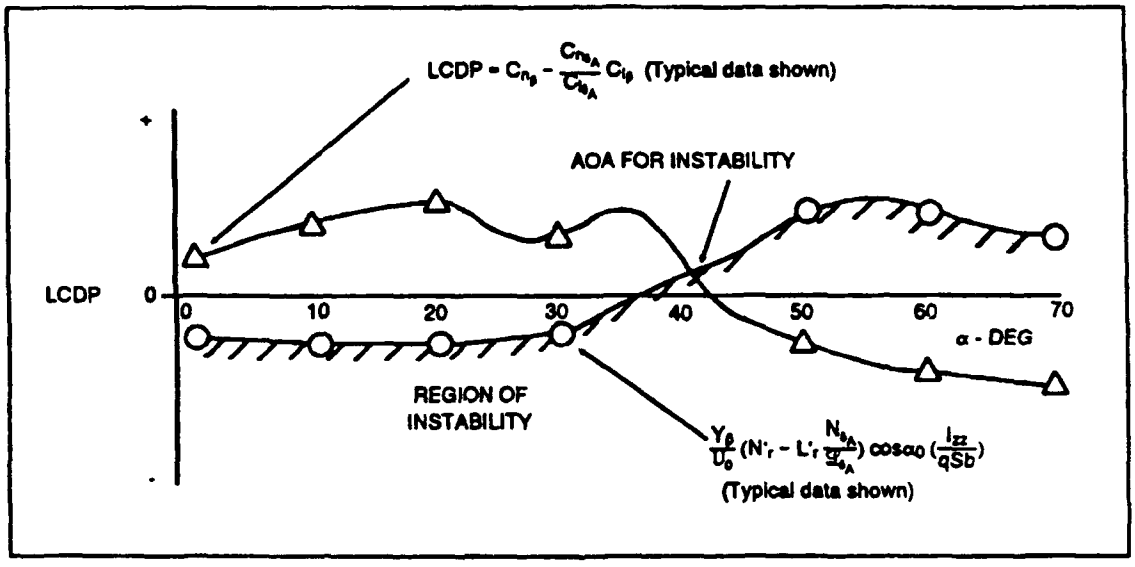

Figure 48 Closed-Loop Lateral/Directional Stability Boundaries of Chody (Extension of LCDP to Include the Aerodynamic Dynamic Deriivatives) (Reference (36))

indicate that the real part of one complex pair of roots (either the conventional "Dutch-roll pair or the lateral-phugoid") is in the unstable RHP which implies one oscillatory divergence will occur). Correlation of these coefficient stability bounderies with aircraft departure susceptibility has yet to be done.

The same analysis approach used to include the aerodynamic dynamic derivatives in the expression for $C_{n_{\beta DYN}}$ was also used to modify the LCDP closed-loop stability parameter. The resulting expression is provided in equation (30c) and is plotted versus angle-of-attack in Figure 48 with some simplification.

TYPE OF CRITERION:

Refinements of the open and closed-loop lateral/directional departure susceptibility parameters $C_{n_{\beta DYN}}$ and LCDP are proposed. Additional open-loop stability bounderies based on the "B", "D" and "E" coefficients of the lateral/directional characteristic equation are also suggested.

CRITERION PLOTS:

See Figures 47 and 48.

DESIGN IMPACT:

As suggested in Reference (33), "One interpretation of the modified criteria is that the currently defined minimum value requirements for $C_{n_{\beta DYN}}$ and LCDP should not be constant for all configurations. Instead minimum acceptable values should be based on the configuration specific dynamic derivatives."

The proposed criteria is an important refinement because it is consistent with modern fighter/attack aircraft configuration aerodynamics which are dominated by the effects of the forebody vortices at high angles-of-attack which tends to result in adequate static stability characteristics but

poor dynamic stability characteristics (As an example see the yaw and roll damping characteristics for the X-31A given in Figure 4) (Reference (33)).

Table V from Reference (33) compares the major differences in design features and characteristics of the fighter/attack aircraft of the 1950's and 1960's to the current design periods beginning with the early 1970's (i.e., F-14, F-15, F-16 generation).

Review of the substantiating data used by Weissman (to correlate regions of $C_{n_{\beta DYN}}$ versus LCDP with aircraft departure susceptibility) (Reference (33)) found that the dynamic data (C_{n_p}, C_{ℓ_p}, C_{n_r} and C_{ℓ_r}) influenced the departure susceptibility characteristics of the aircraft in correlation data base, but were not the dominant factors.

Table V Comparison of the Major Differences in Design Features and Characteristics of Fighter/Attack Aircraft of the 1950's and 1960's versus the Current Design Period. (Reference (33))

	50's ' 60's	70's ' 90's
$\alpha C_{L_{max}}$	17°- 23°	30° - 40°
$C_{L_{max}}$	Relatively Low	High
I_z/I_x	Med - High	High
Forebody Fineness (l/d)	2 - 2.5	4 - 6
Asymmetric Yawing Moment (C_{n_0})	0 - 0.01	0.05 - 0.12
Directional Weathercock Stability (C_{n_β})	Dominated by aft located vertical tail	Dominated by forebody (nose/lex*/ canard) vortices
Effect of Increasing C_{n_β} on Directional Damping (C_{n_r})	Increased damping due to forces acting aft of aircraft CG	Decreased damping due to forces acting ahead of CG
Impact of Rotary Cross Derivatives (C_{ℓ_r}, C_{n_p})	Low due to relatively low $C_{L_{max}}$	High due to increased $C_{L_{max}}$
		*Leading edge extension

As experienced during early X-31A configuration design, work done by NASA has shown that when the high angle-of-attack aerodynamics of a configuration are dominated by the forebody, there is a fundemental interchange between the static and dynamic stability characteristics (Reference (33)). Specifically if the forebody is altered to improve the static directional stability (C_{n_β}) at high angles-of-attack, yaw damping (C_{n_r}) will invariably decrease. Conversely, alterations to the forebody to improve dynamic stability characteristics will invariably degrade the static directional stability characteristics.

CRITERION ADVANTAGES:

The process of determining the stability characteristics of an aircraft without computing the roots of the characteristic equation to gain insight into the dominant vehicle characteristics is a formidible analytical task for the complete linear unaugmented aircraft equations-of-motion. To make this a realistic task, as is often done, Chody utilizes Kalviste's equation development given in Reference (51) which decouples the complete linear equations-of-motion and considers the stability characteristics of just the lateral/directional set. However, unlike the original $C_{n_{\beta DYN}}$ and LCDP stability parameters derived by Moul & Paulson (Reference (35)), Chody does not exclude the aerodynamic dynamic derivative terms (C_{n_r},C_{l_p}, etc.) as second order effects in his derived expressions. As pointed out, the influence of the dynamic derivatives can be significant for the configurations where forebody dynamics dominate the flow. Furthermore, by application of Routh Stability Criteria to the other coefficients[1] of the lateral/directional quartic characteristic equation (A, B, C, D, E and D(BC-AD)-B^2E must all be positive for absolute system stability), Chody has found that dynamic instabilities other than those associated with the "C" - coefficient are also influential to an aircraft configuration being departure prone.

[1]Note, Chody does not address the D(BC-AD)-B^2E term of Routh's Stability Criteria

CRITERION SHORTCOMINGS:

Used as aircraft departure susceptibility criteria the lateral/directional stability criteria proposed by Chody has two shortcomings to consider. First, as Chody suggests, the criteria (with the exception of the extension of the expressions for the $C_{n_{\beta_{DYN}}}$ and LCDP parameters) still need to be further analyzed in terms of correlating the proposed parameters with aircraft departure susceptibility characteristics.

Secondly, because the proposed stability parameters are derived from the uncoupled lateral/directional equation-of-motion set, instabilities due to coupling between the longitudinal and lateral/directional modes of motion which is prevalent at high angles-of-attack can not be addressed. If significant aerodynamic cross-coupling does exist (i.e. $\mathcal{L}_\alpha$, M_β, etc.) the criteria proposed by Johnston of STI ($1/T_{\theta_3}$) and Kalviste ($N_{\beta_{COP}}$,$M_{\alpha_{COP}}$, etc.) may be more appropriate.

CONCLUSIONS

The goal of this research was to provide guidelines to aid in the analytical determination of the departure susceptibility of future fighter aircraft designs. Towards this end the major departure susceptibility criteria developments dating back to the concept of the stability derivative were discussed at length in terms of their derivation, their design impact, their strong points and their shortcomings. As expected, no one analytical criterion can be applied to an aircraft design and provide the "full picture" as to the susceptibility of an aircraft to depart from controlled flight. However, the survey of criteria revealed that although in some cases there is overlap in the existing criteria, on the whole the criteria can be used in an intergrated fashion (from simple to more complex) to follow the design evolution and the associated availability and refinements of the aerodynamic data base.

Without exception each of the departure susceptibility criteria researched were based on linear or quasi-linear frozen point analysis. Although application of linear analysis does still appear to apply to the high angle-of-attack flight regime, caution must be exercised in defining limits of validity of the derived linear models. Additionally, where aerodynamic cross-coupling exists (i.e., C_{m_β}, C_{n_α}, etc.) and/or inertial coupling is an important stability consideration, the lateral/directional-longitudinal equations-of-motion can not be decoupled, and the linearization must be based on the six degree-of-freedom equations-of-motion and trim points that include asymmetric flight ($\beta_0 \neq 0$, $\phi_0 \neq 0$) and nonzero angular rates (P_0, Q_0, $R_0 \neq 0$). Furthermore, the linear analysis based results must address both open- (characteristic equation) and closed-loop (transfer function numerator dynamics) parameters and be verified using nonlinear simulations and available experimental techniques. Table VI summarizes the suggested use of the existing departure susceptibility criteria/stability parameters as they apply in the course of the design evolution.

Table VI Recommended Methodology For Evaluation/Determination Of Aircraft Departure Susceptibility

DESIGN EVOLUTION (INCREASING METHODOLOGY COMPLEXITY)

DATA/ANALYSIS REQUIREMENTS	APPROPRIATE/RECOMMENDED CRITERIA AND OR METHODOLOGY
Inertial Data (I_{xx}, I_{zz}, I_{xz})	Determine significance of aerodynamic cross-coupling (i.e., see vector polygon method of Reference (37)).
Lateral-Directional aerodynamic static data (C_{l_β}, C_{n_β}, $C_{l_{\delta_a}}$, $C_{n_{\delta_a}}$ . . C_{m_β} C_{n_α})	a. If aerodynamic cross-coupling is significant apply Kalviste's Coupled Stability Criteria. b. If aerodynamic cross-coupling is not significant apply STI/Weissman's LCDP versus $C_{n_{\beta DYN}}$ Criterion, Pelikian's $C_{n_{\beta APP}}$ Criterion, and STI's $1/T_{\phi_1}$.
Aerodynamic dynamic data (C_{l_p}, C_{n_r}, etc.)	Apply Chody's Stability Criteria to extend the concept of "$C_{n_{\beta DYN}}$" to include the effects of the dynamic derivatives.
Evaluate the effects of asymmetric flight ($\beta_0 \neq 0$)	Applicable stability parameters include STI's $1/T_{\theta_2}$ and Kalviste's Coupled Stability Parameters.
Assess/determine the effects of maneuvering	Kalviste's (1989) Dynamic Stability Parameters address the effects of steady maneuvering flight. Additionally pilot-in-the-loop simulation is highly recommended.
Assess/determine the effects of the flight control system augmentation	The closed-loop criteria, $1/T_{\theta_2}$ and $1/T_{\phi_1}$,apply equally well to fully augmented aircraft. Augmentation effects can be considered in Chody and Kalviste ('89) criteria using augmented derivatives (i.e., $L_{p_{AUG}} = L_p + K_{p_{\delta_a}} \cdot L_{\delta_a}$, etc.). Additionally the LCDP parameter can be modified to include the effects of an aileron-rudder interconnect. The effects of the FCS (especially digital, full-authority, fly-by-wire FCS) are best assessed using pilot-in-the-loop simulation.

RECOMMENDATIONS

To thoroughly analyze the departure tendencies of an aircraft configuration (note, even small configuration changes can alter the departure characteristics of an aircraft) through the evolution of the design (in terms of data availability and complexity) each of the following factors should be considered:

1. Analysis of both open- and closed-loop departure susceptability should be addressed.

RATIONALE: Aircraft departure from controlled flight can occur without the pilot-in-the-loop as well as be caused by pilot-in-the-loop control. If closed-loop criteria are not addressed, aircraft that are "assumed" departure resistant can in fact be just the opposite when the effects of pilot control are considered.

2. Careful measurement and thorough analysis of static wind tunnel data should be conducted.

   a. Consider the effects of Reynold's number during high angle-of-attack wind tunnel testing.

   b. A sufficient number of data points must be taken with angle-of-attack and sideslip angle to reveal nonlinearities and understand the limits of linear models used for analysis purposes.

   c. Static aerodynamic cross-coupling (i.e., C_{m_β}, C_{ℓ_α},C_{n_α} etc.) effects should be investigated and zero sideslip asymmetric phenomena (i.e., C_{ℓ_0}, C_{n_0}) should not be overlooked or ignored as anomallies.

   d. Functionality of the aerodynamic data should be carefully analyzed, e.g., is control data a function of sideslip angle?

RATIONALE: Formulation of an aerodynamic math model that accurately represents the aerodynamic forces and moments is a prerequisite for any of the proposed criteria to successfully correlate with aircraft departure susceptibility.

3. Include the influence of the aerodynamic dynamic derivatives in the proposed criteria.

RATIONALE: Current and future fighter/attack aircraft designs dominated by forebody vortices at high angles-of-attack can lead to stable statics

($Cn_{\beta DYN}$,0) but unstable dynamics (C_{n_r} >0) in addition to the dynamic cross-coupling derivatives being more significant. When the $Cn_{\beta DYN}$ criteria was developed, aircraft of the time were characterized by the derivatives Y_β, N_r andL_p being negative (stable). The opposite is true for high angles-of-attack for the X-31A and other current fighter/attack aircraft designs.

4. Conduct a sensitivity analysis of the high angle-of-attack aerodynamic characteristics (i.e., M_β, $\mathcal{L}_\alpha$, N_α, N_β, L_β, N_{δ_r}, etc).

RATIONALE: The reason for conducting an aerodynamic sensitivity analysis is two fold. First off, the dominant aerodynamic influences on the aircraft's departure susceptibility characteristics can be determined to aid in addressing design configuration changes and/or establishing a flight control law design for departure resistance. Secondly, the sensitivity analysis provides the aerodynamicist/flight controls engineer with some knowledge as to the robustness properties of the nominal aerodynamic math model. As discussed earlier, one of the biggest challenges of estimating aircraft dynamics at high angle-of-attack flight conditions is the development of an "accurate" aerodynamic math model that can be used with a high degree of confidence. The sensitivity analysis addresses this issue and highlights where model uncertainty is critical.

5. Evaluate the effects of longitudinal-lateral/directional dynamic coupling on aircraft stability which are:

   a. introduced through asymmetric flight conditions ($\beta_0 \neq 0$; $\phi_0 \neq 0$).

   b. introduced through the effects of maneuvering (P_0,Q_0, $R_0 \neq 0$; i.e., inertial coupling effects).

RATIONALE: Departure susceptibility criterion parameters such as $Cn_{\beta DYN}$,$Cn_{\beta APP}$, LCDP, etc., based on decoupling the lateral/directional equations-of-motion from the longitudinal set are based on linearizing the six degree-of-freedom equations-of-motion about a trim flight condition that assumes zero roll and yaw angular rates as well as zero bank angle (typically pitch rate, Q_0 is also assumed to be zero).

Typical of most air combat maneuvers, high angular rates can increase an aircraft's departure susceptibility from two perspectives. Firstly, the pilot workload is increased significantly during maneuvering flight. Secondly, nonzero pitch rate destabilizes the normal modes (primarily dutch-roll) and reduces the available control power, while nonzero roll rate causes lateral/directional-longitudinal coupling which produces mode shapes unfamiliar to the pilot.

6. Evaluate the effects of any flight control system augmentation using the applicable analytical departure susceptibility criteria.

RATIONALE: In light of the fact that future advanced fighter/attack aircraft will invariably contain full authority, digital fly-by-wire/light augmentation systems that "guarantee" stability (provided sufficient control power is available), application of the "static augmented" departure susceptibility criteria (i.e. Pelikan, Kalviste) serves to optimize the unaugmented aircraft dynamics including the effects of the controls to minimize control power requirements from the outset of the design evolution.

7. Investigate the effect of nonlinearities via man-in-the-loop simulation to include:

   a. the effect of the pilot (i.e., determine closed-loop aircraft pilot departure susceptibility).

   b. the effect of nonlinearities such as position and rate limiters, hysteresis, nonlinear dynamic maneuvering effects, atmospheric disturbances.

   c. evaluation of failure states and degraded flight control system modes.

   d. verifying/validating the linear departure susceptibility criteria findings.

RATIONALE: Determining local regions (in terms of M, h, α_0, β_0) of stability/instability associated with large angle, nonlinear maneuvering flight can become very cumbersome using quasi-linear methods (the problem is further compounded if the effects of the flight control system are included). In addition, their determination might not be indicative of aircraft departure susceptibility since the aircraft trajectory might diverge into a "stable region" where the aircraft becomes controllable again.

Utilizing a high fidelity pilot-in-the-loop simulation, closed-loop stability of the aircraft/pilot system can be determined from a nonlinear perspective. "Flying" a test matrix of critical departure prone maneuvers, the normal aircraft flight trajectory can be described as locally stable if after any disturbance (i.e., due to turbulence, gusts, system failure, etc.) from the normal trajectory it converges back to the nominal flight path and/or stabilizes at a new trim condition. If the aircraft/pilot system is locally unstable at some point along a desired flight path trajectory then the aircraft will not return to the nominal flight trajectory. If the instability is not "controllable" (i.e., the aircraft does not follow commanded inputs) at the very least the flying qualities would be degraded. In the worst case scenario the aircraft would diverge from the desired flight trajectory (and not "stabilize" in a different trim condition), with post-stall gyrations to follow and spin susceptibility very high.

8. Support analytical and pilot simulation results with available experimental methods.

RATIONALE: Because of the limitations of wind tunnel data acquisition/interpretation (Reynolds number effects, amplitude/oscillation effects, etc.) and the inherent limits of any mathematical model (be it pilot-in-the-loop or otherwise), it is recommended that aircraft departure susceptibility analysis make full use of experimental techniques such as water tunnel tests (for flow visualization), tethered model tests and drop model testing to refine and validate the high angle-of-attack and departure susceptibility characteristics of the subject aircraft.

REFERENCES

1. Henderson, C., Clark, J. and M. Walters, "V/STOL Aerodynamics and Stability & Control Manual," Report No. NADC-80017-60, 15 January 1980.

2. Anonymous, "Military Standard Flying Qualities of Piloted Aircraft," MIL- STD-1797A, 30 January 1990.

3. Skow, A.M., and A. Titiriga, Jr., "A Survey of Analytical and Experimental Techniques to Predict Aircraft Dynamic Characteristics at High Angles of Attack," AGARD-CP-235, May 1978.

4. Seltzer, R.M., and G.R. Rhodeside, "Fundamentals and Methods of High Angle of Attack Flying Qualities Research," Report No. NADC 88020-60, January 1988.

5. Kalviste, J. and B. Eller, "Coupled Static and Dynamic Stability Parameters," AIAA Paper 89-3362, Atmospheric Flight Mechanics Conference, Boston Massachusetts, 14-16 August 1989.

6. Ruckemann-Orlik, K.J., "Aerodynamic Aspects of Aircraft Dynamics at High Angles of Attack," Journal of Aircraft, Vol 20, No. 9 September 1983.

7. Schellenger, H.G., "Aerodynamic Damping Dataset for Flight Control Analysis of the X-31A Aircraft," Rockwell International TFD-89-1392L, No date.

8. Chambers, J.R., Gilbert, W.P., and Nguyen, L.T., "Results of Piloted Simulator Studies of Fighter Aircraft at High Angles of Attack," Paper 33, AGARD-CP-235, 1978.

9. Grafton, S.B. and Anglm, E.L., "Dynamic Stability Derivatives at Angles-of- Attack From -5° to 90° for a Variable-Sweep Fighter Configuration with Twin Vertical Tails," NASA TN D-6909, 1972.

10. Anon., Dynamic Stability Parameters, AGARD CP-235, 1978 and AGARD LS 114, 1981.

11. Dickes, Edward, "Analysis of Static and Rotational Aerodynamics at High Angles of Attack for Rockwell X-31A Preliminary Configuration," Bihrle Applied Research, Rep. BAR 88-1, January 1988.

12. Orlik-Ruckermann, K.J., "Dynamic Stability Testing of Aircraft-Needs versus Capabilities," Proceedings of International Congress on Instrumentation in Aerospace Simulation Facilities, 1973, pp. 8-23.

13. Johnston, Donald E. et al, "Investigation of Flying Qualities of Military Aircraft at High Angles of Attack. Volume I. Technical Results," Technical Report AFFDL-TR-74-61, June 1974.

14. Ruckemann-Orlik, K.J., "Aerodynamic Coupling Between Lateral and Longitudinal Degrees of Freedom," AIAA Journal Vol 15, December 1977, pp. 1792-1799.

15. Curry, W.H., and K.J. Orlik-Ruckermann, "Sensitivity of Aircraft Motion to Aerodynamic Cross-Coupling at High Angles-of-Attack," Paper 34, AGARD-CP-235, 1978.

16. Langham, T.F., "Aircraft Motion Sensitivity to Dynamic Stability Derivatives," AEDC-TR-79-11, 1980.

REFERENCES (CONT)

17. Orlik-Ruckermann, K.J., "Sensivity of Aircraft Motion to Cross-Coupling and Acceleration Derivatives," Lecture 15, AGARD-LS-114, 1981.

18. Lichtenstein, J.H. and Williams, J.L., "Effect of Frequency of Sideslipping Motion on the Lateral Stability Derivatives of a Typical Delta- Wing Airplane," NACA RML57F07, 1957.

19. Nguyen, Luat T., "Evaluation of Importance of Lateral Acceleration Derivatives in Extraction of Lateral Directional Derivatives at High Angles of Attack," NASA Technical Note D-7739, October 1974.

20. Goodman, Alex and Ronald Altman (of Tracor Hydronautics) "An Experimental Study to Determine the Subsonic Static and Dynamic Stability Characteristics of a 0.19 Scale Model of The X-31A Aircraft Operating at High Angles of Attack," Rockwell International TFD-88-1493L, 11 May, 1987.

21. Chambers, Joseph R., and Sue B. Grafton, "Aerodynamic Characteristics of Airplanes at High Angles-of-Attack," NASA TM-74097 December, 1977.

22. Bihrle, W.Jr., Barnhart, B., and E. Dickes, "Influence of Forebody Geometry on Aerodynamic Characteristics and a Design Guide for Defining Departure/Spin Resistant Forebody Configurations," WRDC-TR-89-3079, September 1989.

23. Roskam, Jan, "Linear or Nonlinear Analysis Methods: When and How?," AGARD CP-235, 1978.

24. Roskam, J., "Airplane, Flight Dynamics and Automatic Flight Controls," Roskam Aviation and Engineering Corporation, 1979.

25. Brogan, W.L. "Modern Control Theory," Prentice-Hall Inc., Englewood Cliffs, N.J., 1985.

26. Greer, D.H., "Summary of Directional Divergence Characteristics of Several High Performance Aircraft Configurations," NASA TN D-6993, November 1972.

27. Weissman, R., "Status of Design Criteria for Predicting Departure Characteristics and Spin Susceptibility," Journal of Aircraft Vol. 12, No. 12., December 1975.

28. Tinger, H.L., "Analysis and Application of Aircraft Departure Prediction Criteria to the AV-8B Harrier II," AIAA-Paper 87-2561.

29. Phillips, W.H., "Effect of Steady Rolling on Longitudinal and Directional Stability," TN 1627, June 1948.

30. Stengel, R.F. and P.W. Berry, "Stability and Control of Maneuvering High Performance Aircraft," NASA CR-2788, April 1977.

31. Stengel, R.F., "Effect of Combined Roll Rate and Sideslip Angle on Aircraft Flight Stability,"Journal of Aircraft, Vol 12, No. 8, August 1975.

REFERENCES (CONT)

32. Stengel, R.F., Taylor J.H., et al, "High Angle of Attack Stability and Control," ONR-CR215-237-1 7 April 1976.

33. Chody, J.R., Hodgkinson, J. and A.M. Skow, "Combat Aircraft Control Requirements for Agility," AGARD Paper No. 4, Madrid, Spain October 2-5, 1989.

34. Seckel, Edward, "Stability and Control of Airplanes and Helicopters," Academic Press, New York, 1964.

35. Moul, M.T. and J.W. Paulson, "Dynamic Lateral Behavior of High-Performance Aircraft," NACA RM-L58E16, August 1958.

36. Chody, J., "High Angle-of-Attack Departure Criteria," Eidetics TR-88-013, 7 October 1988.

37. Johnston, D.E., and R.K. Heffley, "Investigation of High-AOA Flying Qualities Criteria and Design Guides," AFWAL TR-81-3108, December 1981.

38. Mello, John and James Agnew, "McAir Design Philosophy for Fighter Aircraft Departure and Spin Resistance," SAE Paper No. 791081, presented at Aerospace Meeting, Los Angeles, Dec 3-6, 1979.

39. Calico, Robert A., "A New Look at $C_{n_{\beta DYN}}$," Journal of Aircraft, Vol. 16, No.12, Dec 1979.

40. Chambers, Joseph R. and E.L. Anglin, "Analysis of Lateral-Directional Stability Characteristics of a Twin-Jet, Fighter Airplane at High Angles of Attack," NASA TN D-5361, August 1969.

41. DaForno, G., "Theoretical Estimation Methods for Stall Aerodynamics: Ideas and Preliminary Results," presented at High Angle-of-Attack Workshop, Wright- Patterson AFB, 29 Nov. through 2 Dec. 1976.

42. Hodgkinson, J., "Prediction of Lateral and Directional Divergence at High Angles of Attack," Mc-Donnell Aircraft Co. Report No. EN844, 15 October 1971.

43. Pelikan, R.J., "Evaluation of Aircraft Departure Divergence Criteria with a Six-Degree-of-Freedom Digital Simulation Program," AIAA Paper No. 74-68 Washington, D.C. January 30 - February 1, 1974.

44. Weissman, Robert, "Criteria for Predicting Spin Susceptibility of Fighter- Type Aircraft," ASD-TR-72-48, June 1972.

45. Weissman, Robert, "Preliminary Criteria for Predicting Departure Characteristics/Spin Susceptibility of Fighter-Type Aircraft," AIAA Journal of Aircraft, Vol. 10, No. 4, April 1973.

46. McRuer, D.T., Ashkenas, I.L., and D.E. Johnston, "Flying Qualities and Control Issues/Features for Hypersonic Vehicles," NASP Contractor Report 1063, October 1989.

REFERENCES (CONT)

47. Titiriga, A., Jr., J.S. Ackerman and A.M. Skow, "Design Technology for Departure Resistance of Fighter Aircraft," Stall/Spin Problems of Military Aircraft, AGARD Conference Proceedings No. 199, June 1976.

48. Johnston, Donald E., David G. Mitchell and Thomas T. Myers, "Investigation of High-Angle-of-Attack Maneuver-Limiting Factors. Part I: Analysis and Simulation, AFWAL-TR-80-3141, Pt. I, September 1980.

49. Rao, D.M. and D.G. Murri, "Exploratory Investigation of Deflectable Forebody Strakes for High-Angle-of-Attack Yaw Control," AIAA Paper 86-0333, Reno, Nevada, 6-9 January 1986.

50. Ng, T. and G. Malcom, "Aerodynamic Control Using Forebody Strakes, "AIAA Paper 91-0618, Reno, Nevada, 7-10 January 1991.

51. Kalviste, J., "Aircraft Stability Characteristics at High Angles of Attack," Dynamic Stability Parameters, AGARD Conference Proceedings No. 235, May 1978.

52. Kalviste, J., "Coupled Static Stability Analysis for Nonlinear Aerodynamics," AIAA-83-2068, AIAA Atmospheric Flight Mechanics Conference, August 1983.

53. Bihrle, W., Jr. and B. Barnhart, "Design Charts and Boundaries for Identifying Departure Resistant Fighter Configurations," NADC-76154-30, July 1978.

54. Johnston, Donald E. and Jeffrey R. Hogge, "Nonsymmetric Flight Influence on High Angle-of-Attack Handling and Departure," Journal of Aircraft, Vol. 13, No. 2, January 1976.

55. Pelikan, R.J., "F/A-18 High Angle of Attack Departure Resistance Criteria for Control Law Development," AIAA-Paper 83-2126, Gatlinburg, TN, 15-17 August, 1983.

56. Anonymous, "Military Specification Flight Test Demonstration Requirements for Departure Resistance and Post Departure Characteristics of Piloted Airplanes," MIL-S-83691A, 15 April 1972.

APPENDIX A

GLOSSARY OF DEFINED TERMS

DEPARTURE : The event indicating loss of control which may develop into a post-departure gyration, spin or deep stall condition. The departure may be characterized by divergent, large amplitude, uncommanded aircraft motions, such as nose slice or pitch-up. An AOA excursion is not considered a departure (Reference (55)).

DEPARTURE SUSCEPTIBILITY (MIL-S-83691A Definitions) :

Extremely Susceptible to Departure: Departure from controlled flight will generally occur with the normal application of pitch control alone or with small roll, and yaw control inputs.

Susceptible to Departure: Departure from controlled flight will generally occur with the application or brief misapplication of pitch, roll, and yaw controls that may be anticipated in operational use.

Resistant to Departure: Departure from controlled flight will only occur with a large and reasonably sustained misapplicaton of pitch, roll, and yaw controls.

Extremely Resistant to Departure: Departure from controlled flight can only occur after an abrupt and inordinately sustained application of gross, abnormal, pro-departure controls.

POST-STALL GYRATION: An uncontrolled oscillation about any or all axis following a departure.

SPIN: A sustained rotation in yaw at an angle-of-attack greater than the stall angle-of-attack.

DISTRIBUTION LIST
Report No. NADC-90048-60

No. of Copies

Office of Naval Technology 2
800 North Quincy St.
Arlington, VA 22219-5000
(2 for W. King)

Naval Air Systems Command 9
Washington, DC 20361-0001
(4 for AIR-53011; T. Lawrence)
(1 for AIR-53011B; R. Hanley)
(1 for AIR-53011B2; M. Draper-Donley)
(1 for AIR-53011B3; S. Taylor)
(1 for AIR-5114F; J. Jones)
(1 for AIR-05TP1; C. Johnson)

Naval Air Warfare Center 8
Aircraft Division
Patuxent River, MD 20670
(2 for SA-40; B. Kneeland)
(2 for SA-60B; C. Clark)
(2 for SA-60; W. McNamara)
(2 for Code AT)

Center for Naval Analysis 1
4401 Fort Avenue
P.O. Box 16268
Alexandria, VA 22302-0268

USN Test Pilot School 1
Naval Air Test Center
SA-40
Patuxent River NAS, MD 20670-5000

Naval Air Warfare Center 25
Aircraft Division Warminster
Warminster, PA 18974-5000
(1 for Code 60)
(1 for Code 605)
(20 for Code 6053; R. Seltzer)
(1 for 60C; L. Lehman)
(2 for Code 8131)

NASA Langley Research Center 7
Hampton, VA 20350
(1 for J. Chambers)
(1 for W. Gilbert)
(1 for L. Nguyen)
(1 for J. Foster)
(1 for M. Ogborne)
(1 for M. Croom)
(1 for J. Davidson)

DISTRIBUTION LIST (Continued)
Report No. NADC-90048-60

No. of Copies

NASA Ames-Dryden Flight Research Facility 4
NASA ADFRF/OF
Edwards AFB, CA 93523-5000
(1 for J. Gera)
(1 for R. Clarke)
(1 for J. Bauer)
(1 for J. Wilson)

NASA Ames Research Center 1
MS-210-5
Moffett Field, CA 94035
(1 for E. Aiken)

NASA Headquarters 1
600 Independence Ave, SW
Code RX
Washington, DC 20546
(1 for R. Pearce)

DARPA/ASTO 1
3701 N. Fairfax Dr.
Arlington, VA 22203
(1 for M. Francis)

Wright Laboratory 3
WL/FIGCB
Wright-Patterson AFB, OH 45433
(1 for T. Cord)
(1 for F. George)
(1 for T. Gentry)

Aero Mechanics Division 1
Wright Laboratory
WL/FIM
Wright-Patterson AFB, OH 45433-6523

Flight Control Division 1
Wright Laboratory
WL/FIG
Wright-Patterson AFB, OH 45433-6523

Wright Laboratory 1
WL/FI
Wright-Patterson AFB, OH 45433-5000
(1 for R. Borowski)

DISTRIBUTION LIST (Continued)
Report No. NADC-90048-60

No. of Copies

Flight Technology Division 1
Aeronautical Systems Division
ASD/ENFT
Wright-Patterson AFB, OH 45433-6553

Aeronautical Systems Division 1
ASD/ENFTC
Wright-Patterson AFB, OH 45433-6503
(1 For T. Black)

Air Force Flight Test Center 1
6510TW/DORX
Edwards AFB, CA 93523
(1 for F. Webster)

Air Force Flight Test Center 1
6510TW/DOEF
Edwards AFB, CA 93523
(1 for T. Twisdale)

Air Force Flight Test Center 1
6510TW/DOR
Edwards AFB, CA 93523
(1 for R. Evans)

Air Force Flight Test Center 1
6510TW/DORM
Edwards AFB, CA 93523
(I for A. Lawless)

Bihrle Applied Research 2
400 Jericho Turnpike
Jericho, NY 11753
(1 for W. Bihrle)
(1 for B. Barnhardt)

Boeing Advanced Systems Division 2
Mail Stop 33-18
Post Office Box 3707
Seattle, WA 98124
(1 for D. Ilgenfrit)
(1 for M. Burgess)

Eidetics International 2
3415 Lomita Boulevard
Torrance, CA 90505
(2 for A. Skow)

DISTRIBUTION LIST (Continued)
Report No. NADC-90048-60

No. of Copies

General Dynamics Corporation 1
Post Office Box 748
San Diego, CA 92138
(1 for D. Wyatt)

Grumman Aerospace Corporation 3
Bethpage, NY 11714
(1 for H. Beaufrere)
(1 for M. Lapins)
(1 for C. Boppe)

Lockheed Aeronautical Systems Company 1
86 South Cobb Drive
Dept. 73-42
Marietta, GA 30063-0685
(1 for H. Youssef)

Lockheed Corporation 1
4500 Park Granada Boulevard
Calabasas, CA 91399-0510
(1 for J. Retelle)

Northrop Corporation 1
3836/82
1 Northrop Avenue
Hawthorne, CA 90250
(1 for Juri Kalviste)

McDonnell Aircraft Company 4
Post Office Box 516
St. Louis, MO 63166
(1 for D. Riley)
(1 for K. Citurs)
(1 for W. Moran)
(1 for D. Wilson)

Rockwell International 3
Mail Code 011-GB02
Post Office Box 92098
Los Angeles, CA 90009
(1 for M. Robinson)
(1 for H. Schellenger)
(1 for R. Bitten)

Rockwell International 1
Dept 736-MCPJ01-805-273-6000-5404
2825 East Ave P.
Palmdate, CA 93550
(1 for S. Powers)

DISTRIBUTION LIST (Continued)
Report No. NADC-90048-60

No. of Copies

SRS Technologies 1
1500 Wilson Boulevard
Arlington, VA 22209
(1 for G. See)

SRS Technologies
238 Harman Boulevard 1
Dayton, OH 45419
(1 for W. Lamar)

Systems Technology Incorporated 3
13766 South Hawthorne Boulevard
Hawthorne, CA 90250-7083
(1 for D. McRuer)
(1 for T. Myers)
(1 for D. Johnson)

Department of Aero. and Mechanical Sciences 1
Princeton University
Princeton, NY 08540
(1 for Dr. R. Stengal)

Department of Aero and Ocean Engineering 1
VPI & SU
Blacksburg, VA 24061
(1 for F. Lutze)

Defense Technical Information Center 2
ATTN: DTIC-FDAB
Cameron Station BG5
Alexandria, VA 22304-6145